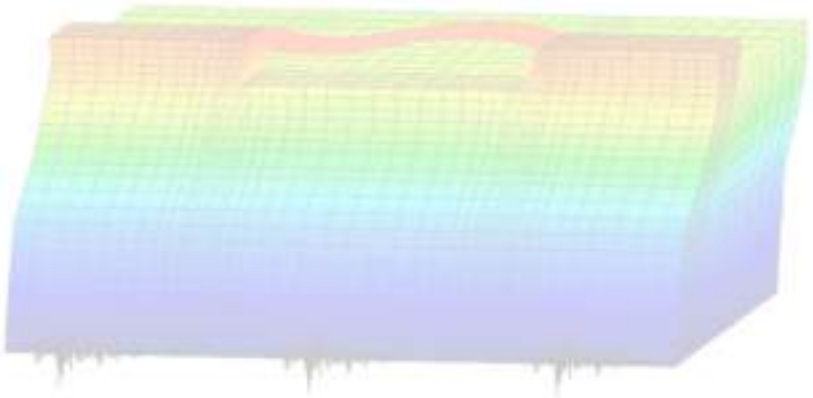

2024 International Workshop

Computational Dynamic Soil-Structure Interaction - CompDSSI

Book of Extended Abstracts

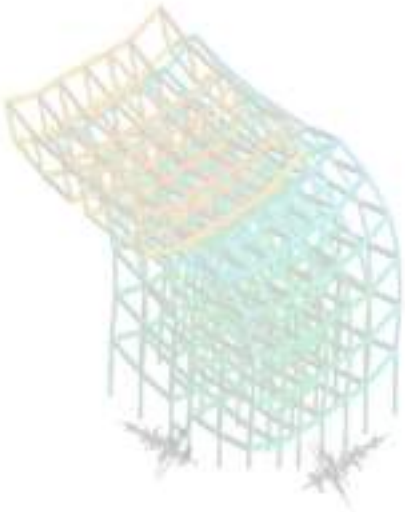

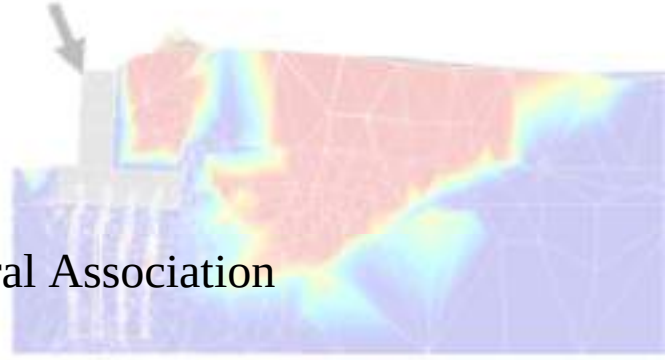

***Published by*:** CompDSSI Cultural Association
***ISBN*:** 979-12-985212-0-9

Organizers

Dr. Davide Noè Gorini
University of Trento, Trento, Italy

Prof. Pedro Arduino
University of Washington, US

Dr. Domenico Gallese
ARUP, UK

Scientific Committee

Prof. Anastasios Sextos (University of Bristol, UK)
Prof. Shideh Dashti (University of Colorado at Boulder, US)
Prof. Guido Camata (University of Pescara G. d'Annunzio, Italy)
Prof. Christopher McGann (University of Canterbury, New Zealand)
Prof. Francesca Dezi (University of Camerino, Italy)
Prof. Nikos Gerolymos (National Technical University of Athens, Greece)
Dr. Federico Pisanò (Norwegian Geotechnical Institute, US)
Prof. Ertugrul Taciroglu (University of California, Los Angeles, US)
Prof. Claudio Tamagnini (University of Perugia, Italy)
Prof. José A. Abell (University of the Andes, Chile)
Prof. Stefania Sica (University of Sannio, Italy)
Prof. James Ricles (University of Lehigh, US)
Prof. Domniki Asimaki (California Institute of Technology, US)
Prof. Paolo Franchin (Sapienza University of Rome, Italy)
Dr. Yu-Wei Hwang (National Taiwan University, Taiwan)
Dr. Massimo Petracca (ASDEA Software Technology, Italy)
Prof. Stavroula Kontoe (University of Patras, Greece)
Prof. Youssef M. A. Hashash (University of Illinois Urbana-Champaign, US)
Prof. Boris Jeremić (University of California, Davis, US)
Dr. Domenico Gallese (ARUP, UK)
Prof. Pedro Arduino (University of Washington, US)
Dr. Davide Noè Gorini (University of Trento, Italy)

Table of Contents

Preface

Advances in the field of soil-structure interaction are impacting design, retrofitting and protection of civil engineering structures against natural hazards. CompDSSI is an in-person International Workshop devoted to new-generation numerical approaches for the dynamic analysis of soil-structure systems of strong practical relevance, investigating critical issues and high-fidelity methods applicable from local to regional scale.

A meeting point to share knowledge, in which researchers and designers of Structural & Geotechnical Engineering will promote solutions for a safer and more efficient urban fabric. The co-presence of Academia and Industry is a key element of CompDSSI, for better orienting new lines of research and implementing them in real cases.

This Book of Extended Abstracts of the CompDSSI contains 32 contributions, which are organized in four major sections:

1. *Large soil-structure systems*
2. *Artificial Intelligence-based approaches to dynamic soil-structure interaction*
3. *Mitigation of natural hazards in urban settings*
4. *Underground structures*

All extended abstracts included here are archived in a downloadable form on the CompDSSI website (https://compdssi.altervista.org/) for wider dissemination.

D. N. Gorini
P. Arduino
D. Gallese

September 2024

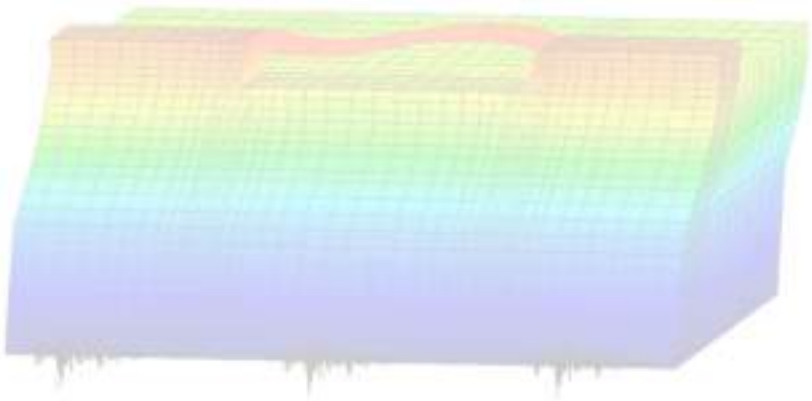

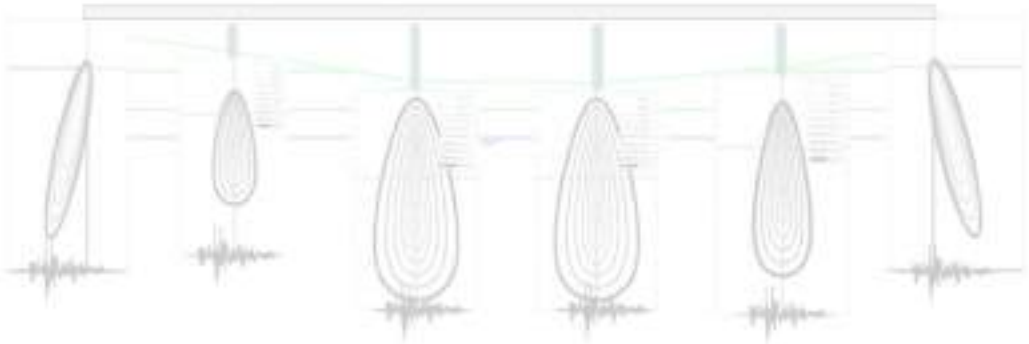

1.Large soil-structure systems

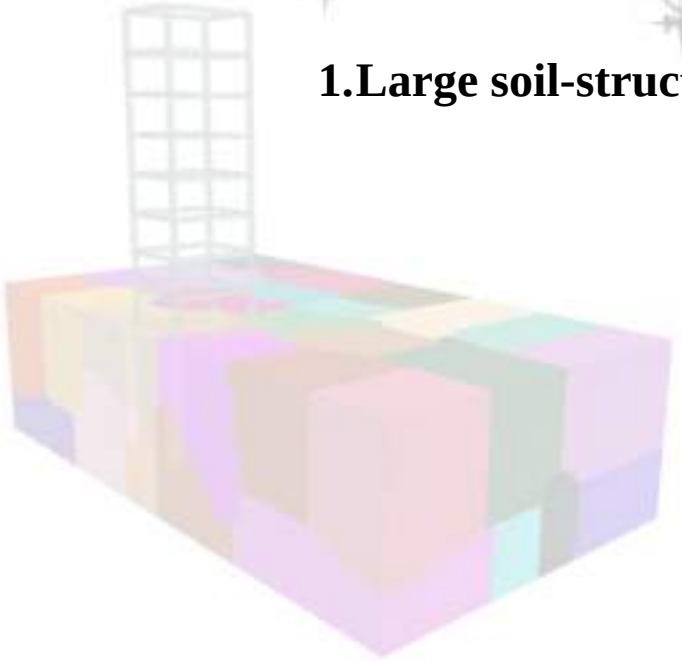

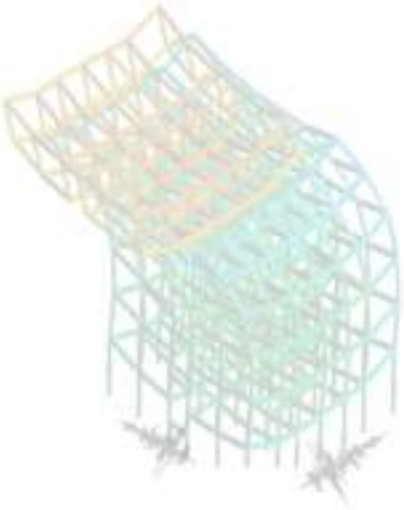

Applications of emerging GPU-accelerated computing at the exascale - exploration of fault-to-structure simulations with regional-scale 3D physics-based models

***D. McCallen*[1]**
[1] *Lawrence Berkeley National Laboratory, Berkeley, California, United States*

Abstract

The continuous advancements in high performance computer platforms, illustrated in Figure 1, are allowing earthquake simulations of unprecedented size and fidelity. With the recent generation of GPU-accelerated exaflop platforms, broad-band, physics-based ground motion simulation at regional scale is becoming a reality. The available memory, compute speeds and massive data manipulation attainable with superfast file systems support the computation of earthquake ground motions across regions 100's of kilometers in extent. Additionally, advanced multidisciplinary earth science - engineering workflows are allowing the rigorous coupling between regional geophysics models with local engineering models of structure-soil systems. This permits fully integrated fault-to structure simulations that include the earthquake source rupture process, propagation of seismic waves through the heterogeneous earth, local soil site response, and soil-structure interaction. This presentation will describe the computational aspects of the U.S. Department of Energy (DOE) **E**arth**Q**uake SIMulation (EQSIM) fault-to-structure framework, which was purpose built to fully exploit the DOE's new exaflop computer systems. In addition, case studies of regional simulations that can yield new insight into the complex regional distribution of earthquake ground motions, site response and the interactions between complex incident seismic waves with engineered structures, are described.

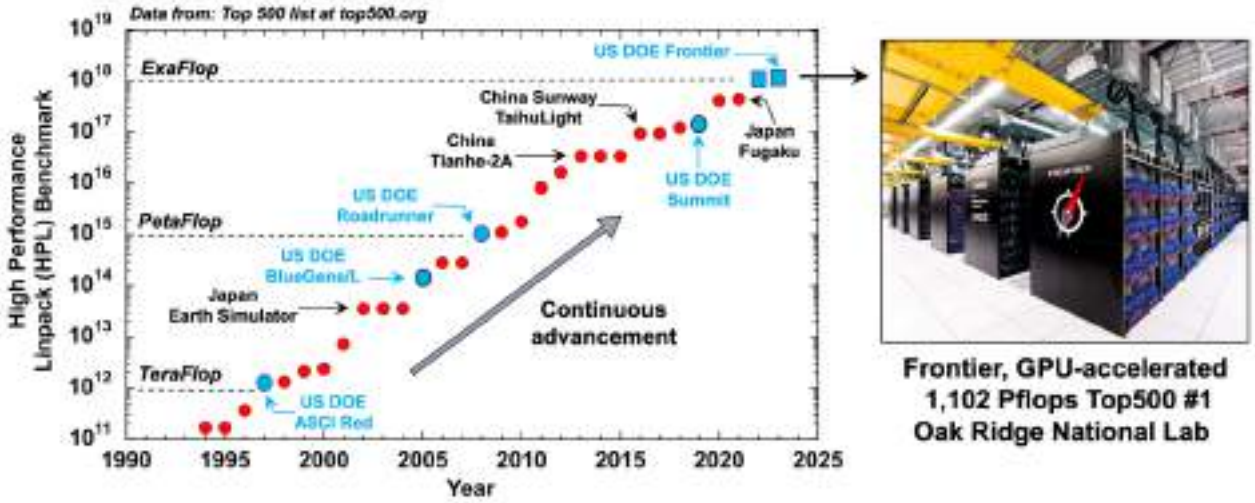

Figure 1. The inexorable advancement of high-performance computing platforms - the world's #1 ranked supercomputer platform by year (from top500.org) and the DOE's new 1.1 exaflop "Frontier" system currently ranked #1.

1. The Earthquake Simulation (EQSIM) workflow for fault-to-structure simulations

In parallel to the DOE developments for building the world's first exaflop computer system, the DOE Exascale Computing Project (ECP) developed science and engineering software applications to be fully ready to utilize these new systems. The EQSIM framework for regional-scale fault-to-structure earthquake simulations is one of 24 selected applications to prepare for the new GPU-accelerated platforms. EQSIM is a multidisciplinary framework with workflow linking regional scale geophysics simulations with local engineering system simulations [1], [2]. The EQSIM workflow utilizes the Graves-Pitarka kinematic fault rupture model [3] to initiate the earthquake process, the SW4 4th order summation by parts seismic wave propagation program [4], to simulate wave motion through an entire

region, and engineering structure response is computed either through traditional fixed base models (no SSI) or through local soil/structure interaction based on efficient implementation of a Domain Reduction Method (DRM) boundary as indicted in Figure 2. The DRM implementation was developed to allow expedient integration with any existing engineering finite element software that has implemented a DRM boundary [1].

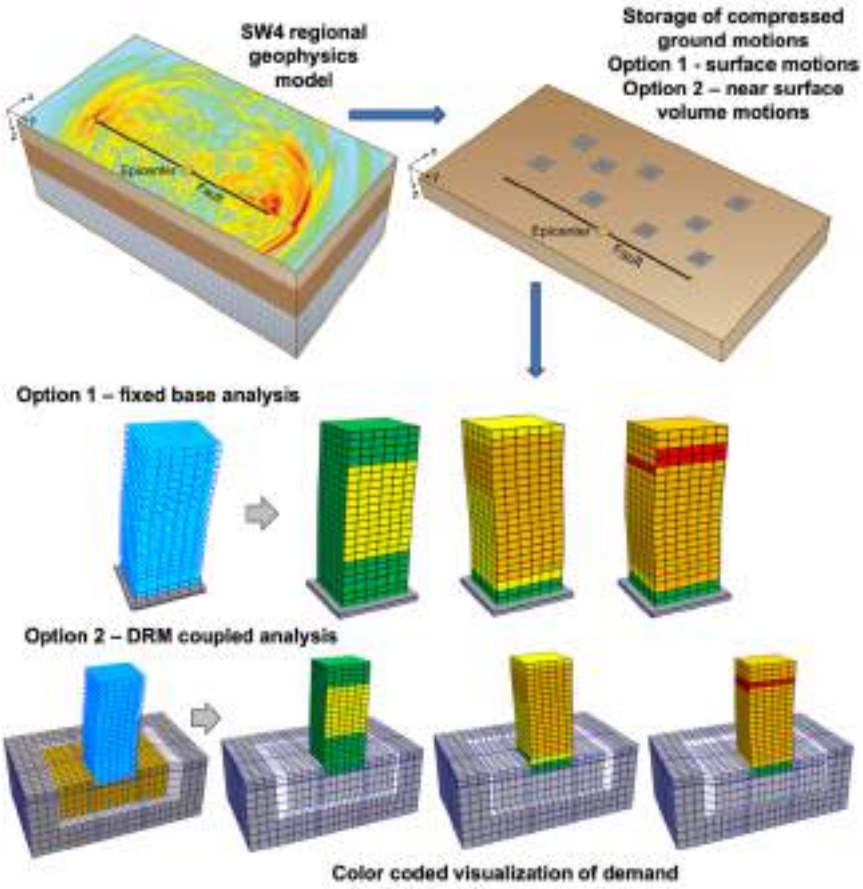

Figure 2. Fault-to-structure workflow for coupling regional geophysics and local engineering models.

The over-arching objectives in EQSIM development included:

- The ability to compute regional earthquake simulations at unprecedented frequency resolution and with resolution of soft low velocity near-surface sediments, both of which present computational challenges,
- Achieve individual earthquake scenario wall clock run times that enable the execution of the large number of earthquake realizations necessary to explore the model parameter space, for example many different fault rupture realizations and sensitivity studies of key geophysical parameters that are not well constrained through observational data,
- Develop a workflow format that allows the EQSIM user to efficiently deal with massive data sets, including both input and output data, in an efficient manner with the objective of making very large-scale simulations routine rather than heroic.

Ultimately, the EQSIM development included implementation of advanced algorithms, optimization of massive data IO, automated fetching of large datasets, and code optimization for efficient execution on massively parallel GPU-accelerated systems. Over the six-year life of the ECP project, major performance advancements were realized. Each ECP application was required to establish a Figure of Merit (FOM) expressing the performance elements of the application. In the case of EQSIM the FOM included an integrated consideration of frequency resolution, soft soil velocity

resolution and wall clock run times. Figure 3 illustrates the FOM trends over the life of the project where the FOM increased from 1.0 at the start of the development to a value of just under 3,500 at the end of the project, indicative of a major advancement in computational performance.

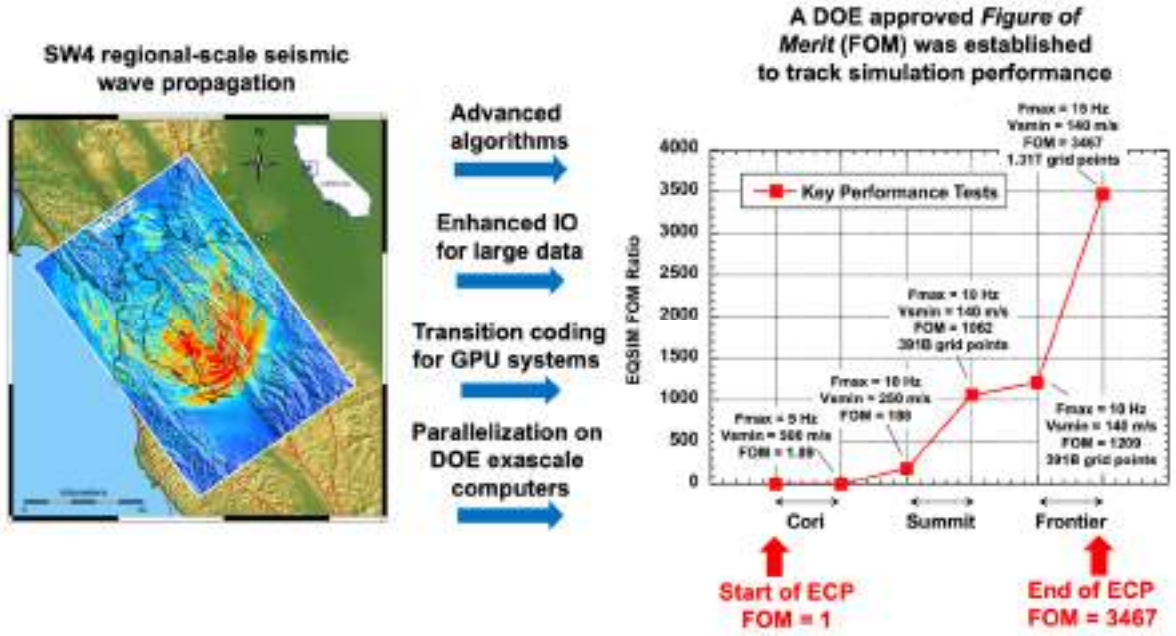

Figure 3. EQSIM computational performance advancements through advanced algorithms and exploitation of massively parallel GPU-accelerated platforms, resulting in a 3,500X performance increase.

With the successful completion of the EQSIM project, the framework is now being pressed into use to develop an open-access regional simulated ground motion database for the San Francisco Bay area that will be created on the Pacific Earthquake Engineering Research Center (PEER) ground motion website. As an important part of the database development, careful evaluation of simulated ground motion realism is being conducted to build confidence for the broader utilization of these massive new datasets [5]. In this presentation, these new applications will be described.

2. References

[1] McCallen, D., Pitarka, A., Tang, H., Pankajakshan, R., Petersson, N.A., Miah, M., Huang, J. (2024). Regional-Scale Fault-to-Structure Earthquake Simulations with the EQSIM Framework: Workflow Maturation and Computational Performance on GPU-Accelerated Exascale Platforms, *Earthquake Spectra*, Early on-line, doi: 10.1177/87552930241246235

[2] McCallen, D., Petersson, A., Rodgers, A., Pitarka, A., Miah, M., Petrone, F., Tang, H. (2021). EQSIM—A Multidisciplinary Framework for Fault-to-Structure Earthquake Simulations on Exascale Computers Part I: Computational Models and Workflow, *Earthquake Spectra*, 37(2), 707-735, doi:10.1177/8755293020970982

[3] Pitarka, A., Graves, R., Irikura, K., Miyakoshi, K., Wu, C., Kawase, H., Rodgers, A., McCallen, D. (2021). Refinements to the Graves-Pitarka Kinematic Rupture Generator, Including a Dynamically Consistent Slip-Rate Function, Applied to the 2019 Mw 7.1 Ridgecrest Earthquake, *Bulletin of the Seismological Society of America*, 112(1), 287-306, doi: 10.1785/0120210138

[4] Petersson, N.A., Sjogreen, B. (2015). Wave propagation in anisotropic elastic materials and curvilinear coordinates using a summation-by-parts finite-difference method, *Journal of Computational Physics*, 299, 820-841, doi: 10.1016/j.jcp.2015.07.023

[5] Petrone, F., Abrahamson, N., McCallen, D., Pitarka, A., Rodgers, A. (2021). Engineering Evaluation of the EQSIM Simulated Ground-Motion Database: The San Francisco Bay Area Region, *Earthquake Engineering & Structural Dynamics*, 50(15), 3939-3961, doi:10.1002/eqe.3540

Leveraging Structure-Soil-Structure Interaction for Enhanced Seismic Resilience in Nuclear Power Plants

C. Kanellopoulos[1] and B. Stojadinovic[1]
[1] ETH Zurich, Zurich, Switzerland

Abstract

The study explores the dynamic structure–soil–structure interaction between idealized Nuclear Power Plant (NPP) reactor and auxiliary building on separate foundations located at a realistic layered soil profile. Drawing inspiration from the main protective mechanism of seismic resonant metamaterials (i.e., out-of-phase oscillation, relatively to the propagating seismic waves, of resonators that are embedded into the soil), the potential for the auxiliary building to provide seismic protection to the reactor building is investigated. Finite element models of increasing complexity are developed and analysed in the Real-ESSI Simulator software employing the Domain Reduction Method (DRM) to generate vertically propagating shear waves. Initially, under linear soil conditions and tied soil–foundation interfaces, the presence of the auxiliary building is found to amplify the rocking vibration mode of the soil–reactor building system through an unfavorable out-of-phase rotational coupling between the two structures. However, incorporating nonlinear soil–structure interfaces and soil nonlinearity, which allow for modelling sliding at the interfaces and soil plastification beneath the foundations, suppressed this detrimental rotational interaction. Thus, a beneficial out-of-phase horizontal coupling emerged between the two buildings, like the protection mechanism of seismic resonant metamaterials. This led to a significant reduction, up to 55%, in the spectral acceleration of critical components within the reactor building, for frequencies near the resonant vibration frequency of the auxiliary building. These findings suggest that properly designing adjacent NPP buildings could enable beneficial interactions among them with the potential to enhance their overall seismic resilience.

1. Methodology

A sophisticated 3D FE model (**Figure 1**) of an idealized — but based on existing designs — Nuclear Power Plant (NPP) was simulated in the Real-ESSI Simulator [1]. The NPP consists of the reactor building surrounded by an auxiliary building, each founded on a separate foundation. The contribution of key aspects of SSSI modelling, such as the soil and interface nonlinearity, is highlighted by gradually increasing the sophistication level of the analysis.

Initially, linear elastic soil conditions are assumed and the soil–structure interfaces are tied. Then, special nonlinear interfaces are introduced, allowing for modelling uplifting and sliding at the soil–foundation interfaces. Specifically, in the normal (vertical) direction, a nonlinear elastic penalty stiffness function representing a soft contact with stiffness increasing exponentially with penetration is used to model the contact behavior. This is considered a realistic representation of the normal soil–structure interface behavior, as the normal contact force changes gradually upon contact and becomes zero upon detachment. For the nonlinear contact behavior in the tangential (horizontal) direction, an Armstrong-Frederick nonlinear hardening model is used, where the shear stress to normal stress ratio ($\mu = \tau/\sigma_n$) increases nonlinearly from 0 to the value of the residual friction coefficient μ_r. Finally, a simple yet realistic nonlinear constitutive soil model is introduced, incorporating a von Mises failure criterion, the Armstrong–Frederick nonlinear kinematic hardening, and an associated flow rule, suitable for modelling the dynamic cyclic response of pressure-independent materials.

The seismic wave field is assumed to consist only of one-component vertically propagating horizontal shear waves (SV), which are inserted into the model using the domain reduction method (DRM) [2], targeting a specific artificial accelerogram at the ground surface.

Since only one configuration of structures, spacing between them, soil layers and excitation is considered, the findings of this study are specific to this configuration and, hence, not all of them can

be generalized. For a detailed description of the employed FE model the reader can refer to the original paper [3].

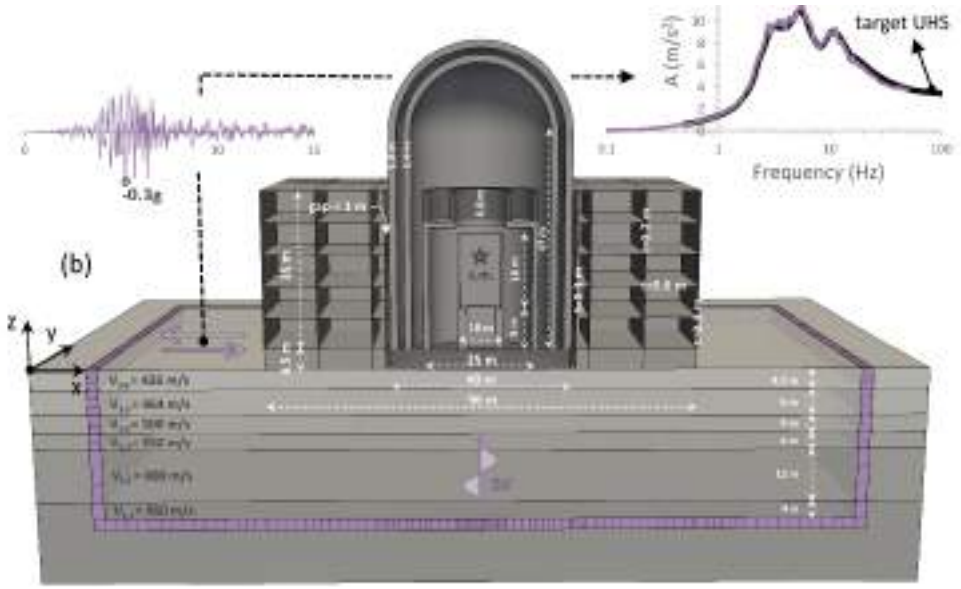

Figure 1. Cross-section of the 3D DRM FE model of the idealized NPP, showing key geometric and material properties. An artificial accelerogram is reproduced at the ground surface using the DRM forces applied at the reduced domain boundary (DRM layer).

2. Study Outcomes

The effect of the auxiliary building on the reactor building is first studied, assuming tied interfaces and elastic soil conditions. The presence of the auxiliary building and the developing SSSI, leads to an overall amplification of the spectral accelerations SA at characteristic critical points of the reactor building, at frequencies close to the resonance of the auxiliary building. This amplification is associated with a *detrimental out-of-phase rotational interaction* mechanism between the two buildings, which leads to an increase of the rotational response of the reactor building. This detrimental effect of the auxiliary building on the reactor building is slightly reduced when nonlinear interfaces are introduced at the soil–foundation level, as limited sliding occurs and dissipates energy, reducing the response of the auxiliary building. The addition, finally, of soil nonlinearity completely reverses the interaction mechanism between the two buildings. Nonlinear soil response leads to a significant suppression of the rocking vibration mode of the reactor building, which changes the *detrimental out-of-phase rotational interaction* of the two buildings, to a *beneficial out-of-phase horizontal interaction* for frequencies near and above the resonance of the auxiliary building. The auxiliary building essentially protects the reactor building by moving out-of-phase (at its resonant frequency and higher) relative to the soil, thus reducing the excitation of the latter, and consequently the response of critical components inside the reactor building. The components that benefit the most are the reactor vessel and the cylindrical wall (see points 3 and 4 in **Figure 2**, respectively), which experience a remarkable reduction in spectral accelerations SA of the order of 55 %, in the frequency range associated with the resonant frequency of the auxiliary building.

Summarizing, SSSI effects can be either *beneficial* or *detrimental* for the response of the structure, depending on the specific studied problem, but also on the selected level of model sophistication. Thus, engineers should be able to gradually increase the sophistication level of their models to account for such complex SSSI effects, and ideally, to optimize the dynamic characteristics of neighboring structures during the design phase, aiming to maximize their beneficial SSSI.

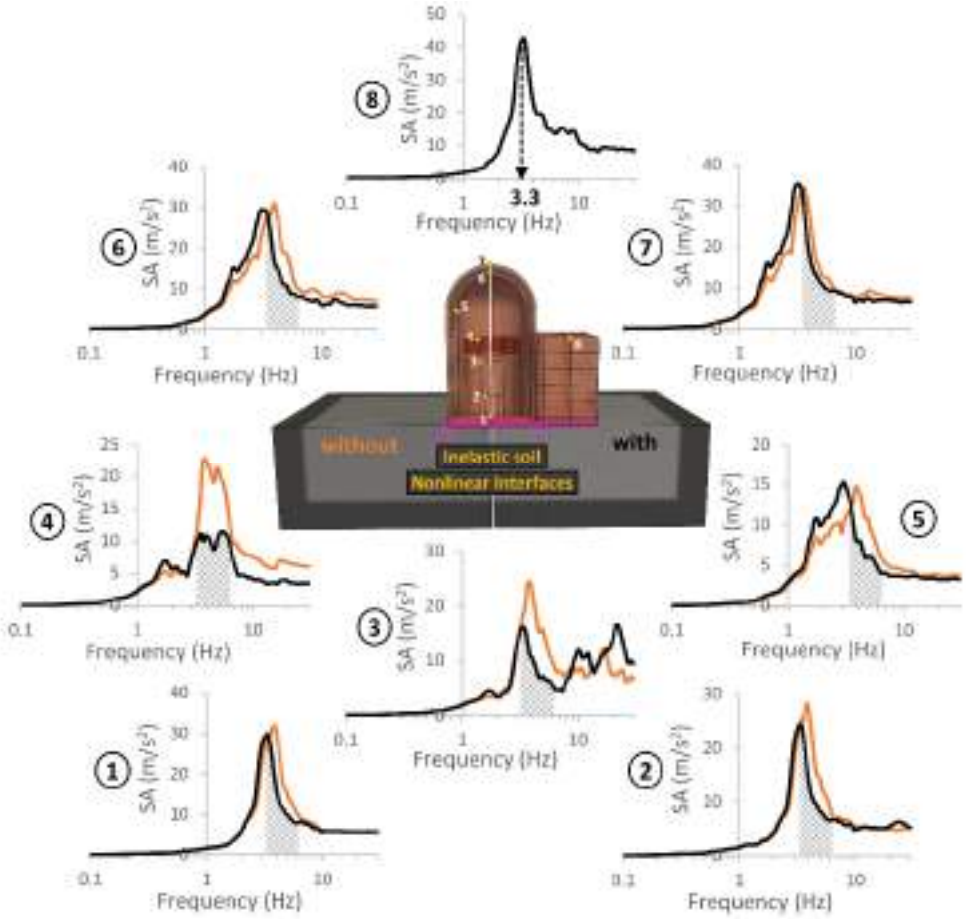

Figure 2. Nonlinear soil and nonlinear interfaces. The effect of SSSI on the response of the reactor building. Comparison of elastic horizontal acceleration response spectra SA at critical points of interest on the reactor building, "with" and "without" the auxiliary building.

3. References

[1] Jeremić, B., Jie, G., Cheng, Z., Tafazzoli, N., Tasiopoulou, P., Pisano, F., et al. (2022). The Real ESSI Simulator System. Univ California, Davis

[2] Bielak, J., Loukakis, K., Hisada, Y., Yoshimura, C. (2003). Domain reduction method for three-dimensional earthquake modeling in localized regions, part I: Theory. *Bull Seismol Soc Am*, 93:817–24. https://doi.org/10.1785/0120010251

[3] Kanellopoulos, C., Rangelow, P., Jeremić, B., Anastasopoulos, I., Stojadinovic, B. (2024). Dynamic structure-soil-structure interaction for nuclear power plants. *Soil Dyn Earthq Eng*, 181:108631, doi: https://doi.org/10.1016/j.soildyn.2024.108631

Advancing Seismic Risk Assessment: Coupled 3D Large-Scale Simulations for a More Accurate Structural Response

M. Korres[1], V. Alves Fernandes[1], I. Zentner[1], F. Voldoire[1], F. Gatti[2] and F. Lopez-Caballero[2]
[1] Electricité de France, R&D Division, Palaiseau, France
[2] Laboratoire de Mécanique Paris-Saclay, Université Paris-Saclay, Gif-sur-Yvette, France

Abstract

Seismic Probabilistic Risk Assessment (PRA) in the nuclear industry evaluates and quantifies the risks posed by earthquakes to nuclear power plants. It involves seismic hazard analysis, fragility evaluation, systems analysis, and risk quantification to ensure plant safety and resilience against seismic events. To this aim, site-specific assessment of seismic load and the impact of SSI on the structural response are key factors for accurate risk/performance estimates. Traditionally, the estimation of seismic structural response is decoupled in two separate steps: i) hazard analysis for ground motion estimation (generally defined in a single point at the site of interest), and ii) the SSI analysis based on the point-wise definition of the input. However, a limitation of this approach is related to the lack of information on the "local'' multidimensional geology in the definition of the seismic input motion, possibly highly influencing the spatial variability of the seismic GM and thus the input signal to be defined.

To address these limitations, a more realistic 3D input excitation is defined in this study based on a SEM – FEM weak coupling using the Domain Reduction Method. The examined case-study focuses on the Unit 7 Kashiwasaki-Kariwa Nuclear Power Plant reactor building during aftershocks of the 2007 Niigata Chuetsu-Oki earthquake, largely investigated thanks to the KARISMA international benchmark. The objective in this work is to demonstrate the influence of different ingredients of the large-scale earthquake simulation on the obtained ground motions and representative critical structure's response.

1. Introduction

Physics-based 3D simulations (PBS) play a key role in predicting seismic response for critical structures adhering to high safety standards and the consideration of SSI is one important factor in this context. The state-of-practice for SSI studies relies on the frequency coupling between the Finite Element Method (FEM), known for its flexibility in handling structural dynamics, and the Boundary Element Method (BEM), for computing the impedance function of stratified unbounded (soil) media. However, this engineering practice simplifies seismic input motion by assuming vertically incident plane waves and neglects possibly important effects such as wave directivity in large infrastructures and surface waves generated from local complex 3D geologies.

The aim of this work is to highlight the impact of each component of the large-scale simulation on the seismic performance of critical structures, relying on state-of-the-art numerical tools for the prediction of earthquake ground motion as well as the assessment of damage for SSCs. The proposed approach makes use of, both 3D PBS for source-to-site wave propagation to provide an accurate description of spatial variability of ground shaking and, on systemic approaches for the evaluation of advanced SSI analysis, accounting for a complex 3D input motion excitation, for the damage analysis of SSCs. The spectral element method (SEM) and FEM in time domain are used as numerical tools for the propagation on a regional and site/structural scales, respectively.

2. Source-to-site propagation

Seismic regional scale simulations using the SEM3D software are performed at first to define the 3D GM at the site of interest and at the boundaries of the SSI model. Earthquake scenarios are simulated using the Ruiz Integral Kinematic (RIK) source model [1] for two different earthquake locations, and 3 different geological profiles proposed in the literature for the Niigata region : i) Z Model, a stratified model with the presence of a folded geology at the surface, ii) R Model, a complex regional geology,

and iii) ZR model, a combination of complexity of the R model in depth and the folded geology of the Z model at the surface. Comparison of the response at surface shows a clear impact of the geological profile on the spatial variability of the observed GM (**Figure**).

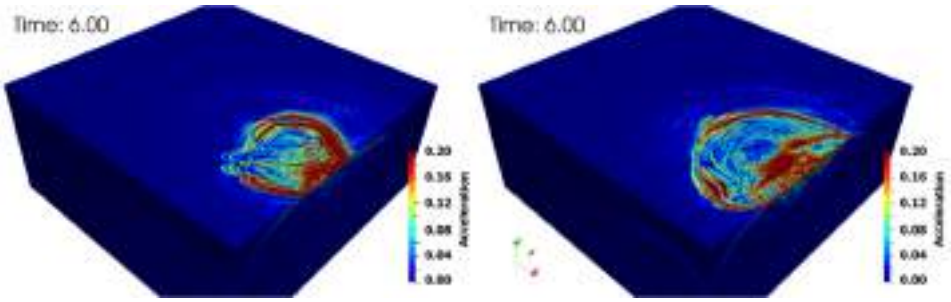

Figure 1. Comparison of the GM at the surface between two geological models: ZR (left), and R (right).

3. Structural Analysis

The link between the regional scale (SEM) and site/structure scale (FEM) is ensured by using the Domain Reduction Method (DRM) [2]. The complex 3D input motion is introduced at the boundary of the SSI model to be solved at the second step of the weak coupling procedure in the FEM framework. Numerical verification of the weak coupling is evaluated at first for a canonical case study while the implemented version allows to account for both complex regional and local geology in SEM and FEM models, via a not-honoring approach [3].

The 3D input motion previously computed for the source-to-site propagation is then introduced on the FEM model to study the dynamic response of the Unit 7 KKNPP reactor building. The state-of-art SSI based on the DRM is compared to the state-of-practice SSI approaches: i) the BEM-FEM coupling and ii) the full-FEM analysis adopting a plane wave excitation of vertical incidence. The analysis examines the dynamic response of a hypothetical electric cabinet situated at the last floor of the reactor building. Comparison is performed using the relative average mean spectral acceleration ASA_{40} as an IM for the GM at the surface and as an EDP for the dynamic response of the electric cabinet. For the same regional geological profile, numerical results (**Figure** – left) demonstrate that the complexity of the input motion plays a key role in the dynamic response of the equipment as the 3D input (DRM) provides higher values of ASA compared to the other two approaches. In a similar way, when the DRM is chosen for the SSI analysis, it is possible to demonstrate that the geological profile ZR provides a higher response compared to the other wo geological models (**Figure** – right).

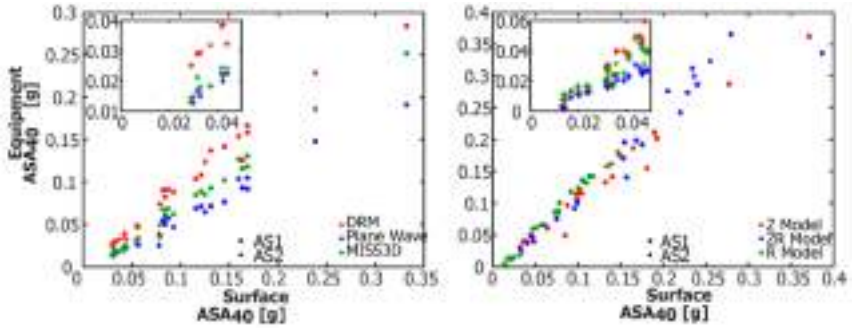

Figure 2. Average spectral acceleration (damping 5%) for the comparison of the SSI approach (left), and the influence of the geological model (right).

4. Structural Demand Hazard Curve

Given the computational cost of the 3D PBS, an optimization of the source-to-structure computation is necessary to account for uncertainties in a probabilistic framework. Synthetic Green's Functions (SGF) are developed here as a surrogate model [4] by means of the SEM simulation. The SGF, are used then to simulate a series of 100 different earthquake scenarios by modifying the RIK source

model parameters and for all three geological profiles. The case of an electric cabinet is examined once again to evaluate the influence of the SSI and the geological profile.

Numerical results are presented in terms of Complementary Cumulative Distribution Function (CCDF) of the ASA_{40} in **Figure** for the DRM approach (left) and the BEM-FEM coupling (middle). By considering a hypothetical damage level of $ASA_{40}^{Equip} = 0.5$ g related to the electric cabinet failure, the distribution of ASA_{40}^{Equip} increases with the different geological models with the ZR model presenting the higher value (25%) of CCDF, the Z Model being in the middle (12.5%) and the R Model remaining 0 for the DRM approach. Similar results are observed for the BEM-FEM approach, only in this case lower values of CCDF are observed for each model and for the same threshold of ASA_{40}^{Equip}, *i.e.*, 12.5% towards 25% (ZR model), 6% towards 12.5% (Z model) showing once again the importance of the SSI approach. Finally, **Figure** – right presented the CCDF for the ZR geological profile, the DRM approach and for the two earthquake locations AS1 and AS2, where is can be observed that for the previously defined threshold, the AS1 location provides a higher probability (25%) compared to the AS2 location (12.5%).

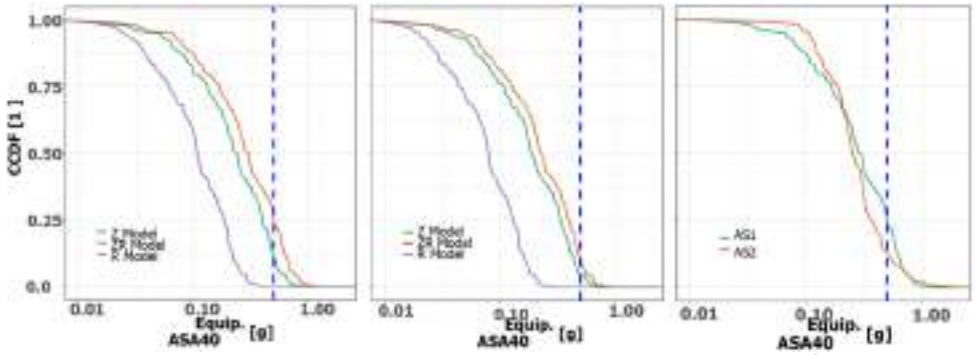

Figure 3. Complementary cumulative distribution function (CCDF) of the ASA_{40}^{Equip}: DRM approach (left), BEM-FEM approach (middle), ZR profile with DRM and for the 2 aftershock locations (right).

5. Conclusions

Coupled 3D PBS based on a SEM-FEM weak coupling and the DRM approach were used in this study to perform a source-to-structure wave propagation. The main objective of this work was to combine the multiple ingredients of the large-scale simulation and to identify the influence of each parameter on the dynamic response of the structure. In this context, the influence of the geological profile and the SSI approach are clearly identified to have major impact on the structural response.

Even though a powerful tool, it is important to keep in mind that 3D PBS necessitate a rigorous validation by comparison to real recordings, are time consuming and need an important amount of available data to be calibrated and used in a site-specific application.

6. References

[1] Gallovič, F. (2015). Modeling Velocity Recordings of the Mw 6.0 South Napa, California, Earthquake: Unilateral Event with Weak High-Frequency Directivity, *Seismological Research Letters*, vol. 87, pp. 2-14

[2] Bielak, J., Yoshimura, C., Hisada, Y., Fernández, A. (2003). Domain Reduction Method for Three-Dimensional Earthquake Modeling in Localized Regions, Part I: Theory, *Bulletin of the Seismological Society of America*, vol. 93, p. 825–840

[3] Korres, M., Lopez-Caballero, F., Alves Fernandes, V., Gatti, F., Zentner, I., Voldoire, F., Clouteau D., Castro-Cruz, D. (2022). Enhanced Seismic Response Prediction of Critical Structures via 3D Regional Scale Physics-Based Earthquake Simulation, *Journal of Earthquake Engineering*, vol. 27, p. 546–574

[4] Castro-Cruz, D., Gatti F., Lopez-Caballero, F. (2021). High-fidelity broadband prediction of regional seismic response: a hybrid coupling of physics-based synthetic simulation and empirical Green functions, *Natural Hazards*, vol. 108, p. 1997–2031

Analysis of Soil-Abutment Interaction in a Frame Bridge

R. Martini[1], A. Brunetti[1], S. Carbonari[1], F. Gara[1], F. Dezi[2] and G. Leoni[2]
[1] Università Politecnica delle Marche, Ancona, Italy
[2] Università di Camerino, Camerino, Italy

Abstract

Assessing the safety of existing bridges against vertical and seismic forces is challenging, especially for structures with unique design features and limited conceptual seismic considerations. This paper evaluates the safety of a frame bridge characterized by unconventional abutments, with struts framed into a surface foundation connected to the inclined backwall and the end cross-beam of the lateral span. The structure includes seven wing walls acting as diaphragms, forming a triangular abutment. The backfill soil within these walls acts as ballast against uplift, and the struts are supported by a rectangular concrete caisson. In detail, the work focuses on the safety assessment of the soil-foundation abutment system, addressing both soil-structure interaction and site effects on the seismic response of the system.

1. Introduction

Bridges are crucial components of roadway systems, and their damage from natural hazards can cause significant direct and indirect losses. As for the seismic risk, bridges are particularly sensitive to Soil-Structure Interaction (SSI) effects [1–3], which have to be considered in the seismic assessment. European seismic codes mandate elastic design for abutments when the deck-abutment interaction is limited to the vertical direction, but when shear forces are transmitted by the deck, the limited ductile capacity of the soil-foundation abutment system necessitates the inclusion of SSI in the analysis, with particular focus on the abutment-backfill interaction effects [4]. Analyzing SSI for geotechnical systems is challenging due to factors like backfills, mixed foundation types, soil slope and approaching embankments. While Finite Element Models (FEM) can address these complexities comprehensively, they are computationally demanding. The substructure method [5] offers a more efficient approach by separating kinematic and inertial effects.

This study uses a method developed by the authors to assess the seismic soil-foundation-abutment response of an existing frame bridge. The method considers SSI and site amplification, taking into account both the stratigraphic and topographic conditions of the soil. The abutment is treated as rigid, with the soil responding elastically, though soil nonlinearity from seismic wave propagation can be included by adopting an iterative linear equivalent approach that adjust the soil properties to reflect its nonlinear response under seismic loading.

2. Overview of the adopted approach

Considering all contributions from the foundation, abutment, and tributary masses of the deck, the following balance equilibrium equation can be written for the soil-foundation-abutment system:

$$\{\mathfrak{J}(\omega) - \omega^2 \mathbf{M}_{\mathrm{SFA}}\}\boldsymbol{\delta}_0(\omega) = \mathfrak{J}(\omega)\boldsymbol{\delta}_{\mathrm{FIM}}(\omega) \tag{1}$$

where

$$\mathbf{M}_{SFA} = \left[\sum_{i=1}^{N} \mathbf{A}_i^T \begin{bmatrix} \mathbf{R}_i & \mathbf{0} \\ \mathbf{0} & \mathbf{R}_i \end{bmatrix}^T \begin{bmatrix} m_i \mathbf{I}_3 & \mathbf{0} \\ \mathbf{0} & \mathbf{T}_i \end{bmatrix} \begin{bmatrix} \mathbf{R}_i & \mathbf{0} \\ \mathbf{0} & \mathbf{R}_i \end{bmatrix} \mathbf{A}_i + \sum_{j=1}^{D} \mathbf{A}_j^T \begin{bmatrix} \mathbf{M}_j & \mathbf{0} \\ \mathbf{0} & \mathbf{0} \end{bmatrix} \mathbf{A}_j \right] \tag{2a}$$

$$\boldsymbol{\delta}_0(\omega) = \begin{bmatrix} \mathbf{u}_0 \\ \boldsymbol{\varphi}_0 \end{bmatrix} \tag{2b}$$

$$\boldsymbol{\delta}_{FIM}(\omega) = \begin{bmatrix} \mathbf{u}(\omega) \\ \boldsymbol{\varphi}(\omega) \end{bmatrix}_{FIM} \tag{2c}$$

are the mass matrix of the soil-foundation-abutment-deck system, the vector of the system displacements and the known vector of the Foundation Input Motion (FIM), respectively. In equation (2a), N is the number of the structural elements in which the soil-foundation system has been divided and D is the number of bridge deck supports at the abutment. In addition, $\mathbf{A}_i$ and $\mathbf{R}_i$ are geometric and rotational matrices, respectively, necessary to address the problem with respect to a global reference system frame, m_i and $\mathbf{T}_i$ are mass and inertia tensor, and $\mathbf{M}_j$ is the mass matrix of the deck tributary mass.

3. The frame bridge

The bridge spans approximately 140 m and features a V-strut frame with a statically determinate scheme composed by two edge cantilever spans supporting a central suspended span with half-joints (Figure a). The suspended span has two fixed supports at one cantilever frame (Abutment A) and two steel rollers at the other one (Abutment B). The restraint layout ensures that transverse seismic forces are equally distributed to both abutments, while the overall longitudinal inertia forces are transferred to Abutment A, which is the most stressed one. Each abutment has a 45° inclined backwall, connecting the deck end box girder diaphragm of the lateral span to the concrete footing. This structure includes a 1 m thick horizontal concrete slab and seven vertical post-tensioned tendons embedded into concrete ties, connecting the horizontal slab to the deck end diaphragm. In the longitudinal direction, the abutments are stiffened by seven orthogonal ribs forming a pseudo-triangular shape (Figure b). The backfill soil within the wingwalls acts as ballast to counteract uplift of the side spans. Each abutment footing is embedded into a rectangular caisson foundation (9.50 × 25 m, 15 m deep). The riverside abutment foundation is unconfined due to the site's morphology. The soils within the volume of interest for the abutment foundation structures primarily belong to the “Laga Formation”, a massive arenaceous geological unit. Based on geophysical investigations, the foundation rock substrate was modelled into four main horizons (Figure a) with mechanical and dynamic parameters provided in Figure a.

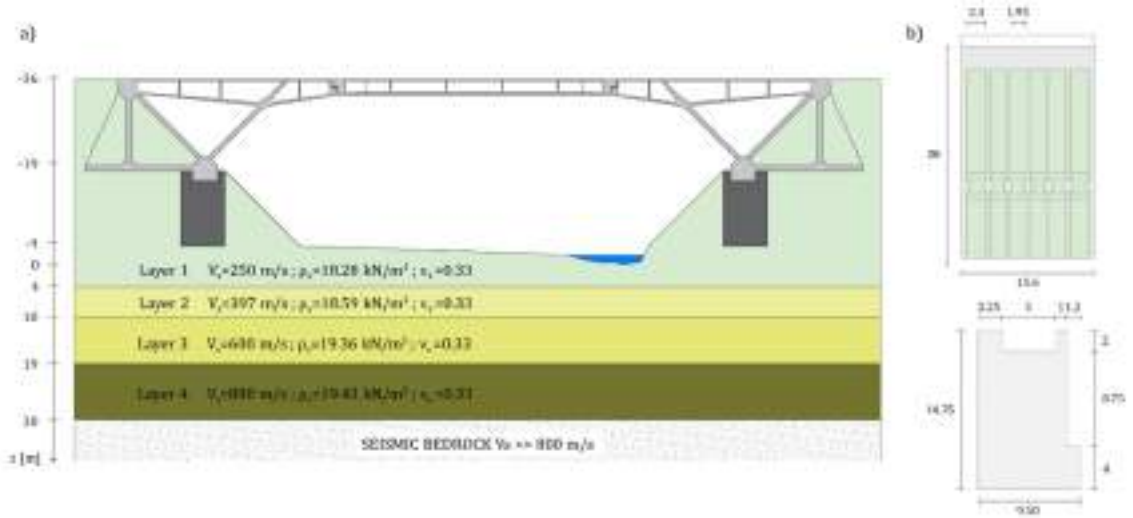

Figure 1. (a) Lateral view of the bridge and soil properties; (b) geometry of the abutment, in meter.

4. Analysis of the soil–foundation-abutment system

Analyses of the abutment were performed using different simplifying assumptions, besides the rigorous approach introduced above (SSI-Rigorous Model). These include the Fixed Base assumption (FB Model) and the simplification of equating free-field motion to the FIM (SSI-Simplified Model).

Due to the site morphology and the unconventional geometry of the abutment-foundation system, a refined 3D FEM was required to evaluate the soil-foundation impedances and the FIM. The soil was modeled in ANSYS [6] using 8-node solid elements with visco-elastic properties in the frequency domain, imposing a rigid soil-foundation interface using the multi-point constraint method.

Ten real accelerograms were selected and scaled to match the Eurocode 8 [7] seismic response spectrum for a return period T_R=2475 years, soil category E, with a PGA of 0.374 g for site category A and a topography amplification factor of 1.20 to account for the soil topography. Figure summarizes seismic analysis results, presenting maximum base shears and moments for each model and seismic action with color-coded bar charts: black for FBM, grey for SSI-SM, and blue for SSI-RM. Figure a refers to the transverse directions, while Figure b refers to the longitudinal direction. In the transverse direction, the soil-structure coupling generates significant moments in the foundation around the *y* and *z* axes, in addition to the shear forces. In the longitudinal direction, moments around the *z* axis and vertical shear forces are observed. These couplings, absent in FBM, are essential for an accurate seismic assessment. The comparisons indicate that neglecting the FIM can lead to an underestimation of the actions at the foundation level.

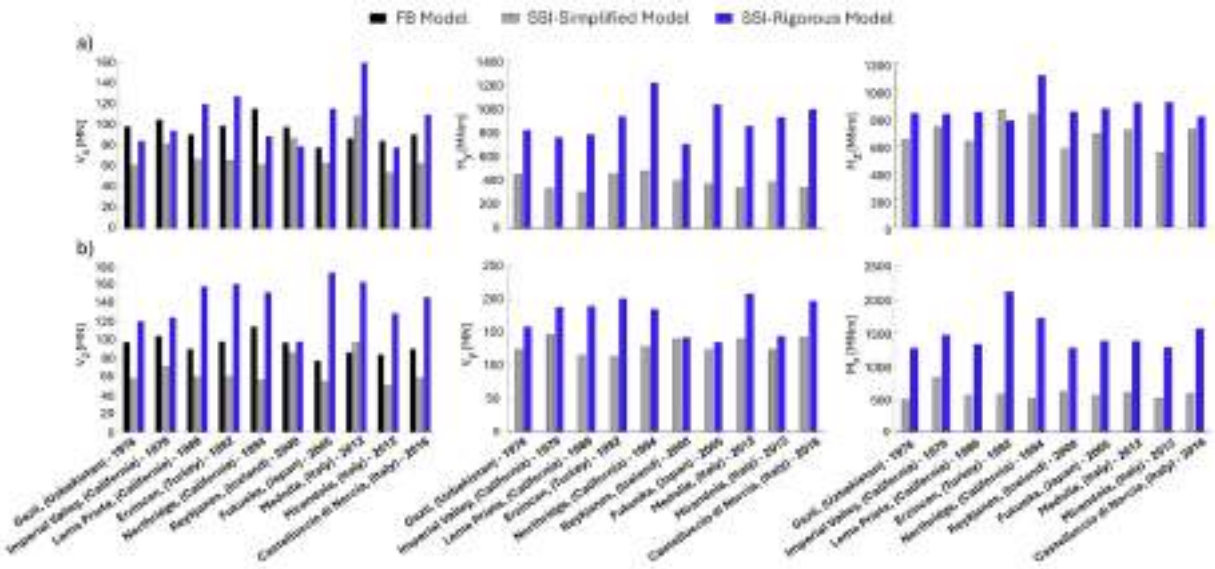

Figure 2. Maximum values of the base reactions from the (a) transverse and (b) longitudinal analyses.

5. References

[1] Spyrakos, C., Loannidis, G. (2003). Seismic behavior of a post-tensioned integral bridge including soil–structure interaction (SSI), *Soil Dyn. Earthq. Eng.*, 23, 53–63

[2] Jeremić B., Kunnath, S., Xiong, F. (2004). Influence of soil–foundation–structure interaction on seismic response of the I-880 viaduct, *Eng. Struct.*, 26, 391–402

[3] İmamoğlu, Ç., Dicleli, M. (2024). Effect of dynamic soil-structure interaction modeling assumptions on the calculated seismic response of railway bridges with single-column piers resting on shallow foundations, *Soil Dyn. Earthq. Eng.*, 181, 108624

[4] European Committee for Standardization (CEN), EN 1998-5 Eurocode 8: Design of structures for earthquake resistance – Part 5: Foundations, retaining structures and geotechnical aspects (2004)

[5] Wolf, J.P. (1985). Dynamic soil-structure interaction, Prentice-Hall, Englewood Cliffs, N.J

[6] ANSYS Inc. (2023). ANSYS Mechanical version 2023 R2 User's Guide

[7] European Committee for Standardization (CEN), EN 1998-2 Eurocode 8: Design of structures for earthquake resistance – Part 2: Bridges, (2004)

Workflow for High-Fidelity Dynamic Analysis of Structures with Pile Foundation

Pedro Arduino[1] and Amin Pakzad[1]
[1] University of Washington, Seattle, WA, United States

Abstract

The increasing demand for high-fidelity soil-structure interaction simulations highlights the need for a standardized workflow. This paper introduces a step-by-step guideline for dynamic analysis of pile foundations, incorporating the Domain Reduction Method for efficient loading, Perfectly Matched Layer elements for wave absorption, Embedded Interface elements for soil-structure interaction, and domain decomposition for optimized processing. Numerical simulations demonstrate the workflow's effectiveness: DRM reduces simulation size without loss of fidelity, PML elements accurately model infinite domains, and Embedded Interface elements efficiently connect structures and soil. Although the study focuses on simplified scenarios, it provides a foundation for future research on more complex structures and loading conditions.

1. Problem Statement

The increasing demand for high-fidelity numerical simulations in soil-structure interaction analysis has highlighted the need for a standardized workflow. Despite the widespread use of finite element simulations in these analyses, no comprehensive guidelines exist to assist in the creation of such simulations for common structures, particularly those involving pile foundations. This study aims to fill this gap by proposing a detailed workflow for the dynamic analysis of structures with pile foundations, focusing on reducing computational complexity while maintaining model fidelity.

2. Scope of Work

The proposed workflow utilizes various methodologies necessary for high-fidelity dynamic simulations. Key components include:

Domain Reduction Method (DRM): This technique integrates earthquake sources efficiently by simplifying the seismic wavefield. It uses a two-stage process: first, a large-scale simulation captures the broad wavefield and seismic forces, then a reduced domain focuses on the structure's surroundings, applying these forces for detailed analysis. This approach reduces computational load and enhances accuracy by concentrating resources on critical areas [1].

Perfectly Matched Layer (PML): A key challenge in finite element analysis is converting an infinite domain to a finite one, which can cause boundary reflections and distorted results. The Perfectly Matched Layer (PML) method addresses this by surrounding the domain with a layer that absorbs outgoing waves, preventing reflections. By matching the layer's properties with the surrounding material, PML reduces computational load while maintaining accuracy[2]. Figure 1-a shows the PML element schematic.

Embedded Interface Elements: Accurate modeling of pile-soil interactions is crucial for realistic pile foundation simulations. Traditional methods require extensive mesh refinement, increasing computational demands. Embedded Interface Elements simplify these interactions by using soil displacement interpolation to model pile displacement and enforce compatibility based on virtual work principles. This approach reduces computational costs while maintaining accuracy, making it ideal for large-scale dynamic analyses [3]. Figure 1-b illustrates the embedded interface element.

Domain Decomposition: Despite the efficiencies of DRM, PML, and Embedded Interface Elements, high-fidelity simulations require substantial computational resources. Domain Decomposition improves feasibility by distributing the workload across multiple processors. By dividing the domain

into subdomains—Regular (soil and structure), DRM (force generation), PML (wave absorption), and, if necessary, Embedded Interface Elements—parallel processing reduces runtime and makes complex simulations more manageable.

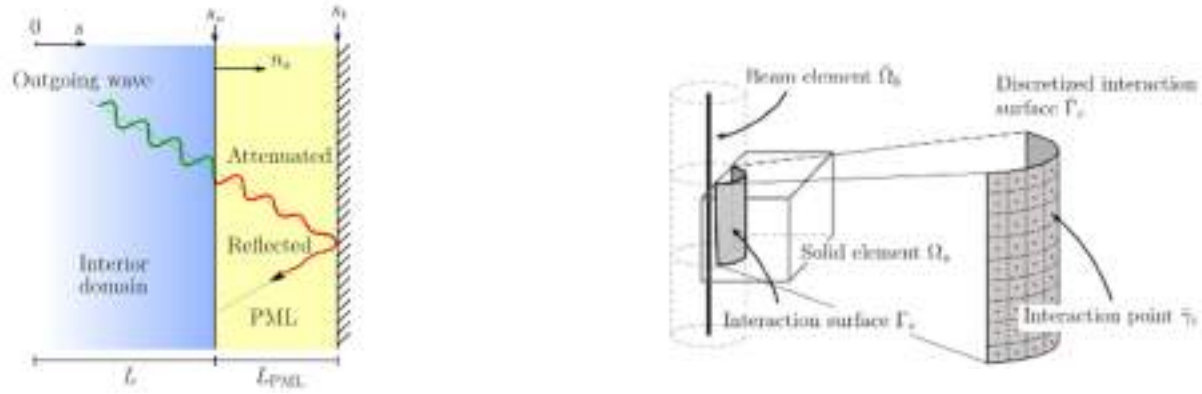

a) PML element [2] b) Embedded Interface element [3]

Figure 1. Schematic of PML and Embedded interface elements.

3. Findings

In this study, the workflow was tested through various examples to evaluate different aspects of its performance. Figure 2 shows one of the models used in this analysis and the result shows the difference when using PML layers around.

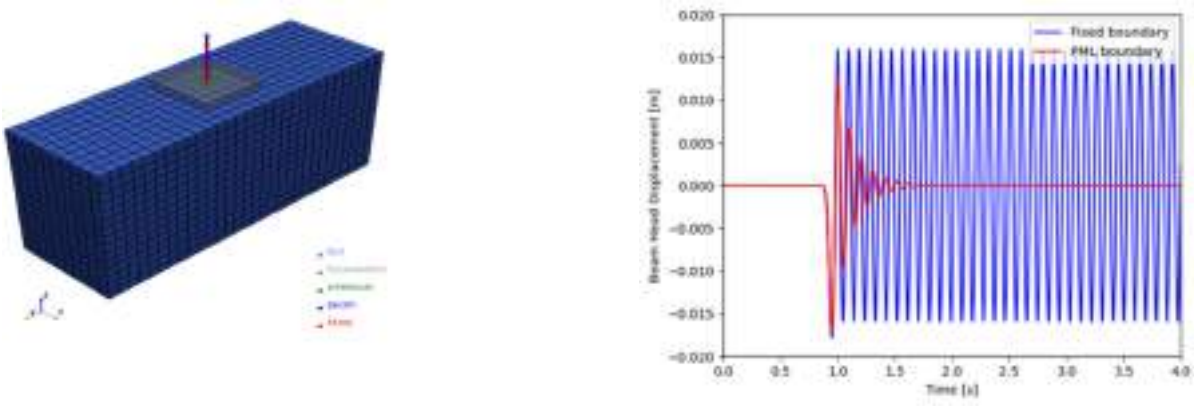

Figure 2. Effect of Perfectly Matched Layer (PML) on model accuracy by absorbing outgoing waves and reducing boundary reflections.

The numerical simulations highlighted its effectiveness in high-fidelity dynamic analyses with optimized computational efficiency with some key findings:

1. Efficiency of Domain Reduction Method (DRM): The DRM was effective in reducing the computational size of the simulations without compromising the essential features of the model. This approach facilitated a more focused analysis on the structure's immediate surroundings, capturing the necessary details of the seismic response.

2. Accuracy of Perfectly Matched Layer (PML) Elements: The PML elements successfully absorbed outgoing waves, thereby modeling the infinite domain accurately. This resulted in improved simulation fidelity, especially in scenarios involving significant wave reflections.

3. Effectiveness of Embedded Interface Elements: These elements proved to be efficient in modeling the soil-pile interaction, allowing for accurate simulations without the need for extensive mesh refinement. This not only reduced computational demands but also enhanced the precision of the interaction modeling.

4. Feasibility of High-Fidelity Simulations: The overall workflow demonstrated its effectiveness in conducting complex, high-fidelity simulations. The use of domain decomposition and parallel computing further ensured that large-scale models could be simulated within a feasible timeframe.

4. Conclusion

This study presents a comprehensive workflow for high-fidelity dynamic analysis of structures with pile foundations, integrating advanced techniques such as DRM, PML, Embedded Interface Elements, and Domain Decomposition. The workflow has proven effective in reducing computational costs while maintaining high accuracy in the simulations. While the current study focuses on simplified structural configurations and loading scenarios, the findings lay the groundwork for future research involving more complex structures and dynamic conditions, paving the way for standardized practices in soil-structure interaction analysis.

5. References

[1] Bielak, J., Yoshimura, C., Hisada, Y., Fernández, A. (2003). Domain reduction method for three-dimensional earthquake modeling in localized regions, Part I: theory, *Bulletin of the Seismological Society of America*, 93 (2): 825–40, doi: 10.1785/0120010251

[2] Fathi, A., Poursartip, B., Kallivokas, L. F. (2015). Time-domain hybrid formulations for wave simulations in three dimensional PML-truncated heterogeneous media, *International Journal for Numerical Methods in Engineering*, 101(3):165-98

[3] Ghofrani, A. (2018). Development of Numerical Tools For the Evaluation of Pile Response to Laterally Spreading Soil, PhD thesis, University of Washington

3D modeling of masonry tower soil-structure interaction in OpenSees using mixed implicit-explicit material integration

Onur Deniz Akan*[1], Massimo Petracca[2], Guido Camata[2,3], Carlo G. Lai[4,5], Enrico Spacone[3] and Claudio Tamagnini[6]

[1] *University School for Advanced Studies IUSS Pavia, Pavia, Italy*
[2] *ASDEA Software Technology, Pescara, Italy*
[3] *University G. D'Annunzio of Chieti-Pescara, Pescara, Italy*
[4] *University of Pavia, Pavia, Italy*
[5] *European Centre for Training and Research in Earthquake Engineering, Pavia, Italy*
[6] *University of Perugia, Perugia, Italy*

Abstract

This study aims to elucidate the possible relationship between foundation deformations and structural cracking, as well as to identify sources of hysteretic energy dissipation within the SSI of shallow-founded masonry structures. A virtual SSI laboratory has been developed by modeling the St. Maria Maggiore Cathedral's bell tower in the town of Guardiagrele, Italy. Analyses reveal that the foundation ratcheting can influence the accelerations experienced by the structure, presenting a trade-off between foundation deformations and structural damage. Increased plastic response in the foundation soil may mitigate structural response, and conversely, reduced foundation deformations may result in increased structural damage.

1. Introduction

Unreinforced masonry (URM) towers are part of the historical heritage and were often constructed as security structures or bell towers during the Renaissance period. They can be found as standalone edifices or as components of larger architectural complexes. The inherent brittleness of masonry renders tower structures particularly hazardous, as collapses can occur without warning and lead to catastrophic results.

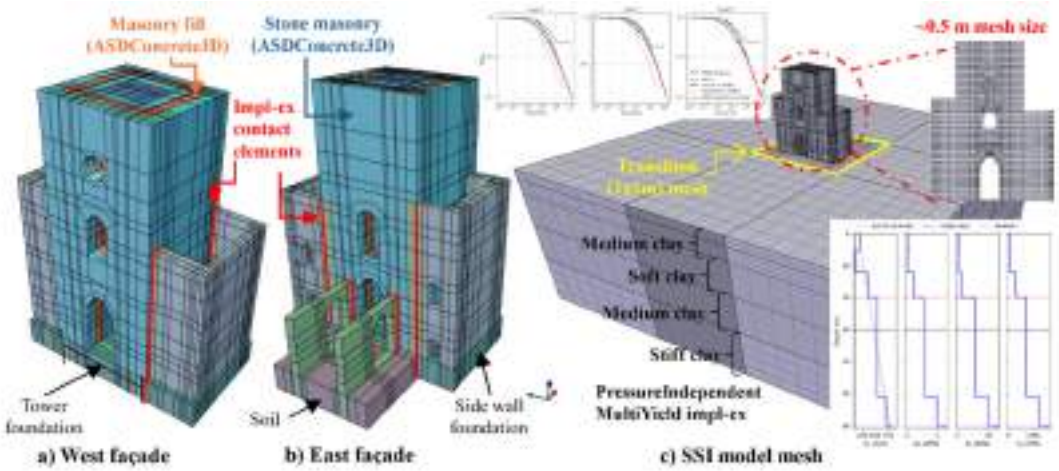

Figure 1. The virtual laboratory in STKO. The material distribution: a) West facade, b) East facade, and c) The meshed view of the SSI model: The soil profile and the G/Gmax curves for each layer.

The mechanisms that lead to the damage and collapse of masonry towers are still an open research question and require studying complex material, geometric, and interaction nonlinearities. Over the years, the numerical investigation of various URM tower systems has received increasing attention from researchers [1]. The modeling of direct soil-structure interaction (SSI) for large structures and

foundation size effects [2], indicates that SSI effects may significantly alter the response of stiff structures due to soil amplification, kinematic, or the inertial effects of an oscillating heavy body.

This study investigates the combined effect of cyclic damage-plasticity behavior in the masonry structures (i.e., the period shift) and stiffness reduction in the foundation soil on the system response. To achieve this, a virtual laboratory is prepared in OpenSees with the help of the STKO pre-processor. The bell tower and the cathedral of Guardiagrele are modeled considering the underlying soil profile up to the bedrock, the nonlinear material characteristics, and the pounding interaction between the bell tower and the church walls. A novel impl-ex contact element and the impl-ex version of the pressure-independent soil material are implemented in OpenSees to make the computation feasible and control the computational cost of running multiple analyses.

2. The modeling of the virtual laboratory

The structure is modeled with 8-node brick solid elements and consists of four separate bodies: the bell tower, the north and south church walls, and the rear church walls. Individual bodies are put in contact with each other using node-to-node ZeroLengthContactASDimplex elements. Contact elements model contact-separation and stick-slip behavior between these bodies during dynamic analysis using a highly stable impl-ex Mohr-Coulomb law [3]. The stone masonry and the fill materials are modeled using the ASDConcrete3D damage-plasticity material [4] (Figure 1). The capabilities of this model include tension-compression damage, fracture energy regularization and impl-ex integration. The soil behavior is modeled with the kinematic hardening PIMY material [5]. The undrained strength of layers is computed as a linear function of the undrained Young's modulus. Finally, the stress-strain backbone is calibrated to match the shear modulus reduction characteristics proposed by Vucetic and Dobry. The mesh size at the structure level is around 0.5m, whereas the soil mesh is tuned to capture a vertically propagating wave with a maximum frequency of 18 Hz. The foundation soil consists of 1x1x1m elements to prevent any size effects. The mismatching meshes are tied to each other using ASDEmbeddedNode elements. The model has around 240,000 elements and is solved in parallel using 24 partitions in OpenSeesMP.

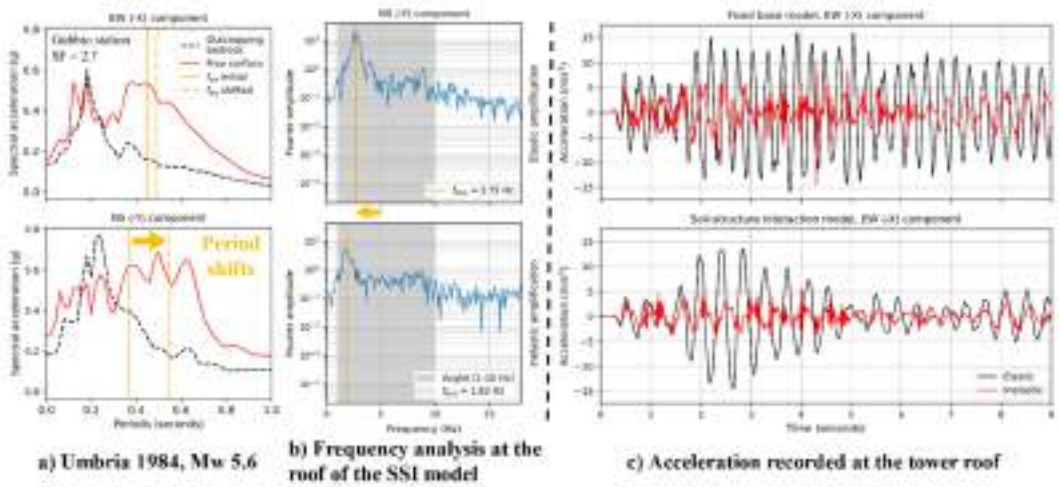

Figure 23. Dynamic response of the bell tower SSI system. a) The input and the amplified motion response spectra. b) Computed system frequency shift (N-S). c) Fixed base versus SSI roof accelerations.

3. Effect of foundation soil nonlinearity on the masonry damage pattern

The input motion is applied at the model base as force history in the SSI model, whereas the surface acceleration history is applied at the fixed base model (Figure 2a). As a result of impl-ex materials, the solution always converges in two iterations. The results do not change significantly after decreasing the time step beyond the 1/4th of the seismic record sampling step.

In Figure 2c, the difference between the roof accelerations recorded in the fixed and SSI models is attributed to the two models' different fundamental periods, which are 0.29s and 0.44s for the EW direction, respectively. The SSI period is a result of elastic foundation rocking. In the fully linear model, the recorded roof displacements strongly match the foundation rotation angle times the tower height. Hence, the SSI behavior is chiefly governed by the foundation rotations with limited contributions from structural modes.

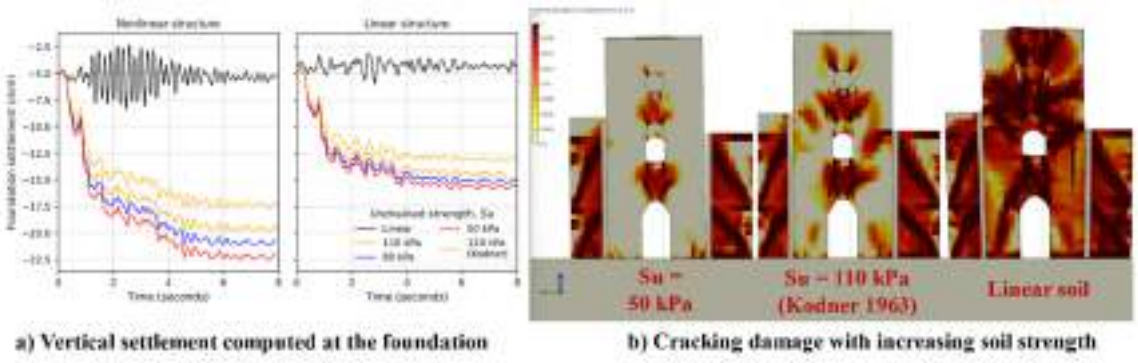

Figure 4. The effect of soil strength and stiffness reduction on a) foundation settlements and b) cracking damage. Moreover, structural nonlinearities lead to increased foundation deformations.

The detrimental effect of increasing soil strength is shown in Figure 3. However, the rate of stiffness reduction is the primary contributing factor. This is proved by comparing the “110kPa” curves in which the stiffness reduction is provided with a reduced rate in the default (Kodner) PIMY soil (Figure 1c). Finally, the nonlinear structure leads to increased settlements due to the shift in the fundamental period. This is due to softening in the foundation material and increased structural response. In Figure 2a, the structure NS initial period shifts towards amplified ranges once the cracking damage accumulates. The increased structural response amplifies settlements.

4. Conclusions

The foundation rotation in shallow-founded towers is identified as a significant factor determining the fundamental period of an SSI system. Furthermore, the rate of stiffness reduction in the foundation soil is shown to affect the damage patterns of a masonry tower. Finally, the inelastic period shift may trigger increased foundation response based on the spectral shape of the input motion.

5. References

[1] Rosell, L. A. (2010). Explicit / Implicit Nonlinear Soil Structure Interaction Study of the Bell Tower of Santa Maria Maggiore, Guardiagrele, Istituto Universitario di Studi Superiori di Pavia

[2] Bullock, Z., Dashti, S., Karimi, Z., Liel, A., Porter, K., Franke, K. (2019). Probabilistic Models for Residual and Peak Transient Tilt of Mat-Founded Structures on Liquefiable Soils, *J. Geotech. Geoenvironmental Eng.*, vol. 145, no. 2, p. 04018108, doi: 10.1061/(asce)gt.1943-5606.0002002

[3] Oliver, J., Huespe, A. E., Cante, J. C. (2008). An implicit/explicit integration scheme to increase computability of non-linear material and contact/friction problems, *Comput. Methods Appl. Mech. Eng.*, vol. 197, no. 21–24, pp. 1865–1889, doi: 10.1016/j.cma.2007.11.027

[4] Petracca, M., Camata, G., Spacone, E., Pelà, L. (2022). Efficient Constitutive Model for Continuous Micro-Modeling of Masonry Structures, *Int. J. Archit. Herit.*, vol. 0, no. 0, pp. 1–13, doi: 10.1080/15583058.2022.2124133

[5] Gu, Q., Conte, J. P., Yang, Z., Elgamal, A. (2011). Consistent tangent moduli for multi-yield-surface J2 plasticity model, *Comput. Mech.*, vol. 48, no. 1, pp. 97–120, doi: 10.1007/s00466-011-0576-7

A thermodynamic standpoint for enhancing soil-structure systems

***D. N. Gorini*[1]**
[1] *University of Trento, Trento, Italy*

Abstract

In this study the foundation soil, the structure and additional protection devices are regarded as a hazard resistant unicum against natural hazards. Factors governing the dynamic problem are pointed out and handled through a macroscopic use of the Laws of Thermodynamics. To this end, a Generalised Thermodynamic-based Inertial Macroelement (TIMg) is proposed as a unified framework to simulate the nonlinear & frequency-dependent multiaxial response of geotechnical systems in structural analysis. The application of the TIMg from the scale of the single structure to territorial assessment shed light on critical components of code-conforming infrastructures under seismic or wind loading. Hazard resistant solutions have been developed accordingly, for optimal control of inertia and dissipation of the entire soil-structure layout.

1. Balancing complexity and accuracy: the TIMg standpoint to structural analysis

Under dynamic loading, significant inertial forces can develop in the soil interacting with a foundation (*participating soil*), that control its frequency-dependent features [1-3]. The resulting dynamic amplification of the geotechnical system (foundation + participating soil) produces complex load patterns exchanged with the superstructure exalting irreversible effects in the whole system [4]. Modelling these effects still requires numerical representations of the entire layout with refined description of the behaviour at the micro/meso-scale, which can be warranted only for specific cases due to the related complexity and computational burden.

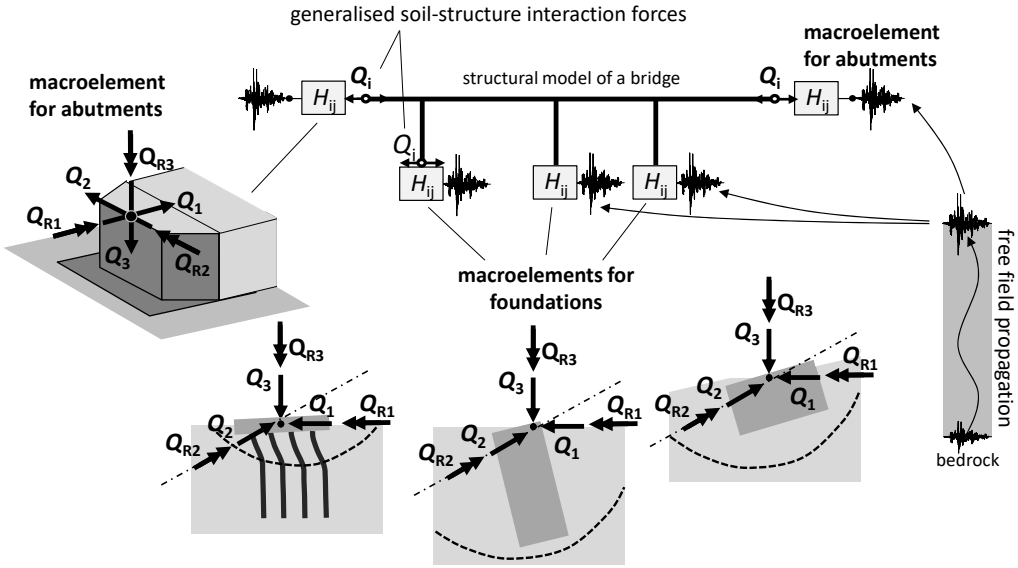

Figure 1. Application of the TIMg in the seismic analysis of structures.

A macroscopic standpoint is therefore proposed, as a convenient balance between complexity and reliability of numerical modelling. It consists of a Thermodynamic Inertial Macroelement (TIMg) [5] extending the original TIM approach [2,3] to a unified formulation able to describe the macroscopic response of a broader class of systems, namely: shallow, piled, monopile and caisson foundations, semi-integral and integral seat- or cantilever-type bridge abutments, resting on shallow or deep foundations. The TIMg lumps the nonlinear and frequency-dependent multiaxial response of the systems above into a single relationship between the generalised forces Q_i exchanged at the

foundation-superstructure contact and the corresponding displacements and rotations q_i, such that $Q_i=H_{ij}q_j$ (global degrees of freedom *i,j* taken as in Fig. 1). The tangent stiffness matrix, H_{ij}, is derived through a thermodynamic framework defined by potential functions, according to the multi-surface plasticity theory with hardening. The TIMg is available in the open-source analysis framework OpenSees [6] and can be used in structural analysis following the procedure in Fig. 1, corresponding to earthquake loading: the free-field motion represents the seismic input for the TIMg; the latter is included in the global structural model to carry out nonlinear dynamic analyses.

2. Seismic assessment at the territorial scale

By virtue of the residual computational demand, the TIM and TIMg approaches have being increasingly employed to simulate the performance of soil-structure systems. For instance, this was the case of a regional-scale assessment of the seismic reliability of Italian code-conforming bridges [7]. Many 3D soil-bridge models were developed with the aim of detecting vulnerable components in typical layouts. For instance, consider an archetype tall viaduct located in the earthquake-prone L'Aquila region (Italy), resting on five supports with piled foundations. The subsoil belongs to Category C (EN 206-1), has a friction angle between 24° and 26° and a cohesion of 10 kPa.

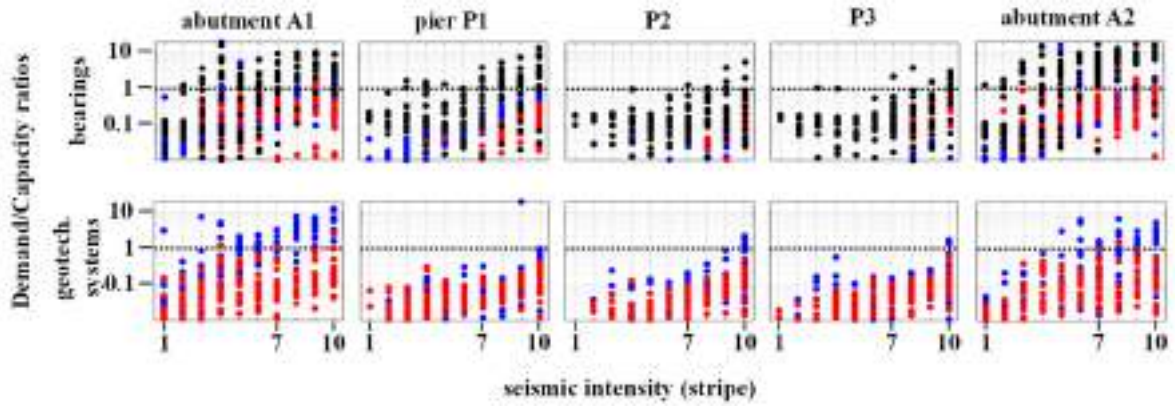

Figure 2. Severe-damage Demand/Capacity ratios for the deck bearings and the geotechnical systems in the longitudinal (in blue), transverse (in red) and vertical (in black) directions, varying the seismic intensity.

The performance of the bridge subjected to 200 spectrum-compatible seismic records is illustrated in Figure 2, in terms of the Demand-over-Capacity ratio for the Severe Damage performance level of the most vulnerable components, which were found to be the deck bearings and the geotechnical systems. Critical mechanisms (D/C>1) occur from stripe No. 5, before the seismic intensity corresponding to the Life-safety Limit State (NTC 2018). Critical mechanisms consist of the attainment of the capacity in the bearings and in the foundation piles of the abutments.

3. Soil-driven hazard resistant structures

The identification of critical performances has led to the development of so-called inertia-control geotechnical systems maximising the resilience of buildings and bridges against natural hazards. These solutions concern piled foundations, bridge abutments, and isolated shallow footings [8-10], with optimal design criteria devised by the aid of artificial intelligence.

As an example, inertia-control geotechnical systems were used for the bridge in Section 2 [8-10]. The bridge model with the new TIMg was subjected to a three-component seismic motion representing a Near-Collapse earthquake scenario. The performance is illustrated in Figure 3 in terms of the shear force-drift relationships of the bearings and the force-deformation responses of the geotechnical systems in the longitudinal direction. Compared to the standard layout (in black), the inertia-control systems (in red) reduce permanent deformations and forces in the geotechnical systems, as the dissipative layers included in the foundation soil (red lines in the top images of Fig.

3) limit soil inertia exalting concurrently energy dissipation. Consequently, this mitigates the displacement/ductility demand for the bearings (dashed lines in Fig. 3 are the respective capacities).

Balancing inertia and dissipation of the whole soil-structure system can therefore improve significantly the resilience of structures under dynamic loading. These considerations are currently being extended to different structural typologies and interacting hazard scenarios of different nature.

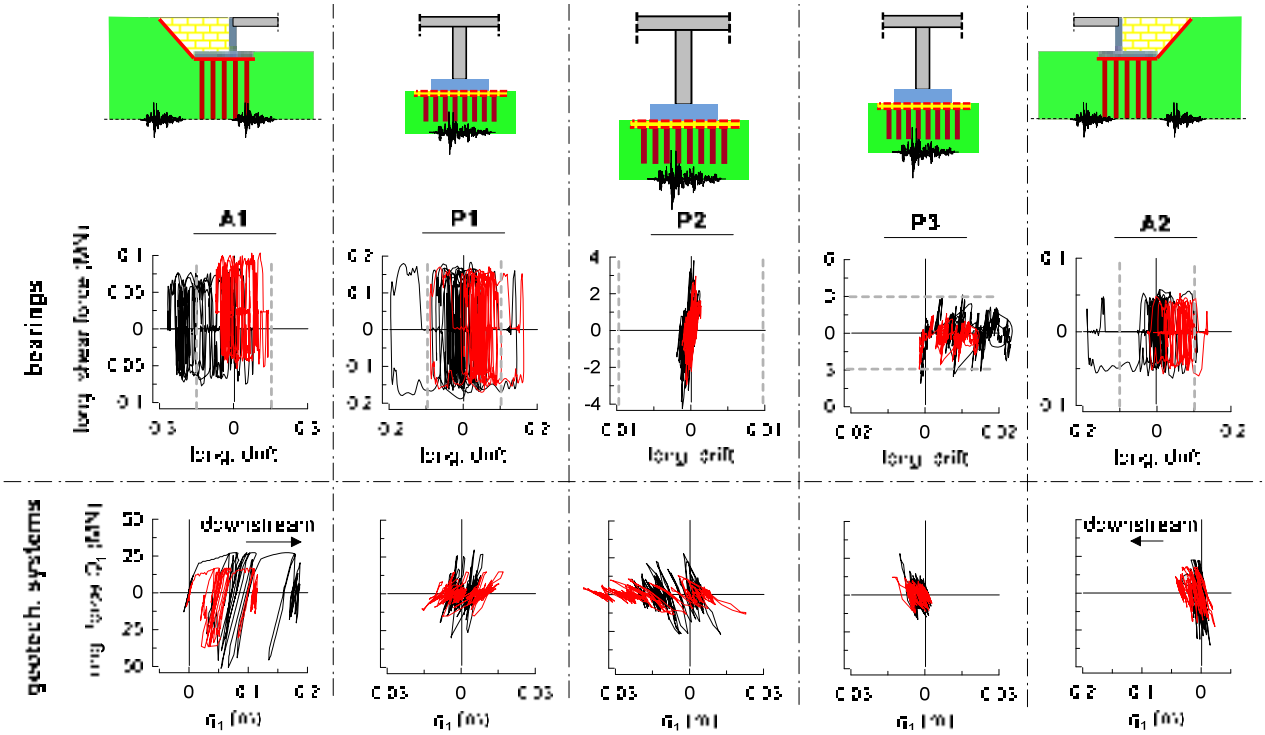

Figure 3. Longitudinal force-deformation relationships for the deck bearings and the geotechnical systems of all supports of the reference bridge (in black) and of the one with inertia-control supports (in red).

4. References

[1] Paolucci, A., Pecker, A. (1997). Soil inertial effects on the bearing capacity of rectangular founda-tions on cohesive soils, *Eng. Struct.*, 19(8), 637-643

[2] Gorini, D.N., Callisto, L., Whittle, A.J., Sessa, S. (2023). A multiaxial inertial macroelement for bridge abutments, *Int. J. Numer. Anal. Methods Geomech*, 47(5), 793-816

[3] Gorini, D.N., Callisto, L. (2023). A multiaxial inertial macroelement for deep foundations, *Computers and Geotechnics*, 155, 105222

[4] Gorini, D.N., Callisto, L., Whittle, A.J. (2022). An inertial macroelement for bridge abutments, *Geotechnique*, 72(3), 247-259

[5] Gorini, D.N. (2024). A unified thermodynamic-based macroelement approach, Submitted to *Acta Geotechnica*

[6] McKenna, F., Scott, M.H., Fenves, G.L. (2010). Nonlinear finite-element analysis software architecture using object composition, *Journal of Computing in Civil Engineering*, 24(1), 95-107

[7] Franchin, P., et al. (2023). Seismic reliability of Italian code-conforming bridges, *Earthq Eng Struct Dyn*, 52(14), 4442-4465, doi: 10.1002/eqe.3958

[8] Gorini, D.N., Whittle A.J., Callisto, L. (2020). Ultimate limit states of bridge abutments, *J. Geotech. Geoenviron.*, 146(7), doi: 10.1061/(ASCE)GT.1943-5606.0002283

[9] Gorini, D.N., Callisto, L. (2019). Seismic performance and design approach for friction dissipative foundations, *Soil Dyn Earthq Eng*, doi: 10.1016/j.soildyn.2019.05.006

[10] Gorini, D.N., Callisto, L. (2023). Effect of the failure mode on the macro-response of pile groups, *10th NUMGE*, doi: https://doi.org/10.53243/NUMGE2023-220

Nonlinear 3D Soil-Structure Dynamic Interaction Modelling for Railway Tracks

J.N. Varandas Ferreira [1]
[1] *CERIS, Faculdade de Ciências e Tecnologia da Universidade NOVA de Lisboa, Lisboa, Portugal*

Abstract

The dynamic response of railway systems may involve complex interactions between moving vehicles, track superstructure, and continuous foundations, embodying a typical soil-structure interaction problem. Accurately modeling these interactions often requires constructing large-scale, three-dimensional models, and the consideration of nonlinear behaviors such as the response of geomaterials or the wheel-rail contact. To address these challenges, a three-dimensional finite element method program, *Pegasus*, was fully coded in MATLAB. *Pegasus* incorporates several computational optimizations to enhance efficiency, such as reconstructing the large stiffness matrix during simulations, using a mixed implicit-explicit solver, and managing memory effectively. The capabilities of Pegasus are demonstrated through simulations of trains passing over tracks with inhomogeneous support at various speeds. Each dynamic simulation is completed in under an hour, showcasing *Pegasus*'s effectiveness in handling large-scale nonlinear dynamic problems.

1. Program *Pegasus*

Realistic computational representation of railway systems often requires the construction of three-dimensional models that will eventually lead to a large-scale mathematical system. Additionally, various nonlinear aspects need to be considered in detailed analyses of the problem, including e.g. the nonlinear behavior of geomaterials, wheel-rail contact, sleeper-ballast contact, and load-deformation state dependency (force non-linearity). All-together, these aspects pose significant computational challenges, that are still unpractical with commercial programs. To address these issues, a three-dimensional nonlinear soil-structure dynamic interaction program based on the finite element method, referred to as *Pegasus*, was fully coded in MATLAB®.

The complete railway system is composed of several sub-systems with very different mechanical properties and dimensions that interact through contact forces of a non-linear nature. The *Pegasus* program incorporates this diversity, considering each sub-system separately: i) the vehicle model; ii) the track superstructure (rails, sleepers and fasteners); and iii) the track substructure, which includes the supporting layers of the track (including the ballast) and in this case also a small bridge, as schematically represented in Figure 1. The vehicle system is an assemblage of rigid bodies, springs and dampers. The track superstructure is built with Euler-Bernoulli beam elements representing the rails and the sleepers. The ballast-substructure system is discretised with low-order eight-node solid hexahedral elements. At the lateral boundaries of the model local transmitting boundaries, consisting of visco-elastic dampers are placed to absorb impinging waves.

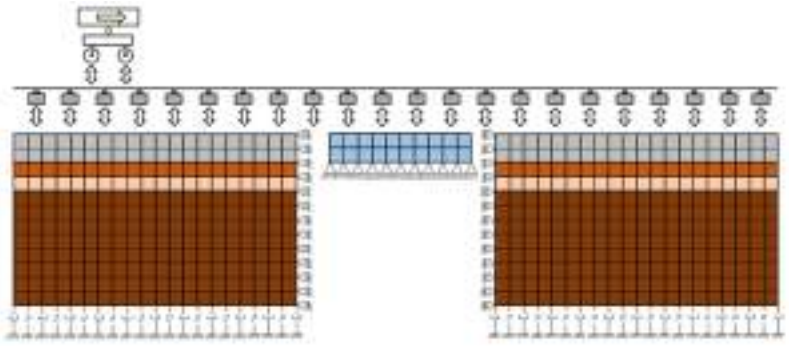

Figure 1. Longitudinal schematic representation of the 3D FEM model composed of three sub-systems: the vehicle, the track superstructure (rails and sleepers) and the track substructure (ballast, soils and bridge).

The coupled equations of motion of the three systems reads:

$$\begin{cases} \mathbf{K}_v\mathbf{u}_v + \mathbf{C}_v\mathbf{v}_v + \mathbf{M}_v\mathbf{a}_v = \mathbf{f}_{g.v} + \mathbf{f}_{a.w} \\ \mathbf{K}_t\mathbf{u}_t + \mathbf{C}_t\mathbf{v}_t + \mathbf{M}_t\mathbf{a}_t = \mathbf{f}_{g.t} - \mathbf{f}_{a.w} + \mathbf{f}_{a.b} \\ \mathbf{K}_s\mathbf{u}_s + \mathbf{C}_s\mathbf{v}_s + \mathbf{M}_s\mathbf{a}_s = \mathbf{f}_{g.s} - \mathbf{f}_{a.b} \end{cases} \quad (1)$$

where the subscripts v, t and s refer to the vehicle, track superstructure and ballast-substructure systems, respectively. Irrespective of the subscripts, **K**, **C** and **M** are the global stiffness, damping and mass matrices of the structural systems, **u**, **v** and **a** are, respectively, the vectors of nodal displacements, velocities and accelerations, $\mathbf{f_g}$ is the vector of the gravity loads, $\mathbf{f_{a.w}}$ is the vector of the interaction forces between the wheels and the rails, calculated using the nonlinear Hertzian contact theory, and $\mathbf{f_{a.b}}$ is the vector of the interaction forces between the sleepers and the ballast, calculated using the nonlinear spring-dashpot model in the normal direction and the linear spring Coulomb limit model in the transverse direction. In *Pegasus*, the ballast-substructure system and the vehicle system are solved using Zhai's explicit integration scheme, and the track superstructure system is solved using the implicit Newmark constant acceleration method. This choice considerably reduced the computational time compared to alternatives using the same integrator for the three systems [1].

Regarding the material behaviour, linear elasticity is assumed for all materials, with exception for the ballast layer which follows a pressure dependent hypo-elastic material law, commonly known as the k-θ model. In this model, the resilient modulus, E_r, is a function of the sum of the normal stresses (θ), defined positive for compression, according to Eq. (2):

$$E_r(t) = \max\left(\boldsymbol{K_1}\left(\frac{\boldsymbol{\theta(t)}}{\boldsymbol{\theta_0}}\right)^{\boldsymbol{K_2}}, \boldsymbol{E_{min}}\right) \quad (2)$$

leaving the Poisson's ratio constant. The reference stress, θ_0, is taken as 100 kPa. Further description of the program can be found in [1,2,3].

2. Application example

The case-study selected to demonstrate the capacities of program *Pegasus* corresponds to a simplified model of an underpass with a small span metallic bridge, in which, when crossing the span, the track rests directly on the bridge, without ballast, as shown in Fig. 2.

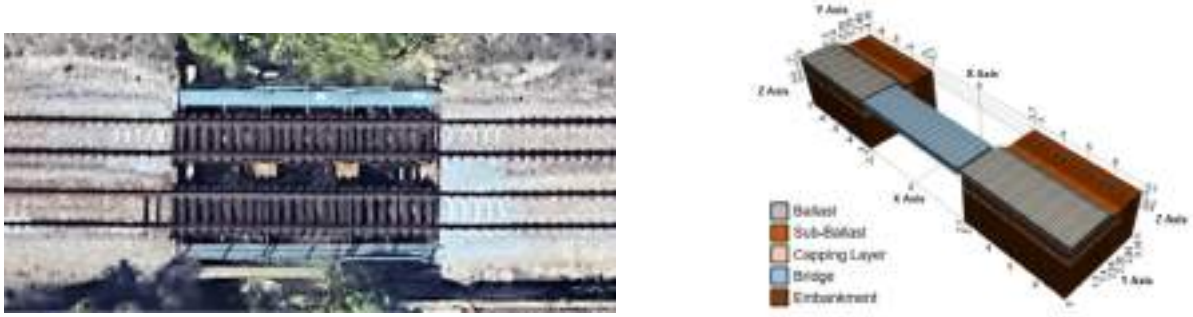

a) b)

Figure 2. a) top view of a non-ballasted underpass, b) Partial 3D view of the track substructure model.

The track superstructure system is composed of two UIC60 steel rails, concrete monoblock sleepers with a mass of 322 kg spaced 0.6 m, and railpads with a vertical stiffness of 160 kN/mm and a damping constant of 9.6 kNs/m, each. Regarding the ballast material, the considered model parameters of the K-θ model defined in Eq. 2 were K_1 = 105 MPa, K_2 = 0.60, E_{min} = 16 MPa, with $\nu = 0.20$. The constant resilient modulus of the sub-ballast, capping layer and subgrade were, respectively, 200 MPa, 250 MPa and 100 MPa, with $\nu = 0.25$. The model comprises 65 sleepers, having 204000 degrees-of-freedom, with 58500 solid elements, of which 10020 present nonlinear behaviour.

The dynamic simulations were performed considering isolated passages of a bogie of the Portuguese “Alfa Pendular” (AP) tilting passenger vehicle. For the study of the influence of the train speed on the dynamic response, four speed values were considered: 110, 180, 250 and 320 km/h.

Figure 3 shows the maximum downward displacements of the rail caused by the passage of the AP model when crossing the underpass from left to right. The dashed vertical lines indicate the location of the bridge ends. It is possible to observe that the stiffness of the track increases considerably and rapidly over the bridge. It is also shown that the effect of the speed on the rail vertical displacements is relatively small, with the exception for highest speed considered.

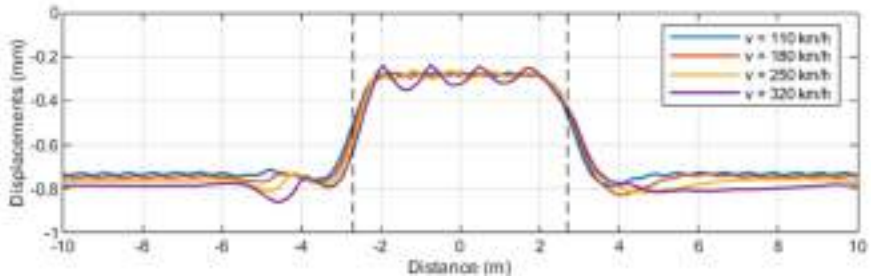

Figure 3. Maximum downward displacements of the rail for different values of train speeds.

Fig. 4 now shows the normal wheel-rail contact forces of the rear axle wheel, for the four speed values considered. It is noted that the static component is 66 kN. It can be observed that the dynamic effect associated with the higher speed is very significant, whereas for the lower speed it is practically negligible.

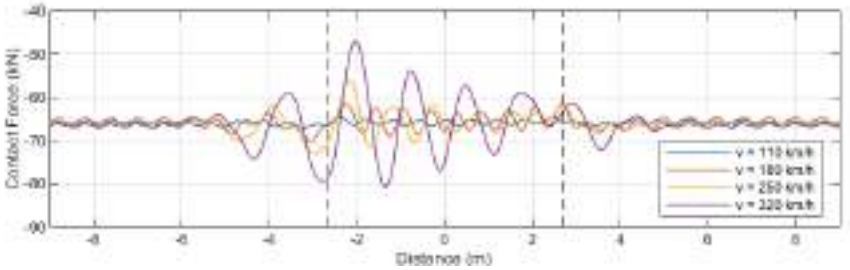

Figure 4. Wheel-rail interaction force of the rear axle wheel as a function of the wheel position.

The total calculation time depends on the train speed considered, varying between about 2 h for the slowest speed and less than one hour for the fastest. This, considering that each time-step calculation requires the reconstruction of the nonlinear part of the stiffness matrix, demonstrates Pegasus's effectiveness in handling large-scale nonlinear dynamic problems involving contacting materials (steel, concrete and soils) with contrasting mechanical properties.

3. References

[1] Varandas, J.N., Paixão, A., Fortunato, E. (2017). A study on the dynamic train-track interaction over cut-fill transitions on buried culverts, *Computers & Structures*, Vol. 189: 49-61, doi: doi.org/10.1016/j.compstruc.2017.04.017

[2] Paixão, A., Varandas, J.N., Fortunato, E., Calçada, R. (2018). Numerical simulations to improve the use of under sleeper pads at transition zones to railway bridges, *Engineering Structures* Vol. 164: 169-182, doi: doi.org/10.1016/j.engstruct.2018.03.005

[3] Varandas, J.N., Paixão, A., Fortunato E., Zuada Coelho, B., Hölscher, P. (2020). Long-term deformation of railway tracks considering train-track interaction and non-linear resilient behaviour of aggregates. *Computers and Geotechnics*, Vol. 126, doi: doi.org/10.1016/j.compgeo.2020.103712

Assessment of Soil Constitutive Models for Predicting Seismic Response of Sheet Pile Walls: A LEAP2022 Project Study

Pedro Arduino[1] and Amin Pakzad[1]
[1] University of Washington, Seattle, WA, United States

Abstract

This paper presents the findings of a study conducted as part of the LEAP2022 project, which aims to investigate the seismic response of a sheet-pile retaining structure supporting liquefiable soils. The study compares the accuracy of two different constitutive models, namely Manzari-Dafalias [1] (MD) and PM4Sand [2], calibrated using element tests provided for Ottawa-F65 sand in the project. The calibrated models are used to build finite element models that simulate centrifuge experiments. Results show that both MD and PM4sand models can reasonably capture the behavior of liquefiable soils and wall displacements. The study further highlights the importance of calibrating for the response at the toe of the wall and the passive zone for accurate prediction of wall behavior. The study also recommends improvements in the material models to accurately capture soil and wall behavior under dry conditions. Finally, the study finds that using the PM4sand and MD models calibrated for F-65 can still provide good predictions for centrifuge tests with different sands.

1. Problem Statement

Predicting soil behavior under seismic loading, especially the behavior of liquefiable soils, remains a significant challenge in geotechnical engineering. Numerical models, like the Manzari-Dafalias (MD) and PM4Sand models, have been developed to simulate such behavior. However, their reliability and accuracy in predicting real-world phenomena where liquefaction occurs are not fully established. The LEAP project addresses these uncertainties by comparing the performance of constitutive models in predicting the seismic response observed in centrifuge experiments[3]. Specifically, LEAP2022 focuses on the response of sheet-pile walls retaining liquefiable soils. This study aims to evaluate the effectiveness of the Manzari-Dafalias (MD) and PM4Sand models in capturing key aspects of soil behavior under seismic loading, including wall displacement, excess pore water pressure generation, and soil-structure interaction.

2. Scope of Work

The LEAP2022 project aimed to create a reliable database of centrifuge experiments for assessing the predictive capabilities of numerical tools used in soil liquefaction analysis. The scope of this study involved conducting a series of centrifuge tests at five different facilities worldwide, each focusing on the seismic response of a sheet-pile retaining structure embedded in liquefiable soils. These experiments varied in terms of initial relative densities, base excitations, and soil types (including Ottawa F-65 sand and Silica 306 sand), allowing for a comprehensive evaluation of the models under diverse conditions. Figure 1 illustrates the baseline schematic of the centrifuge model experiments, which consisted of a layer of medium-dense Ottawa F-65 sand on top, supported by a sheet pile wall made of aluminum.

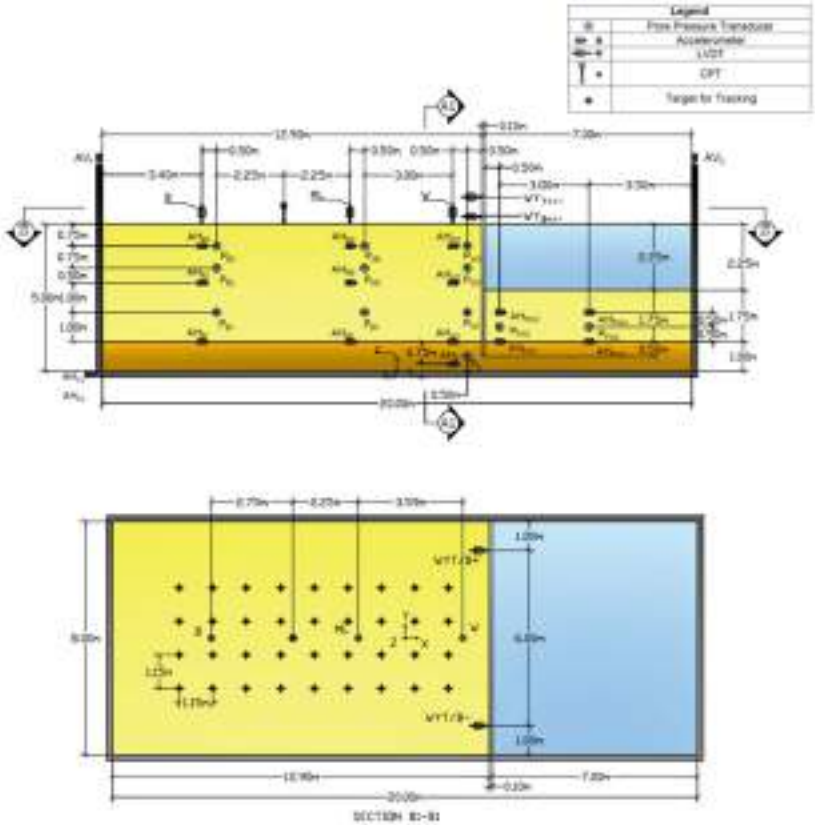

Figure 1. Experimental setup and instrumentation for LEAP-2020 centrifuge tests[3]

Two primary soil constitutive models, Manzari-Dafalias (MD) and PM4Sand, were selected for analysis. These models were calibrated using element tests and then employed in finite element models (FEM) developed in OpenSees[4]. The study also incorporated a dry soil scenario to and a different sand (Silica 306) further challenge the predictive capabilities of these models. Key performance metrics included wall displacement, excess pore water pressure generation, spectral acceleration responses, and shear stress profiles.

3. Findings

The results showed that both the MD and PM4Sand models could effectively predict the seismic behavior of liquefiable soils and the resulting wall displacements. However, several discrepancies were observed:

Calibration Challenges: Both models exhibited difficulties in calibration, particularly in accurately reproducing observed demands from centrifuge tests. The accuracy of the predictions was sensitive to the calibration of parameters, especially for the behavior at the toe of the wall and in the passive zone.

Model Performance: The MD model generally provided better predictions for wall displacement trends compared to PM4Sand, especially in scenarios involving different relative densities and cyclic stress ratios. However, the PM4Sand model demonstrated superior performance in predicting excess pore water pressure trends, particularly when applied to Silica 306 sand.

Dry Soil Conditions: Significant limitations of both MD and PM4Sand models in predicting the behavior of dry soils were observed. The SANISAND-MS model, an enhanced version of MD, showed better performance under these conditions, suggesting that improvements in constitutive models are necessary for accurate predictions in dry soil scenarios.

Overall, the findings underscore the importance of careful calibration and the need for continued

development of soil constitutive models to improve their predictive accuracy under a range of loading conditions. These insights are particularly relevant for geotechnical engineers involved in the design and analysis of structures subjected to seismic loading.

4. Conclusion

The LEAP2022 project successfully demonstrated the capabilities and limitations of the MD and PM4Sand models in predicting the seismic response of sheet-pile walls in liquefiable soils. While both models showed potential, their performance varied depending on the specific conditions and parameters involved. The study suggests that further refinement of these models, particularly for dry soil scenarios, is necessary to enhance their reliability and accuracy. The results contribute valuable knowledge to the ongoing development of more robust numerical tools for geotechnical earthquake engineering.

5. References

[1] Dafalias, Y.F., Manzari, M.T. (2004). Simple plasticity sand model accounting for fabric change effects, *J Eng Mech* 2004, 130(6):622–34

[2] Boulanger, R. W., Ziotopoulou, K. (2015). PM4Sand (Version 3): A sand plasticity model for earthquake engineering applications, Center for Geotechnical Modeling Report No. UCD/CGM-15/01, Department of Civil and Environmental Engineering, University of California, Davis, California

[3] El Ghoraiby, M., Park, H., Manzari, M. T. (2020). Physical and mechanical properties of Ottawa F65 sand, Model tests and numerical simulations of liquefaction and lateral spreading: LEAP-UCD-2017, 45–67. Springer

[4] “OpenSees.” (2007). Open system for earthquake engineering simulation, University of California. Berkeley: Pacific Earthquake Engineering Research Center (PEER), 2007, http://opensees.berkeley.edu

Trends and gaps in the numerical analysis of offshore wind turbine foundations

F. Pisanò [1,2]
[1] *Norwegian Geotechnical Institute, Boston, Massachusetts, United States*
[2] *Delft University of Technology, Delft, The Netherlands*

Abstract

The growth of the offshore wind energy sector presents significant engineering challenges, particularly in the design and installation of monopile foundations. Monopiles, commonly used for offshore wind turbines in waters up to 60 meters deep, face issues such as cyclic/dynamic tilting, penetration during installation, and interaction with difficult soils. Advanced numerical models are crucial for optimizing monopile design and supporting global decarbonization goals. This summary elaborates on the need for further research with regard to the mentioned knowledge gaps, underscoring the importance of collaboration between industry and academia to address complex engineering problems.

1. Introduction

With the accelerating growth of the offshore wind energy sector worldwide, the installation of ever-larger offshore wind turbines (OWTs) in harsh marine environments poses serious engineering challenges. As OWT foundations mobilize approximately 20-30% of the capital expenditure costs, questions and open gaps related to foundation design emerge as some of the most pressing concerns. In this regard, it is worth noting that monopiles are the most common type of foundation used for OWTs in water depths of up to approximately 60 meters. To accommodate the increasing size of wind towers, monopiles with larger diameters (up to 8-10 meters and beyond) are being adopted in the construction of modern offshore wind farms. As a consequence, monopiles have been – and continue to be – at the core of important geotechnical research initiatives. Recent studies have focused on various aspects of monopile performance, including driveability and assessment of different installation methods, lateral capacity and stiffness, interaction with difficult geomaterials such as chalk and glauconitic soils and, more recently, dynamic/seismic response. All these aspects are crucial for optimizing monopile design, a focus of numerous research programs and advanced consulting projects. Given the high costs and extended timeframes associated with field testing (and, in general, of experimental work), numerical analysis tools are ever more used for design assignments. Therefore, the accuracy and reliability of numerical models are essential for producing suitable designs that can support the attainment of the world's ambitious decarbonization goals. Despite significant advancements in numerical modelling of soil-structure interaction problems, also in the presence of dynamic effects, there are still areas that require further research and collaboration between industry and academia.

The following explores the relationship between advanced numerical modeling and monopile design, highlighting three examples from the author's experience where further research is particularly needed:

1) analysis of cyclic/dynamic monopile tilting;
2) simulation of monopile penetration;
3) monopile-soil interaction in difficult soils.

2. Analysis of cyclic/dynamic monopile tilting

The assessment of monopile serviceability under cyclic/dynamic loading conditions, particularly in terms of predicting lateral deflection/tilt accumulation, remains a subject of debate. While the offshore industry often requires simplified approaches (such as p-y methods) for repetitive, location-

specific calculations, advanced physical and numerical modelling work continues to be carried out to inform the development of simplified design methods [1].

Figure 1 illustrates the suitability of the SANISAND-MS model for the 3D FE simulation of cyclic monopile behavior in sandy soils [2]. Building on previous research, the primary focus is to evaluate the model's ability to reproduce the accumulation of permanent deflection and tilt under cyclic lateral loads. Experimental data from the PISA field campaign, specifically medium-scale cyclic tests conducted at the Dunkirk site in France, are utilized. This marks the first attempt to simulate the reference data set using a fully step-by-step 3D FE approach, offering novel insights into calibrating and employing advanced cyclic models for monopile analysis and design, particularly regarding the quantitative influence of pile installation effects and the microstructural evolution of sand under cyclic loading.

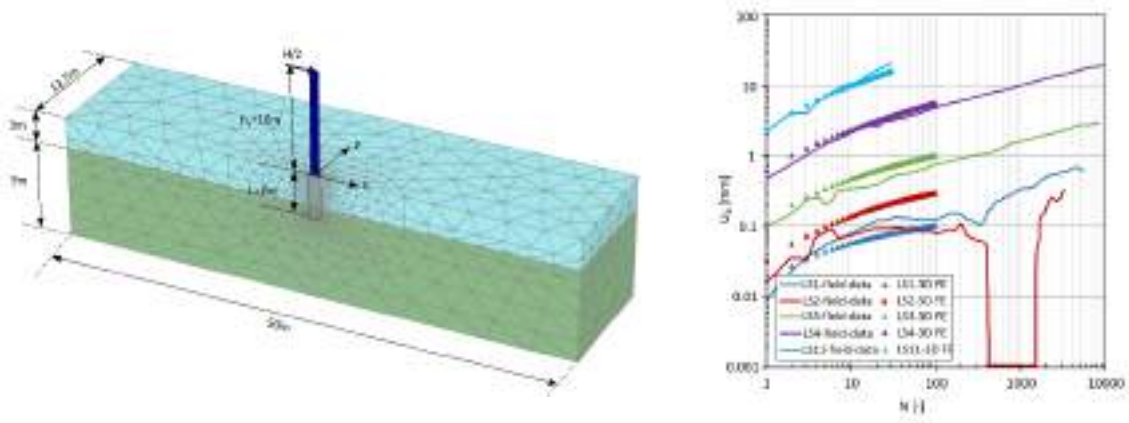

Figure 1. 3D FE SANISAND-MS simulation of cyclic monopile behaviour [2].

As the development of offshore wind expands in the Asia-Pacific region, fulfilling similar monopile design criteria becomes increasing challenging in the presence of seismic loading. During seismic shaking, soils exhibit strongly non-linear behavior, including changes in stiffness and strength, permanent deformations, and pore pressure build-up. Excess pore pressure can lead to soil liquefaction, resulting in excessive displacement or catastrophic collapse of structures. These issues are the core of DONISIS, a new research programme aiming to inform the development of seismic design models for monopiles, building on advanced physical and 3D FE modelling work.

3. Simulation of monopile penetration

Dynamic effects are particularly pronounced during installation operations. This second section concerns numerical simulation challenges associated with pile run, which is the sudden and uncontrolled penetration of a pile or pile/hammer system during impact driving. Two primary mechanisms can trigger pile run: transitioning from high- to low-strength soil and soil strength loss during hammering. While acceleration and velocity of the pile/hammer system can be calculated using simple Newtonian mechanics principles combined with CPT-based methods for soil resistance evaluation, the complexity of soil behavior under high strain-rate deformation would require more advanced analysis methods (Figure 2). Techniques such as large deformation MPM or PFEM simulations can provide greater insight into the impact of non-linear soil behaviour and hydro-mechanical effects, especially given the typical scarcity of experimental data for validating simpler engineering methods. The need to advance large-deformation methods for pile penetration problems is also linked to the analysis of pile driving using vibratory methods [3]. These methods are gaining popularity due to environmental concerns related to underwater noise emission during traditional impact piling. This second section of the oral presentation will conclude by reflecting on the existing gaps that hinder the application of advanced numerical simulation methods for solving these penetration problems in practical engineering projects.

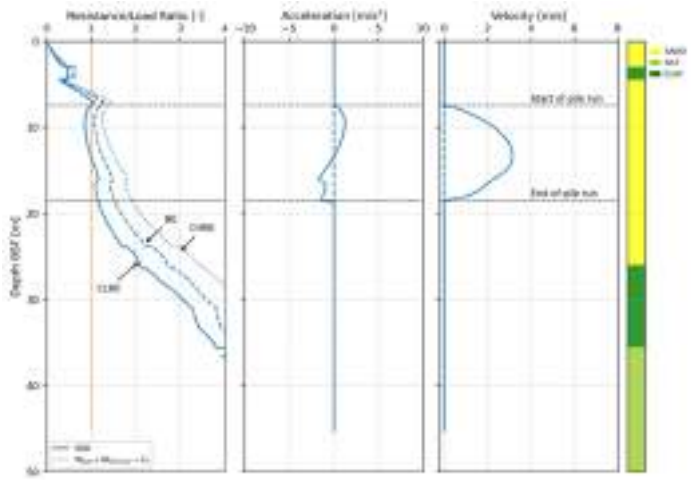

Figure 2. Numerical analysis of pile run during installation in layered deposits (courtesy of NGI).

4. Monopile-soil interaction in difficult soils

Offshore wind development in the US is rapidly expanding, especially on the Atlantic Coast, due to high energy demand, suitable shallow water depths, and strong wind speeds. However, the Atlantic Outer Continental Shelft is designated a “frontier” region by the Bureau of Ocean Energy Management (BOEM) due to limited geological and geotechnical experience. The area presents numerous challenges, including high spatial variability, boulders, calcareous sediments, glauconite sands, shallow bedrock, micaceous soils, and sediment mobility. Serious difficulties for goetechnical design and field operations are associated with the presence of glauconite, an iron potassium mica, which behaves as sand but transforms into a fine-grained soil upon shearing due to particle crushing. During pile driving, a shear zone of crushed glauconite forms around the pile shaft, affecting shaft friction and limiting penetration depths. In addition to the mentioned challenges regarding the simulation of penetration processes and dynamic operational performance, glauconitic soils introduce fundamental challenges related to soil characterization and constitutive modeling. These soils exhibit behavior that evolves from granular-like to cohesive-like depending on geological history and exposure to loading excitations [4].

5. Acknowledgements

Part of the contents mentioned herein relate to the MIDAS (https://www.grow-offshorewind.nl/project/midas) and PIGS (https://www.ngi.no/en/projects/pigs/) research projects. The author gratefully acknowledges the collaboration and support of industry partners, the Dutch Enterprise Agency (RVO), and numerous international colleagues (not listed in detail for brevity).

6. References

[1] Pisanò, F. (2019). Input of advanced geotechnical modelling to the design of offshore wind turbine foundations, In *XVII European Conference on Soil Mechanics and Geotechnical Engineering-Reykjavík, Iceland*, Vol. 1, No. 6

[2] Pisanò, F., Del Brocco, I., Ho, H. M., Brasile, S. (2024). 3D FE simulation of PISA monopile field tests at Dunkirk using SANISAND-MS, *Géotechnique Letters*, 1-30

[3] Tsetas, A., Kementzetzidis, E., Gómez, S. S., Molenkamp, T., Elkadi, A. S. K., Pisanò, F., Tsouvalas, A., Metrikine, A. V. (2024). Gentle Driving of Piles: field observations, quantitative analysis and further development, In *Offshore Technology Conference* (p. D021S019R001). OTC

[4] Westgate, Z., Rahim, A., Senanayake, A., Pisanò, F., Maldonado, C., Ridgway-Hill, A., Perikleous, Y., De Sordi, J., Roux, A., Andrews, E., Ghasemi, P. (2024). The Piling in Glauconitic Sands (PIGS) JIP: reducing geotechnical uncertainty for US offshore wind development, In *Offshore Technology Conference* (p. D031S001R007). OTC

Modeling Soil-Foundation Response of Offshore Wind Turbines Under Realistic Dynamic Loading using the Thermodynamic Inertial Macroelement

J. M. Ricles[1], D. N. Gorini[2], F. N. Malik[1], S. Al-Subaihawi[3], Q. Abu Kassab[1], M. Suleiman[1], and R. Sause[1]

[1] Lehigh University, Bethlehem, Pennsylvania, United States

[2] University of Trento, Trento, Italy

[3] California Polytechnic State University, San Luis Obispo, California, United States

Abstract

Wind, wave and periodic blade forces subject Offshore Wind Turbine (OWT) structures to multidirectional cyclic loads that have varying amplitudes, frequencies, and patterns. The fundamental frequency of the structure changes during the life of the OWT, depending on the behavior of the structure and the Soil-Foundation Structure Interaction (SFSI) that occurs. Therefore, understanding the SFSI of the OWT under realistic loading conditions is needed to improve the design and performance of OWT structures subjected to different environmental and mechanical loading conditions. The computational formulations used to model SFSI effects in OWT requires calibrating the models using test data from experiments performed under realistic loading conditions. This paper describes applying real-time hybrid simulation (RTHS) to OWT structures to acquire such data. The response of the foundation of a monopile OWT subjected to operational and extreme loading conditions is then predicted using a calibrated Thermodynamic Inertial Macroelement (TIM) The TIM is an efficient computational tool, enabling faster solutions by avoiding the modeling of the complete soil-foundation domain. The TIM is shown to provide reasonable agreement with the experimental results in terms of secant stiffness and ratcheting of the soil-foundation system. Recommendations for improving the prediction of SFSI effects in monopile OWT structures using the TIM are given.

1. Introduction

Offshore wind power is a renewable and infinite source of energy. The conversion of wind into power creates no harmful greenhouse gas emissions. Thus, OWT will play a major role in the future of electricity generation.

This paper presents a study that uses a TIM formulation to account for the effects of soil-foundation interaction on the response of monopile OWT structures subjected to wind, wave, and operational loads. The fundamental frequency of the structure changes during the life of the OWT, depending on the behavior of the structure and the extent of SFSI that occurs [1]. The effects of SFSI on the behavior of a OWT under both normal operating and extreme loading conditions is therefore necessary in order to improve OWT designs. Investigating SFSI effects can be performed computationally, however such attempts must use calibrated formulations that are efficient and accurate. This issue is addressed here using the TIM approach [2-4]. A TIM is a constitutive relationship between the generalized forces exchanged at the foundation-superstructure contact and the corresponding displacements and rotations of the soil-foundation system. In the present study, the TIM models the monopile foundation and the soil interacting with it, with reference to a 5 MW OWT developed by NREL [5].

Real-time hybrid simulations (RTHS) [6] are initially performed on the considered structure to produce realistic loading conditions under wind, wave, and energy generation equipment vibration loadings. The experimental results from the RTHS are used to assess the accuracy of the TIM in predicting the response of a monopile OWT under operational and extreme loading conditions.

2. Thermodynamic Inertial Macroelement: formulation and OWT foundation modeling

TIMs simulate the nonlinear and frequency-dependent multiaxial response of a suite of geotechnical systems at a residual computational demand [3,4]. TIMs are available in OpenSees [7] as multiaxial

materials, that can be assigned to a zero-length finite element providing a fully coupled, 6D response (three translations and three rotations) between the two nodes [3]. Each TIM represents a multi-surface plasticity law with kinematic hardening, whose incremental response is obtained through a rigorous thermodynamic-based framework fully defined by consistent potential functions, i.e., free energy and its dissipation.

For the reference OWT, the TIM was employed to reproduce the response of the monopile and of the soil region interacting with it. The TIM calibration required a few parameters to be determined: the initial stiffness matrix, the matrix of the participating masses of the soil-foundation system, and the multiaxial ultimate capacity of the latter. The respective identification procedures followed the ones delineated in [4] and are omitted for conciseness.

3. Real-time Hybrid Simulation of OWT concept

Real-time hybrid simulation is a testing technique where the system is divided into analytical and experimental substructures [8, 9]. The former uses well-established computation models to create a numerical model of a portion of the system. The remaining components of the system, for which there is no existing well-established computational model, is modeled physically in the laboratory. The two substructures are kinematically coupled, and equilibrium is maintained at their common degrees of freedom (DOFs), as depicted in Figure 1. The embedded foundation and surrounding soil of the OWT are modeled physically in a soil box in the laboratory while the remaining parts of the system and loading are modeled analytically. The program OpenFAST [10], developed by the National Renewable Energy Laboratory (NREL), is linked to a RTHS coordinator to determine the hydrodynamic and aerodynamic loads acting on the OWT, along with modeling the dynamics of the electric power generation equipment and associated controller for the OWT. Further details about the framework can be found in [6].

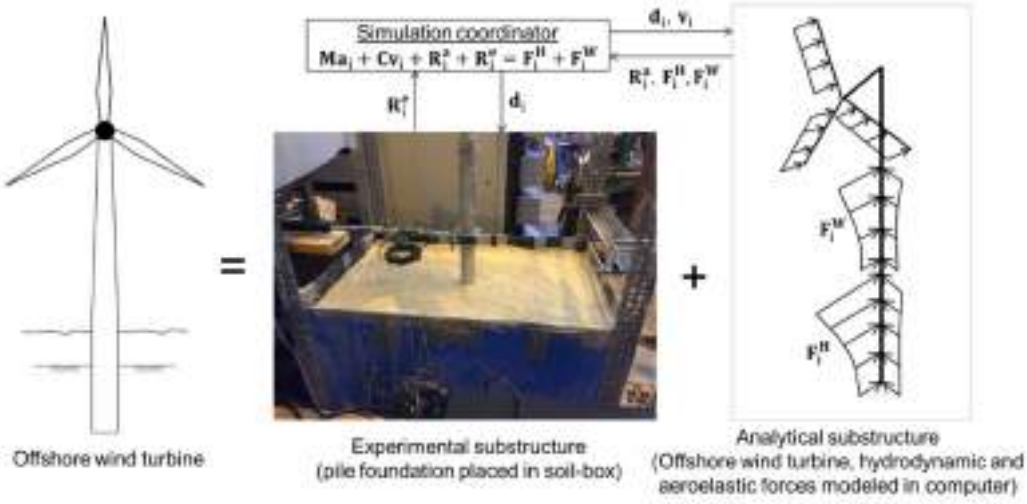

Figure 1. Generalized schematic of the real-time hybrid simulation concept for offshore wind turbines.

4. Comparison of TIM and Real-time Hybrid Simulation results

The matrix for the RTHS included two tests: (1) Test 1 – having a steady state wind speed of 12 m/s and regular wave height of 6 m; and (2) Test 2 – having a steady state wind speed of 20 m/s and regular wave height of 12 m. Test 1 represented normal operational conditions, whereas Test 2 more extreme conditions. Shown in Figure 2 are the pile head force-displacement hysteretic response for the two tests. The cyclic response is seen to be nonlinear, where in all of the RTHS there is a presence of accumulated pile displacement with a shift towards the positive displacement in the direction of the loading, along with pinching in the hysteresis loops. The degree of shifting and pinching is more predominant in Test 2, which had the more severe conditions for wind speed and wave height causing

larger deformations and nonlinear behavior to develop in the pile foundation. The TIM captures the response quite well in terms of the secant stiffness and ratcheting. However, the TIM is not able to reproduce the pronounced pinching observed in the experimental data (i.e., RTHS). The TIM formulation will need further extension to capture the pinching effect, and is the topic of ongoing research by the authors.

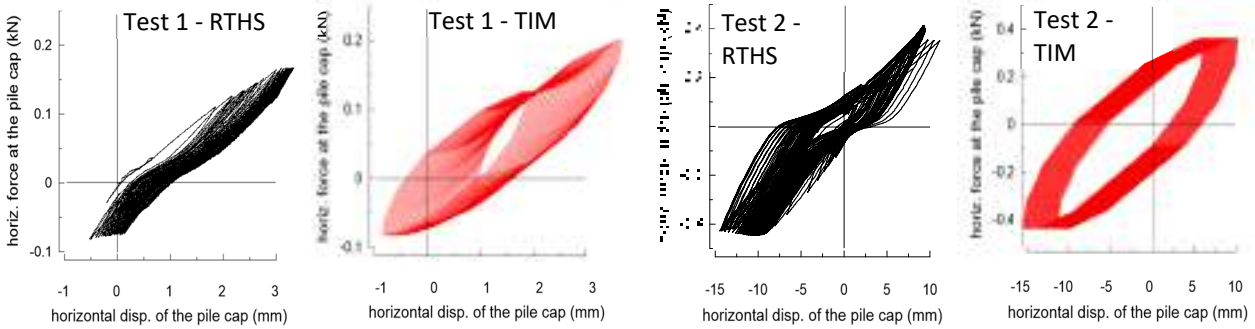

Figure 2. Pile head force-displacement response for Tests 1 and 2.

5. References

[1] Bhattacharya, S. (2019). Design of foundations for offshore wind turbines. John Wiley & Sons, ISBN 9781119128120

[2] Gorini, D. N., Callisto, L., Whittle, A. J., and Sessa, S. (2023). A multiaxial inertial macroelement for bridge abutments. *International Journal for Numerical and Analytical Methods in Geomechanics*, 47(5): 793-816

[3] Gorini, D. N., and Callisto, L. (2023). A multiaxial inertial macroelement for deep foundations. *Computers and Geotechnics*, 155, 105222

[4] Gorini, D. N. (2024). A unified thermodynamic-based macroelement approach. *Submitted to Acta Geotechnica*

[5] Jonkman, J., Butterfield, S., Musial, W., Scott, G. (2009). Definition of a 5-MW reference wind turbine for offshore system development. Golden (CO): National Renewable Energy Laboratory (US); 2009 Feb. Report No.: NREL/TP-500-38060

[6] Al-Subaihawi, S., Ricles, J., Abu-Kassab, Q., Suleiman, M., Sause, R., and Marullo, T. (2024). Coupled aero-hydro-geotech real-time hybrid simulation of offshore wind turbine monopile structures, *J of Eng. Struc.*, 303 117463, https://doi.org/10.1016/j.engstruct.2024.117463

[7] McKenna, F., Scott, M. H., and Fenves, G. L. (2010): OpenSees. Nonlinear finite-element analysis software architecture using object composition. *Journal of Computing in Civil Engineering*, 24(1): 95-107

[8] Kolay, C., Ricles, .J, Marullo, T., Mahvashmohammadi, A., Sause, R. (2015). Implementation and application of the unconditionally stable explicit parametrically dissipative KR-α method for real-time hybrid simulation, *Earthquake Eng. & Struct Dyn.*; 44(5):735-55. https://doi.org/10.1002/eqe.2484

[9] Al-Subaihawi, S., Ricles, J., Quiel, S, and T. Marullo, (2024). development of multi-directional real-time hybrid simulation for tall buildings subject to multi-natural hazards, *Engineering Structures*, 315 (2024) 118348, https://doi.org/10.1016/j.engstruct.2024.118348, 2024

[10] OpenFAST documentation. (2023). Release v3.1.0. National Renewable Energy Laboratory

Towards practice-oriented procedures for analysing monopile-supported offshore wind turbines

D. Gallese[1], J. Go[1], J. Sasaki[2]
[1] Ove Arup and Partners, London, UK
[2] Ove Arup and Partners, Tokyo, Japan

Abstract

Amid the global transition to renewable energy, offshore wind power stands out as a key player. Nevertheless, the construction of offshore wind farms in seismic-prone regions highlights the urgent need for practice-oriented methods to ensure adequate performance during earthquakes. In fact, current codes offer limited guidance on analysing such complex soil-structure interaction problems under seismic loading. Current practices involving full three-dimensional dynamic soil-structure interaction (DSSI) models are proven to be computationally burdensome and economically unfeasible for routine design. To tackle these challenges, Arup has devised practice-oriented design methodologies for use in routine design.

A 3D DSSI model was developed within the LS-DYNA environment and used as a reference for the validation of simpler approaches based on beam-on-nonlinear springs, as defined by Japanese provisions. These springs are used in the context of a decoupled approach, in which the seismic action is defined by means of a manageable free-field soil response. In detail, this study explores the application of two spring typologies, namely visco-elastic and nonlinear springs. Their efficacy in capturing intricate 3D soil-structure interaction responses in terms of displacements and internal forces is discussed. However, caution is warranted, particularly in highly seismic regions, as the adoption of visco-elastic springs may lean towards conservatism, emphasizing the importance of accounting for soil nonlinearity in soil-structure interaction problems. Finally, it is shown that simplified 1D models effectively capture 3D response attributes, significantly reducing computational run times for offshore wind farms with around 100 turbines.

1. Introduction

Offshore wind energy has emerged as a crucial renewable power source, with the global average size of turbines increasing from 1.5 MW in 2000 to 8.1 MW by 2021, and projections suggesting it will exceed 12 MW by 2025 [1]. In addition, it is expected that 680 GW of wind capacity will be installed globally by 2027, of which 130 GW will be offshore [2]. Monopiles are the preferred support for these turbines in shallow waters due to their cost-effectiveness. However, accurate seismic response modeling is essential in seismically active regions such as Japan, Taiwan, and the Western United States to ensure safety and performance.

Current design codes provide limited guidance on soil-structure interaction (SSI) under seismic loading, necessitating the use of complex and time-consuming three-dimensional dynamic soil-structure interaction (3D DSSI) analyses. These analyses are crucial for understanding monopile compliance effects and foundation internal forces. Recent advancements in design methodologies, such as the PISA methodology, have improved efficiency by using three-dimensional finite element analysis to calibrate 1D non-linear springs in static conditions. Nevertheless, there is a need for further guidance on dynamic SSI problems.

Recent studies by Gallese et al. [3,4] demonstrate that simplified 1D models can effectively capture complex 3D DSSI responses. These advancements are essential for developing cost-effective and timely design solutions that meet the demands of the offshore wind industry.

2. Methodology

The study focuses on an idealised offshore site resembling conditions in East Asia, with a 30-meter water depth and a soil profile consisting of stiff clay layers overlying fine-grained sedimentary rock

(mudstone). The analysis involves a 15 MW Offshore Wind Tower (OWT) as per International Energy Agency [5] data, with a monopile (MP) diameter of 10.5 meters and a length of 47 meters.

A comprehensive 3D dynamic soil-structure interaction (DSSI) model created using LS-DYNA software to simulate the offshore wind turbine is depicted in Figure 1. The model includes solid elements for the soil and shell elements for the embedded sections of the monopile. The superstructure is modeled with elastic beam elements and lumped masses to simulate non-structural elements and hydrodynamic loads. The input earthquake motion is applied at the base of the model, with non-reflecting boundary conditions, whilts free field conditions are reproduced at the edges.

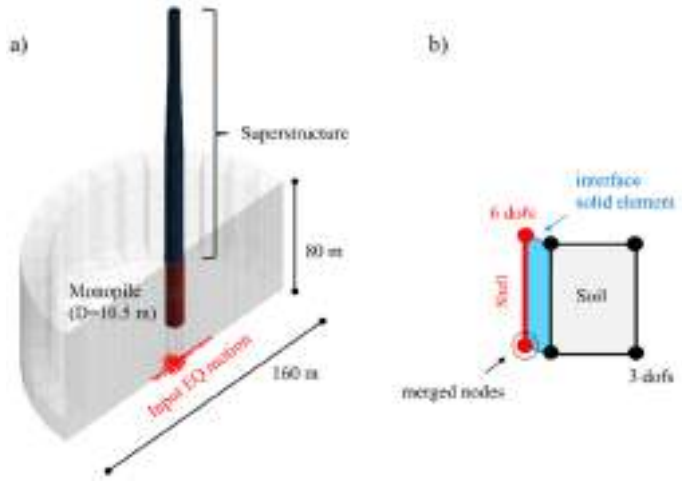

Figure 1. (a) Half-isometric view of the 3D soil-structure model developed in LS-DYNA; (b) detail of the soil-structure contact.

Two simplified methods for modeling soil-structure interaction were investigated, based on Japanese provisions. The first method follows the Japan Society of Civil Engineers (JSCE, [6]) guidelines, which use elastic springs and viscous dampers to model soil behavior. The spring stiffness and damping are derived employing common solutions of proven validity taking into account the results of the site response analysis (SRA).

The second method adheres to the Japanese Specifications for Highway Bridges (JRA, [7]). This approach uses a bilinear curve to define soil resistance, with the strength determined by passive resistance around the pile whilts the initial stiffness is based on the horizontal subgrade reaction coefficient, adjusted for the installation procedure.

The flowchart of the 1D simplified procedure is shown in Figure 2 and it is based on the decoupled approach where displacement time histories along the depth of the MP are carried out from a 1D SRA and then applied along the springs of the beam-on-nonlinear-Winkler-foundation model. The masses of the foundation nodes are lumped at the discretized points considering the sum of the structural part and the soil inside the cylinder.

The study examined seismic responses using three spectrally matched bedrock time histories to assess the system under different levels of seismic excitation, denominated as low, medium, and high intensity in the following.

3. Results and conclusions

Results show that the 1D JRA model closely matches the 3D model across all seismic intensities, while the 1D JSCE model tends to overestimate internal forces and bending moments, particularly under high seismicity. This overestimation is attributed to the use of linear springs in the JSCE model, which do not fully capture the nonlinear soil response.

Despite some limitations, these findings suggest that, with proper calibration against 3D models, 1D models can provide cost-effective and time-efficient solutions for seismic analysis in offshore

wind turbine design, even in regions with high seismic activity. This advancement supports the growing demand for sustainable and resilient offshore wind energy infrastructure.

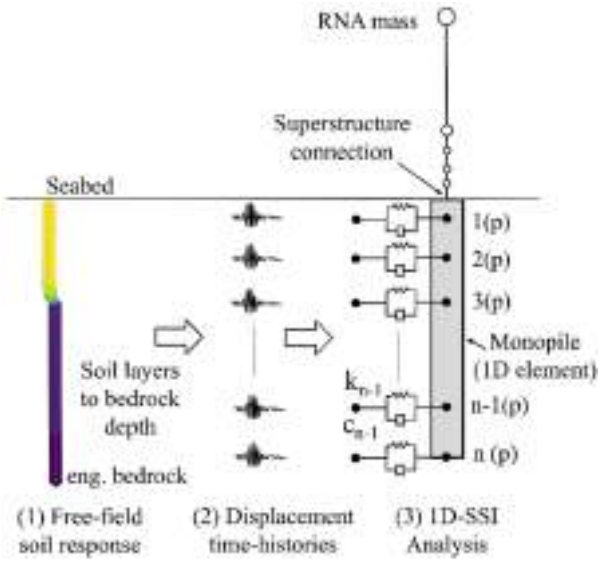

Figure 2. Flowchart of the simplified procedure for the 1D-SSI analysis: (1) free-field soil response analysis and (2) evaluation of the displacement time histories at each depth along the monopile; (3) 1D-SSI analysis.

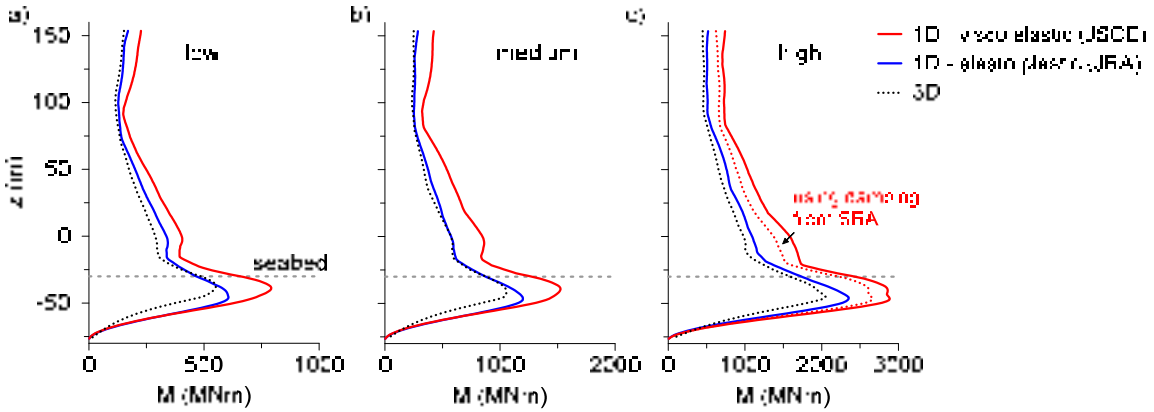

Figure 3. Average of the maximum bending moments reached in each seismicity level; (a) low, (b) medium and (c) high seismicity.

4. References

[1] Global Wind Energy Council (GWEC 2022). https://gwec.net/global-wind-report-2022/

[2] Global Wind Energy Council (GWEC 2023). https://gwec.net/globalwindreport2023/

[3] Gallese D., Go J., Hokmabadi A.S., Tsang H.T., Sasaki J., Shirai Y., Miyoshi T., Hisamatsu A. Yoshida M., Miura N. (2023). Simplified methods for seismic design of monopile-supported offshore wind turbines. OSIG 2023, doi: https://doi.org/10.3723/JFPJ4372

[4] Gallese D., Go J., Sasaki J. (2024). A comparative study of simplified models and complex 3D dynamic soil-structure interaction analysis for monopile-supported offshore wind turbines, 18th World Conference on Earthquake Engineering 2024, Milan

[5] IEA Wind TCP Task 37 (2020). Definition of the IEA Wind 15-Megawatt Offshore Reference Wind Turbine, Technical Report

[6] JSCE (2010). The Guideline for Design of Wind Turbine Sup-port Structures and Foundations, Japan Society of Civil Engineers

[7] JRA (2020). Design Specifications for highway bridges, Part IV: Seismic Design. Japan Road Association

Seismic response of large shallow buried water reservoirs – Centrifuge testing and numerical modeling

Y. M. A. Hashash[1], K. AlKhatib[2] and K. Ziotopoulou[3]
[1] University of Illinois Urbana-Champaign, Urbana, Illinois, USA
[2] Mott MacDonald, Cleveland, Ohi
[3] University of California, Davis, California 95616, USA

Abstract

Large, buried water reservoirs are increasingly utilized to store and deliver water in major urban centers. They are considered critical infrastructure that must continue to operate during and after an earthquake. This presentation will discuss the results of a detailed simulation-experimental program aimed at understanding the seismic behavior of these reservoirs and developing reliable and calibrated numerical models that captures the seismic fluid-structure-soil interaction (FSSI). The experiments and simulations showed conclusively that the response of buried water reservoirs is three-dimensional, and that two-dimensional simplification misses important damage modes, and the importance of fluid interaction. Advanced nonlinear three-dimensional (3D) FSSI numerical models of reservoirs were successful in capturing measured behavior. Parametric numerical analyses were conducted considering reservoir size, embedment depth, soil profile, and ground motion variability. The analyses show that the seismic response of reservoirs is strongly correlated with PGA, unlike conventional underground structures. Reservoir columns around the center experienced the highest demands and appear to be the point of initiation of failure. The roof in-plane shear stresses accumulate along the walls and towards the corners. 3D FSSI numerical models are reliable tools for the seismic evaluation of large, buried water storage reservoirs.

1. Problem statement

Buried water reservoirs are increasingly being built to replace open aboveground municipal water supply reservoirs in urban areas to enhance water quality and utilize their surface footprint for other purposes such as public parks or placement of solar arrays. Many of these lifeline structures are in seismically active regions and as such need to be designed to remain operational after severe earthquake shaking. However, evaluating their seismic response is challenging and involves accounting for the interaction of the structure with the stored fluid and the retained soil, in other words, accounting for fluid-structure-soil interaction (FSSI). Reasonably so, the code-based and simplified methods commonly used for their design are not always applicable which raises concerns regarding the reliability and performance of these structures. In order to properly study their resilience to earthquake damage, one needs to cumulatively consider the interactions between the surrounding soil, the structure itself, and the enclosed water during an earthquake.

2. Scope of research

The work presented herein was performed to advance our understanding of the seismic fluid-structure-soil-interaction in buried water reservoirs using centrifuge tests and numerical modeling. With the lack of available centrifuge experiments that focus on water hydrodynamics, it was first deemed important to examine the complex dynamic response of water in a scaled environment under shaking. Moreover, the reliability of numerical models and commonly used analytical and simplified methods in predicting the centrifuge measurements needed to be evaluated as well before upscaling to the full engineering system featuring the components of structure, soil, and water.

First, a series of five centrifuge model tests were performed where water tanks with a range of dimensions and configurations were subjected to sine waves and earthquake motions (a total of 130 tests) to isolate and investigate the hydrodynamic pressures generated inside the tank. The motions

used varied in peak ground acceleration (PGA) ranging from 0.003 to 0.74 g which excited the water at several frequencies, including its natural frequencies. Numerical simulations were performed using the Arbitrary Langrangian Eulerian (ALE) solver in LS-DYNA [1], a commercial FE package (Figure 1 – [2]). The numerical models prediction capability was first tested against available 1g shake table experimental data and analytical solutions in the literature. Then, the centrifuge experimental data of this study were employed to validate the numerical predictions under a scaled environment. Commonly used analytical, simplified, and code-based methods were also compared to determine their reliability when used in quantifying water dynamic response.

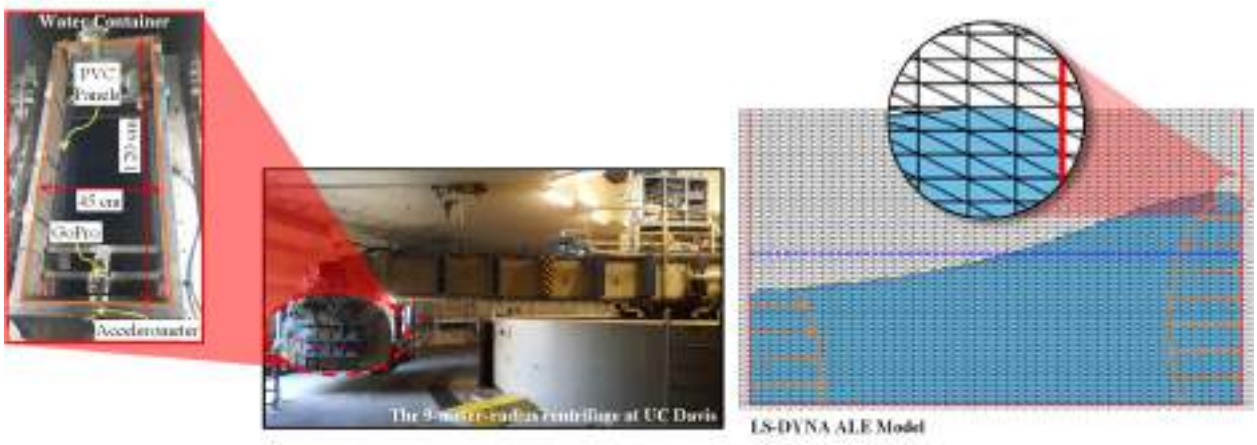

(a) (b)

Figure 1. Study of water hydrodynamics through (a) centrifuge testing and (b) ALE numerical modeling.

Then, seismic FSSI response of buried water reservoirs was studied through centrifuge model testing and advanced FE numerical modeling. Two series of centrifuge model tests were performed at different reservoir orientations to investigate one-dimensional (1D) and two-dimensional (2D) motion effects under full, half full, and empty reservoir conditions. Corresponding numerical models were developed whereby the structure, and the soil were represented by continuum Lagrangian finite elements, while the fluid was again modeled via the ALE formulation. Soil-structure and fluid-structure interface parameters were calibrated using the experimental measurements (Figure 2 – [3]). The simulations successfully captured the measured reservoir responses in terms of accelerations, bending moment increments, and water pressures, as well as the near- and far-field soil. The validated numerical models were further employed to have a more in-depth evaluation by having access to data that are not measured in the experiments.

3. Findings

The results from the first stage of this research showed that the ALE models yield a good match to the experimental recordings. Most importantly, ALE numerical modeling was found suitable for use in a performance-based design approach of complex fluid-structure-soil interaction problems. The analytical and simplified solutions showed reasonable performance under earthquake motions. However, the analytical solutions were found to overestimate the dynamic response when resonance is present. The simplified solutions were also found to underestimate the peak response when sloshing is significant.

The results from the second stage of this research found that the common assumption of plane strain is not applicable for reservoirs as their behavior was found to be truly three-dimensional (3D). This was observed by the non-uniform distribution of earth pressures, localized stress concentrations, water dynamic pressures, and the racking deformation shape of the roof. The roof slab acted as a diaphragm that distributed the lateral forces to the vertical structural elements based on their relative stiffnesses. It was found that the lateral forces were mainly resisted by the walls parallel to the motion

direction and least resisted by the columns. Furthermore, the full reservoir resulted in the highest seismic demands in the reservoir walls and roof while the empty reservoir yielded the highest base slippage. The study demonstrates that the complex reservoir seismic response is best captured by carrying a 3D FSSI numerical simulation.

The study highlighted the limitations of traditional design practices for reservoirs, emphasizing the need for more comprehensive analysis methods. Simplified approaches may underestimate or misrepresent demands due to the complex, three-dimensional nature of reservoir behavior under seismic conditions. To ensure the accurate assessment and robust design of this class of structures, it is recommended that full fluid-structure-soil interaction (FSSI) simulations are performed, considering 3D geometry and bidirectional shaking, and accounting for the presence of water.

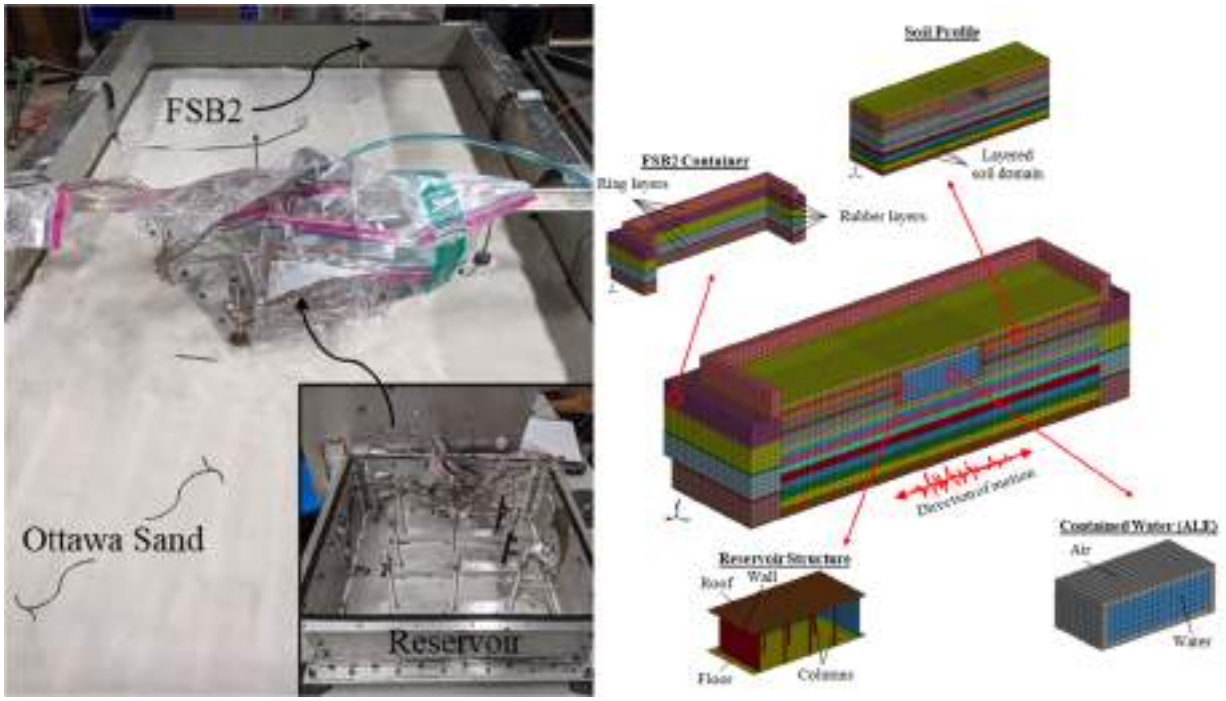

(a) (b)

Figure 2. Study of reservoir fluid structure soil interaction through (a) centrifuge testing and (b) advanced numerical modeling.

4. References

[1] LSTC. (2020). LS-Dyna keyword user's manual. Livermore Software Technology Corporation

[2] AlKhatib, K., Hashash, Y. M. A, Ziotopoulou, K., and Morales, B. (2023). Hydrodynamic pressures on rigid walls subjected to cyclic and seismic ground motions, *Earthq Eng and Str Dyn*, 53, 279–302, doi: https://doi.org/10.1002/eqe.4020

[3] AlKhatib, K., Hashash, Y. M. A., Ziotopoulou, K., and Heins, J. V. (2024). Centrifuge and numerical modeling of seismic response of buried water supply reservoirs, *ASCE J of Geotech & Geoenv Eng*, 150(3), doi: https://doi.org/10.1061/JGGEFK.GTENG-11758

Use of capacity curve in the seismic analysis of geotechnical systems

D. Gallese[1], D. N. Gorini[2], L. Callisto[3]
[1] Ove Arup and Partners, London, UK (formerly Sapienza University of Rome)
[2] University of Trento, Trento, Italy
[3] Sapienza University of Rome, Rome, Italy

Abstract

Nonlinear dynamic analysis of soil-structure systems requires advanced and time-consuming computations that may not be feasible for most practical applications. The present research is devoted on conceptualizing and validating simplified procedures that are easier to implement, yet capable of capturing the essential features of the dynamic response of the systems at hand, consistently with modern concepts of seismic performance and capacity design. The geotechnical systems herein considered include retaining structures, bridge abutments, multi-propped excavations, and tunnels. The seismic capacity of a geotechnical system is studied through nonlinear static numerical analysis (NLSA), in which equivalent inertial forces, proportional to a seismic coefficient, are applied to the system until the activation of a global plastic mechanism. The overall deformability of the system, from static conditions to failure, can be represented by a capacity curve, relating accelerations to seismic displacements of scrutiny points. The capacity curve proves to be a versatile representation of the system response under seismic loading in both displacement-based and equivalent force-based design approaches, discussed in the first and second parts of this work, respectively. The first part pertains to systems that may accumulate permanent displacements under seismic loading such as earth retaining structures, whereas the second refers to systems that cannot experience important seismic deformations, otherwise, the structural integrity of the entire structure/infrastructure would be compromised. Bridges with integral abutments (IABs) and multi-propped excavations belong to the latter category. Both methodologies are extensively validated and underscore the essential role of the capacity curve in the seismic assessment of geotechnical systems within the framework of the decoupled approach.

1. Introduction

Seismic design of geotechnical systems involves evaluating their performance under earthquake loading, which can significantly differ based on whether the system is able or not to accumulate permanend displacements. Displacing systems, such as slopes, unsupported excavations, and certain retaining structures, exhibit asymmetric behavior under seismic loading. They tend to displace both the soil and structural members towards weaker zones, leading to irreversible deformations. For these systems, a common assumption is that the structural members interacting with the soil do not reach their capacity during strong motions and are therefore regarded as non-dissipative elements. On the contrary, the soil can mobilise its strength, acting as a dissipative element. Conversely, non-displacing systems, such as deep excavations, underground frame structures, and bridge abutments, are characterized by the fact that, if the structural members are designed to remain in the elastic range, these systems cannot accumulate displacements. Therefore, it is logical to expect that the design of the first type of system adheres to the philosophy of the displacement-based approach, while the design of the second type follows the philosophy of the force-based approach.

The distinction between these systems is crucial for selecting appropriate seismic design-methodology. Among the simplified methods to be employed for a practical design, there are the ones based on the decoupled approach, whereas, differently from the advanced and complicated coupled soil-structure interactions systems, the seismic action and system response are evaluated separately and combined only at the end. This design-approach allows for a more manageable assessment of complex systems. In this context, the capacity curve is one of the way to characterise the system response following the modern philosophy of the performance based design.

In summary, identifying whether a geotechnical system is displacing or non-displacing guides the design strategy for controlling seismic performance. Nevertheless regardless of the approach, the capacity curve can be effectively used for both types of systems.

2. Methodology and discussion

The seismic capacity of a geotechnical system can be evaluated through NLSA, in which equivalent inertial forces are applied to the system, taken to be proportional to a seismic horizontal coefficient k_H representing the ratio of the horizontal acceleration to the gravity acceleration. In this context, the capacity curve can be expressed as a relationship between the seismic coefficient k_H and the corresponding horizontal displacement u_R of a point of interest, for instance the top of the embedded retaining wall depicted in Figure 1 [1]. In this analysis, commonly known as a 'incremental pseudostatic analysis' the seismic coefficient is increased progressively, until the results of the analysis indicate that a plastic mechanism in correspondence of the critical acceleration k_C is activated.

Due to the tendency of displacing systems to accumulate deformations under seismic loading, this curve can be employed in a time-domain calculation to characterise both the tangent stiffness — evaluated either on the first loading branch of the curve or along an unloading-reloading cycle (Figure 1b) — and the ultimate strength k_C of an equivalent SDOF system. In the logic of a decoupled approach, the input motion applied to the equivalent SDOF system corresponds to the seismic demand obtained from a free-field one-dimensional ground response analysis at a representative depth of the soil domain. A more detailed and comprehensive picture of this methodology, successfully validated with both numerical analyses and centrifuge tests, is discussed in [1,2,3,4,5].

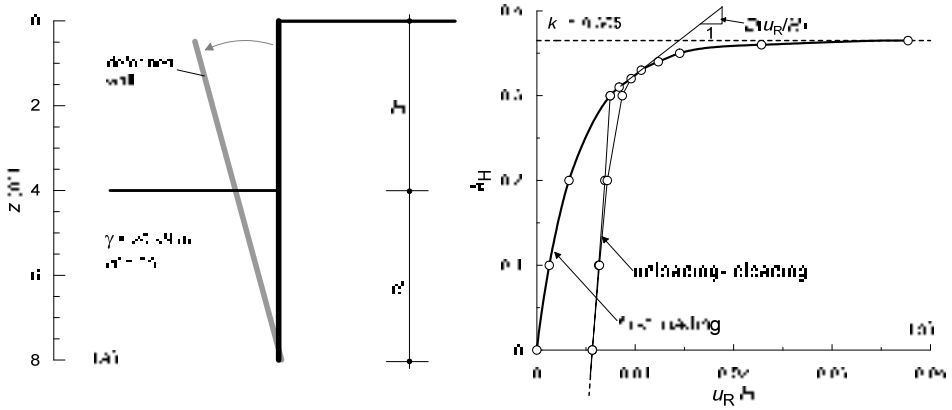

Figure 1. (a) Example embedded retaining wall; (b) non-dimensional capacity curve [1].

In contrast to displacing systems, the seismic design of non-displacing systems generally includes the evaluation of the maximum internal forces in the structural members. Using a single-span integral abutment overpass recently built in Italy as a reference, an advanced coupled 3D soil-bridge model was developed in OpenSees. To facilitate more efficient dynamic computations, a more manageable and validated equivalent 2D model was also created, as detailed in [6,7]. This 2D model serves as a benchmark for validating a simplified procedure to study the seismic behavior of the bridge in the longitudinal direction, which generally governs the overall seismic response.

In IABs, the monolithic connection between the deck and the abutments is such that the seismic response tends to be controlled by the interaction of the abutments with the surrounding soil, and especially with the approach embankments. In the context of the Capacity Spectrum Method (CSM) [8] commonly used for the seismic analysis of civil engineering structures, the capacity curve obtained from a NLSA is combined with a seismic demand, evaluated with a decoupled approach, in the form of an acceleration-displacement (AD) response spectrum. Specifically, the capacity of the system is evaluated through the application of two different distributions of equivalent inertial forces

replicating the main two deformation patterns associated with dominant vibration modes. These modes are primarily controlled by the soil response and can be reasonably determined through a modal analysis of the soil deposit including the approach embankment. The entire methodology, implemented in OpenSees and validated against results of several dynamic analyses conducted on a reference case study is summarised as a flowchart in Figure 2, where only the pattern of k_H reproducing the first soil-bridge mode is shown for simplicity.

In summary, for practical design, the seismic assessment of geotechnical systems (both 'displacing' and 'not displacing') can effectively use practice-oriented methods based on the decoupled approach. In this contect, the capacity curve, obtained through nonlinear static analysis (NLSA), plays a key role in describing the response of the systems at hand.

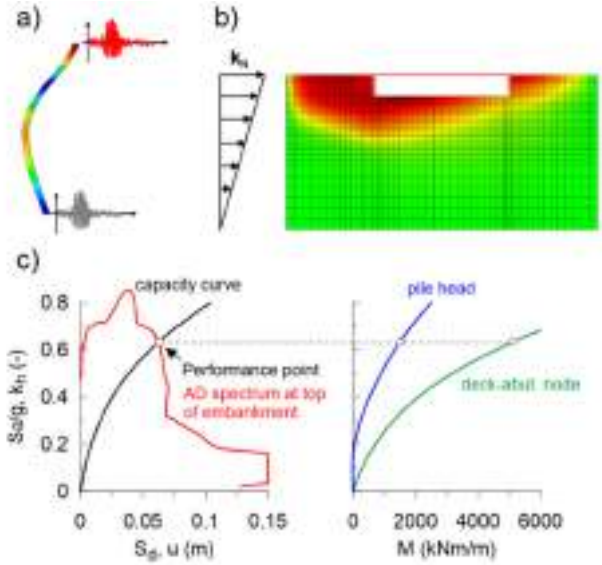

Figure 2. Recap of the simplified tool developed for the seismic design of a single-span IAB: a) Free field response used to determine acceleration at the abutment-deck node, b) Nonlinear static analysis replicating one of the two main deformation modes, c) Superimposition of the capacity curve with the seismic demand and definition of the performance point employing an iterative procedure for the determination of the equivalent damping.

3. References

[1] Callisto, L. (2019). On the seismic design of displacing earth retaining systems, In: Proceedings of the 7th ICEGE. Associazione Geotecnica Italiana, Rome, pp 239–255

[2] Callisto, L. (2014). Capacity design of embedded retaining structures, Geotechnique 64:204–214, doi: https://doi.org/10.1680/geot.13.P.091

[3] Laguardia, R., Gallese, D., Gigliotti, R., Callisto, L. (2020). A nonlinear static approach for the prediction of earthquake-induced deformation of geotechnical systems, *Bull. Earthq. Eng*, 18, No. 15, 6607–6627, doi: https://doi.org/10.1007/s10518-020-00949-2

[4] Callisto, L. (2024). A method for the seismic design of multi-propped retaining walls, *Italian Geotechnical Journal* (1), doi: dx.doi.org/10.19199/2024.1.0557-1405.044

[5] Gallese D., Callisto L. (2024). A simple tool for the capacity curve of embedded retaining systems – part I and part II, Ground Engineering, July and August/September issue, doi: https://www.geplus.co.uk/

[6] Gallese, D. (2022). Soil–structure interaction for the seismic design of integral abutment bridges: from advanced numerical modelling to simplified procedures, PhD thesis, Sapienza University of Rome. See https://hdl.handle.net/11573/1666837

[7] Gallese, D., Gorini, D.N., Callisto, L. (2023). A nonlinear static analysis for the seismic design of single-span integral abutment bridges, Gèotechnique, doi: https://doi.org/10.1680/jgeot.22.00229

[8] Freeman, S.A., Nicoletti, J.P., Tyrell, J.V. (1975). Evaluations of existing buildings for seismic riska case study of Puget sound naval shipyard, Bremerton, Washington, In: Proceedings of the 1st US National conference on earthquake engineering. Berkeley, USA

Kinematic interaction between two nearby foundations

E. Zeolla[1], F. de Silva[2] and S. Sica[1]
[1] University of Sannio, Benevento, Italy
[2] University of Federico II, Naples, Italy

Abstract

The dynamic interplay between soil and foundation may significantly influence the response of a construction during an earthquake. Deep foundations can filter the seismic excitation, causing the foundation input motion to differ substantially from the free-field ground motion. In the sub-structure approach, this phenomenon is called kinematic interaction and has been deeply investigated in the literature. Uncoupled methods are often used as valid alternatives to handle soil-structure interaction problems to optimize computational accuracy and analysis time. Several authors have derived frequency-dependent transfer functions that relate the steady-state harmonic motion experienced by the foundation to the amplitude of the corresponding free-field motion of the soil. Nevertheless, these functions have been obtained assuming rigid, massless, and isolated foundations (i.e., no other foundations nearby). Foundations, however, have their own mass. Furthermore, they are often built in densely urbanized areas, where buildings and infrastructure may be very close to each other, thus experiencing multiple interaction phenomena through the soil. This paper presents a numerical study aimed at evaluating the effect of Foundation-Soil-Foundation Interaction (FSFI) on the classical kinematic interaction coefficients I_u and I_θ. The parametric study was conducted through a 2D finite difference code, varying the embedment of the deep foundation and the distance at which a nearby shallow foundation is placed. From the numerical results obtained, new transfer functions were derived so that the foundation motion of the target structure may be computed considering those factors typically neglected in practice, such as the proximity among structures and their foundations.

1. Introduction

The dynamic behavior of a structure may strongly be affected by the constraints assumed at its base. The fixed-base assumption is not always suitable due to soil-foundation compliance, which could modify the dynamic and seismic response of the superstructure. In addition, the foundation input motion (FIM) can differ substantially from the free-field ground motion, leading to the so-called kinematic interaction ([11], [3], [10]).

For a rigid, massless, cylindrical or rectangular foundation, embedded in a homogeneous elastic or linear viscoelastic half-space, kinematic effects are relevant ([3]-[9]): under seismic actions, the foundation, due to its stiffness, cannot follow the ground deformations, and the wave field reflected from its walls interferes with the incident waves propagating in the subsoil. Kinematic transfer functions, I_u and I_θ, were thus defined to link in steady-state conditions the translation and rotation motion of the foundation to that of the free-field soil ([1]-[3], [10]).

However, these functions were derived assuming a stand-alone foundation, i.e., a foundation without any other foundations nearby. Nevertheless, structures are often placed in urbanized environments with very small building-building distance [12], so that Foundation-Soil-Foundation Interaction (FSFI) phenomena through the underlying soil could arise in addition to the classical soil-structure interaction (SSI).

This paper presents the results of a numerical study aimed at evaluating the effect of FSFI on the well-known kinematic interaction coefficients, I_u and I_θ. The parametric study was conducted through the finite difference code FLAC2D, varying embedment of the deep foundation and the distance at which a shallow foundation is placed nearby. New transfer functions, I_u and I_θ were derived from the numerical results to compute the FIM in the case of a shallow foundation close to a deeper one (caisson).

2. Numerical model description

The reference scheme of the numerical study is shown in Fig. 1 and depicts a shallow foundation of width, B, placed at a distance, S, from a deep foundation of height, H, and base, B. In the performed time-domain parametric analyses, the depth, H, of the caisson and the distance of the caisson from the shallow foundation, S, were varied such that the values of H/B and S/B were varied between 0.5 and 2, for a total amount of nine cases analyzed.

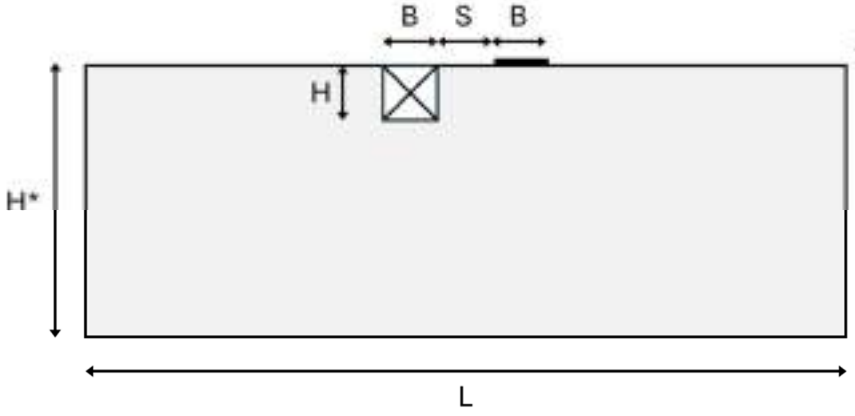

Case	H/B	S/B
1	0.5	0.5
2	0.5	1
3	0.5	2
4	1	0.5
5	1	1
6	1	2
7	2	0.5
8	2	1
9	2	2

Figure 1. Reference scheme with a list of parameters used in the numerical study.

To unravel the physics of the problem, the soil was assumed to be an isotropic linear viscoelastic material (ρ=1900 kg/m^3, V_S=100 m/s and Poisson's coefficient ν=0.3). Rayleigh viscous damping (1.2 % at the center frequency of 3.3 Hz) and perfect contact between the foundations and the soil elements were assumed. The rigid and massless foundations were modeled through elastic beams with low mass density ($\rightarrow$ 0) and high stiffness (E=5 GPa; A=7 m^2; I=6 m^4; ρ=8 kg/m^3).

Free-field boundary conditions were applied along the sidewalls of the model, while viscous dampers and dynamic input, defined as a time history of horizontal velocity with increasing amplitude, duration of 60 s, and frequency rising linearly over time from 0.5 to 10 Hz, were applied at the base of the model to reproduce an upward shear wave propagation. The mesh elements have a maximum size of 0.5 m near the foundation to correctly describe the minimum wavelength of the applied signal ($\lambda_{min}=V_S/f_{max}$=10 m).

During the analyses, the time histories of the horizontal displacement, u_h, at the center of both the caisson and the shallow foundation together with the vertical displacements, u_{v1} and u_{v2}, of the same points were recorded. The complex kinematic interaction functions were obtained through the following relations:

$$I_u = u_{FIM}/u_{FF0} \tag{1}$$

$$I_\theta = \theta_{FIM} \cdot H/u_{FF0} \tag{2}$$

where u_{FF0} is the Fourier transform of the horizontal displacement at the ground surface, u_{FIM} is the Fourier transform of the horizontal displacement of the caisson (or shallow foundation), and θ_{FIM} is the caisson (or shallow foundation) rotation obtained as $(u_{v1}-u_{v2})/B$.

3. Results and discussion

For brevity, only the results obtained for the shallow foundation will be provided to highlight how its motion could be affected by a nearby caisson. Figure 6 shows the kinematic interaction coefficients, I_u and I_θ, as a function of H/λ for fixed values of the S/B and B/H ratios. With reference to I_u, it may be observed that a very slender caisson (e.g., B/H=0.5) is always beneficial for a nearby shallow foundation when H/λ<0.3, irrespectively of S/B. For H/λ > 0.3, the beneficial contribution of the

caisson ($I_u < 1$) is assured only at very short distance from it (S/B ≤1). For squatter caisson (B/H equal to 1 or 2), the higher the B/H ratio the higher I_u, especially at short distance S/B. In this case, the caisson presence is detrimental for the neighboring shallow foundation since an amplification of its horizontal motion up to 20% with respect to the free-field soil motion was obtained. An opposite trend may be observed for the rotational component of the motion experimented by the shallow foundation, i.e. the closer the deep caisson (B/H=0.5) is to the shallow foundation (S/B=0.5), the greater its rotation. It is worth underlining that for a shallow foundation under vertically propagating SH waves this spurious kinematic rotation would have been zero if the nearby caisson had not been present. This is a further aspect of FSFI (Zeolla et al., 2024).

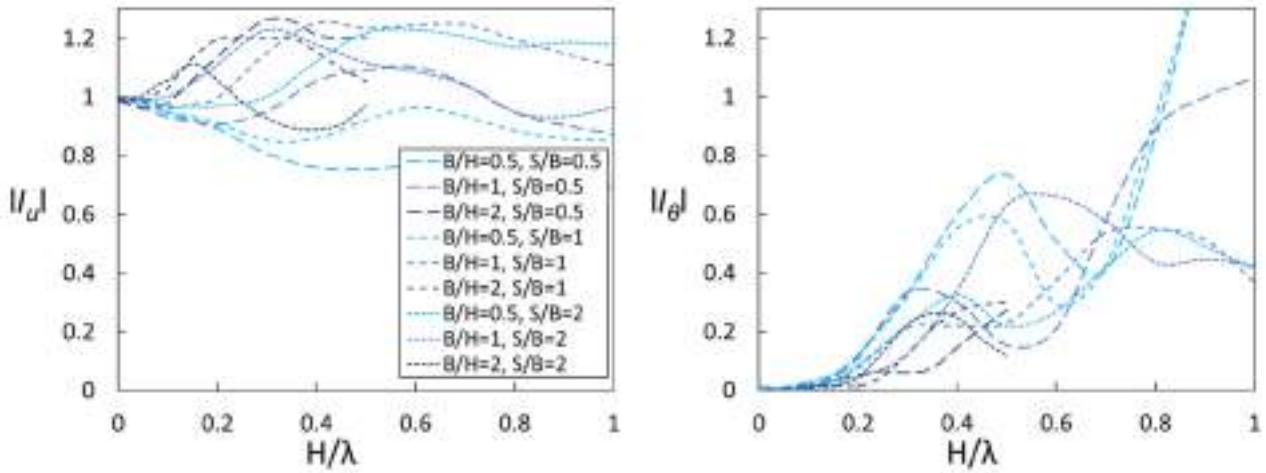

Figure 2. Kinematic interaction coefficients, I_u and I_θ for a shallow foundation close to a caisson.

4. References

[1] Conti, R., Morigi, M., & Viggiani, G. M. (2017). Filtering effect induced by rigid massless embedded foundations, *Bulletin of Earthquake Engineering*, 15, 1019-1035

[2] Conti, R., Morigi, M., Rovithis, E., Theodoulidis, N., & Karakostas, C. (2018). Filtering action of embedded massive foundations: New analytical expressions and evidence from 2 instrumented buildings, *Earthquake Engineering & Structural Dynamics*, 47(5), 1229-1249

[3] Elsabee, F., Morray, J.P. (1977). Dynamic behavior of embedded foundation. Rep. No. R77-33, Department of Civil Engineering, Massachusetts Institute of Technology, Cambridge

[4] Fan, K., Gazetas, G., Kaynia, A., Kausel, E., & Ahmad, S. (1991). Kinematic seismic response of single piles and pile groups, *Journal of Geotechnical Engineering*, 117(12), 1860-1879

[5] Gazetas, G. (1984). Seismic response of end-bearing single piles, *International Journal of Soil Dynamics and Earthquake Engineering*, 3(2), 82-93

[6] Gerolymos, N., & Gazetas, G. (2006). Winkler model for lateral response of rigid caisson foundations in linear soil, *Soil Dynamics and Earthquake Engineering*, 26(5), 347-361

[7] Karabalis, D. L., & Beskos, D. E. (1986). Dynamic response of 3-D embedded foundations by the boundary element method, *Computer Methods in Applied Mechanics and Engineering*, 56(1), 91-119

[8] Luco, J.E., Wong, H.L. (1987). Seismic response of foundations embedded in a layered half-space, *Earthqu Eng Struct Dyn*, 15, 233–247

[9] Mita, A., Luco, J.E. (1989). Impedance functions and input motions for embedded square foundations, *J Geotech Eng ASCE*, 115, 491–503

[10] Mylonakis, G., Nikolaou, S., Gazetas, G. (2006). Footings under seismic loading: analysis and design issues with emphasis on bridge foundations, *Soil Dyn Earthq Eng*, 26(9), 824–853

[11] Veletsos, A.S., Prasad, A.M., Wu, W.H. (1997). Transfer functions for rigid rectangular foundations, *Earthqu Eng Struct Dyn*, 26, 5–17

[12] Zeolla, E., de Silva, F., Sica, S. (2024). Towards a practice-oriented procedure to account for static and dynamic interaction among three adjacent shallow foundations, *Computers and Geotechnics*, 170, 106242

Soil-Structure Interaction Solution in Liquefiable Soils: Direct Method vs Substructure Method

M. Batuhan Kocak [1], Y. Dizman[1], O. Alver[2] and E. E. Eseller Bayat[1]
[1] Istanbul Technical University, Istanbul, Turkey
[2] Delft University of Technology, Delft, The Netherlands

Abstract

Within the scope of the study, superstructure analyses were carried out to examine the effect of soil-structure interaction on the structure response in liquefiable soil. Building properties and soil properties were created according to a reference model published in the literature, and parametric analyses were planned by changing H_L (liquefiable soil layer thickness). Analyses for the direct models and sub-structure approaches were carried out in Plaxis2D and ETABS programs. Non-liquefiable and liquefiable soil models were created, and the effects of the liquefiable soil layer on the superstructure and foundation responses were examined by considering the soil-structure interaction. In order to investigate the effect of liquefied soil in the soil-structure interaction response, analyses were carried out by both PM4Sand and HS-Small models. The created Plaxis2D and ETABS models were generated for two different liquefiable soil thicknesses and a single structure for a given earthquake. The foundation input motions and the structure responses such as the roof spectral accelerations were compared based on the acceleration time history analyses. The effectiveness of the sub-structure method in the design of structures built in liquefiable soils has been discussed.

1. Introduction

The code-based design spectrum is used for the traditional seismic design of structures in earthquake-prone areas. However, the code-based design method is insufficient in liquefiable locations, necessitating site-specific analysis. The main objective of site-specific analysis is to determine the strain-compatible soil parameters (damping ratio and degraded soil modulus), which are the input for soil-structure interaction (SSI) calculations, as well as the foundation input motion (FIM).

The impact of liquefied soil layers on the structural reactions has been studied by a number of researchers (Tokimatsu et al., 2019, Kirkwood and Dashti, 2018, Dashti et al., 2010). In this study, the effect of liquefiable layer beneath the structure was studied using both HS-Small and PM4Sand (susceptible to liquefaction) and the differences in terms of roof spectral acceleration values were compared and evaluated. The analyses were performed for two different liquefiable soil thicknesses (3m and 6m) for both direct and substructuring methods.

2. Numerical Models

Within the scope of the study, in order to investigate the effect of soil-structure interaction on the structure response in liquefiable soils, superstructure analyses were carried out in ETABS and Plaxis2D programs. First, liquefiable and non-liquefiable soil models were created in Plaxis2D and a direct model was created by considering the soil-structure interaction in order to investigate the effects of the liquefiable soil layer on the superstructure and foundation responses. Then, an inertia model was created with the sub-structure approach in the ETABS program to investigate the effects of the liquefiable soil layer on the superstructure and foundation responses. The direct model (a) and the inertial model (b) created are shown in Fig. 1. the numeric models and input parameters were reported in detail by Kocak et al. (2024). Structural features and soil properties were formed according to the baseline model, and parametric analyses were performed in terms of the liquefiable soil layer thickness (HL) which were selected as 3m and 6m.

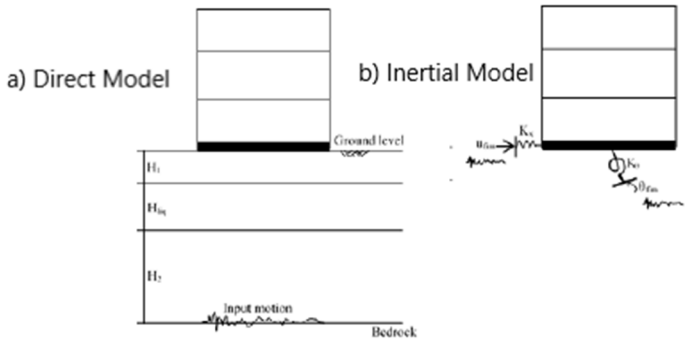

Figure 1. Soil-Structure Interaction Analysis a) Direct Method b) Inertial Model in Sub-structure Approach.

In this context, the structure geometries were selected as a 12m foundation width, 3 stories with 12m height, and 1m embedded shallow foundation.

The study utilized both PM4Sand and HS-Small models to explore the impact of liquefaction on soil-structure interaction. The HS-Small (Brinkgreve et al., 2010) soil constitutive model was exclusively employed to generate the non-liquefiable models. Additionally, PM4Sand (Boulanger & Ziotopoulou, 2017) characterized the behavior of the liquefiable soil layer. The linear elastic bedrock layer, 1 meter thick, was defined as the bottom boundary in each analysis.

The model dimensions were set to 120m width and 21m height to minimize boundary effects. Above the liquefiable layer, there was a 2m thick very dense sand layer with a relative density (D_r) of 90%. The liquefiable layer, with a D_r of 50%, was modeled at depths of 3m and 6m for two different groundwater levels (HL). Below this liquefiable layer, a 20m depth included a very dense sand layer with D_r of 90%.

2.1. Direct Model for Soil-Structure Interaction Analysis

The superstructure was simulated in a direct model and inertia model using a 2D reinforced concrete frame system incorporating the building configurations detailed in Bray and Macedo (2017) The parameter values such as flexural stiffness (EI) and axial stiffness (EA) of beams, columns, and foundations were used the same as in Bray and Macedo (2017) modeled as frame elements in ETABS and Plaxis2D software. The analysis was performed according to the plane strain method. The super-structural columns and the mat element were defined as plate elements. Direct models were created for non-liquefiable (a) and liquefiable soils (b) as shown in Fig. 2.

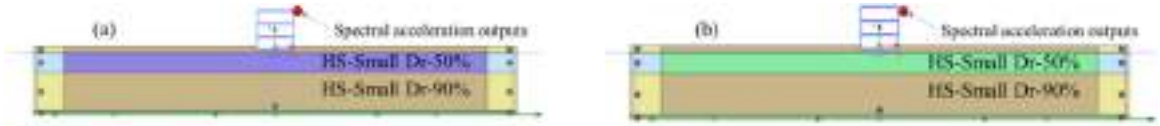

Figure 2. Plaxis2D Direct Model with 3m and/or 6 m non-liquefiable (a) and liquefiable (b) layer.

2.2. Sub-structuring Approaches for Soil-Structure Interaction Analysis

The soil-structure interaction analyses were performed as acceleration-dependent and the kinematic and inertial interaction results were combined through superposition principle. The acceleration records obtained from the kinematic interaction analyses were superposed with the inertial interaction results.

Impedance parameters representing the soil-foundation system spring constants and damping ratios were derived from the Plaxis2D program, using the degraded shear modulus (G) of the soil analyzed with HS-Small and PM4Sand models, based on shear strain variations with depth.

To model the interaction, stiffness and damping ratios of springs were defined for rotational, horizontal, and vertical degrees of freedom using link elements. A connection element was placed at

each end of the foundation, ensuring appropriate rigidity and damping characteristics were considered.

3. Comparison of numerical models and analysis results

The structural responses in terms of spectral roof accelerations considering both direct and substructure method were represented in Figs 3(a). These analyses were performed for both HS-Small and PM4sand constitutive models to represent the effect of liquefaction on the structural responses. The spectral accelerations values obtained from liquefiable model (PM4Sand) were calculated lower than non-liquefiable model (HS-Small). The same effect was observed for the inertial analysis due to the both the lower spring values which were defined at the bottom of the structure and the base input motions. Additionally, the effect of the thickness of the liquefiable layer was studied. The Figure 3 (b) shows the response spectra of the accelerations obtained from the 6m liquefiable soil model analysis. It is observed that the damping effect is directly related with the thicknesses of the liquefiable soil layer and relative density.

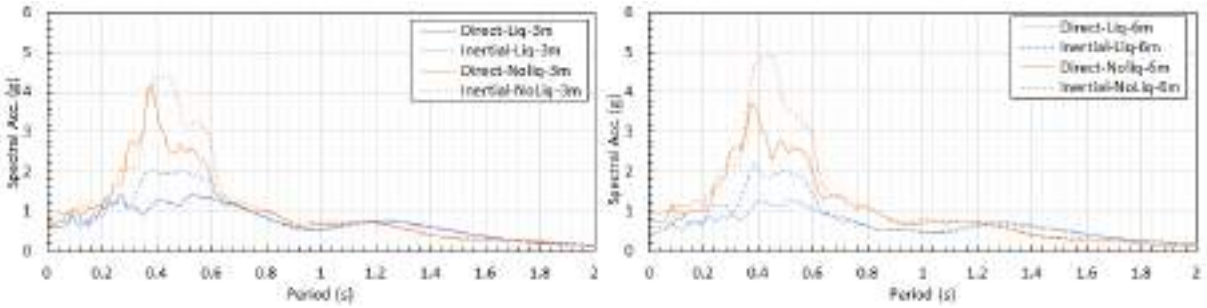

Figure 3. a) Spectral acceleration comparison for 3m liquefiable soil model, b) Spectral acceleration comparison for 6m liquefiable soil model.

4. References

[1] Tokimatsu, K., Hino, K., Suzuki, K., Ohno, K., Tamura, S., Suzuki,Y. (2019). Liquefaction-induced settlement and tilting of buildings with shallow foundations based on field and laboratory observation. *Soil Dynamics and Earthquake Engineering*, 124, 268-279

[2] Bentley Systems (2022). PLAXIS 2D CONNECT Edition (V22 Update 2) [Computer Software]

[3] ETABS 2019 (2019). Extended Three Dimensional Analysis of Building Systems. California. Computer and Structures Inc. [Computer Software]

[4] NEHRP. (2012). Consultants Joint Venture. Soil-structure interaction for buildings structures, Technical Report NIST GCR 12-917-21, National Institute of Standards and Technology.

[5] Brinkgreve, R. B. J.,Engin, E. Engin, H. (2010). Validation of empirical formulas to derive model parameters for sands. In T. Benz, S. Nordal (eds.), 7th European Conference Numerical Methods in Geotechnical

[6] Boulanger, R. W., Ziotopoulou, K. (2017). PM4Sand (version 3.1). A sand plasticity model for earthquake engineering applications. Report No. UCD/CGM-17/01, March, Boulanger_Ziotopoulou_PM4Sand_v31_CGM-17-01_2017.pdf, 112pp.

[7] Bray, J., Macedo, J. (2017). 6th Ishihara lecture: Simplified procedure for estimating liquefaction induced building settlement. *Soil Dynamics and Earthquake Engineering*, Berkeley, University of California

[8] Kocak, M. B., Dizman, Y., Alver, O., Eseller-Bayat, E. E. (2024). Effect of Soil-Structure Interaction (SSI) on the Surface Accelerations in Liquefiable Soils, 8th International Conference on Earthquake Geotechnical Engineering (8ICEGE), Osaka, Japan

FLAC2D Simulation of a Bulkhead Wall in Liquefiable Soil Subject to Earthquake Excitation

N. Goswami[1], K. Syngros[2] and G. Xing[3]
[1] Langan Engineering and Environmental Services, San Francisco, California, Unites States
[2] Langan Engineering and Environmental Services, New York City, New York, United States
[3] Langan Engineering and Environmental Services, San Jose, California, United States

Abstract

The main objective of our study was to assess the effectiveness of a ground-improvement scheme that would densify the potentially liquefiable soils behind a proposed 70-foot-deep bulkhead wall and optimize the design of the wall itself while satisfying the project's performance-based criteria per ASCE 61-14. We evaluated the effects of wall design to understand the moment demands and the consequent displacements at the end of the design earthquake excitations at the bulkhead wall.

FLAC2D was used to model the soils, bulkhead wall, and slope behind the wall, for three ground motions corresponding to a design earthquake level of shaking per ASCE 61-14. Soils that have a high relative density were modeled as a Mohr Coulomb material with calibrated damping parameters. Liquefiable soils, before and after proposed improvement were modelled using the PM4SAND model. The bulkhead wall was modeled using elastic beam elements.

The soil-model parameters were based on field measurements for large-strain and small-strain stiffness parameters. A two-dimensional-plane strain analysis was conducted which is representative of the central portion of the 130-foot-long bulkhead wall.

The residual displacement values at the end of the base excitation were about 7 feet at the top of the wall. The moment magnitudes varied from about 800 kip-ft to about 1,000 kip-ft, depending on the different Design Level motions. The location of high moment demands on the wall roughly coincided with the depth of interface between liquefiable and competent soil.

1. Project Overview and Background

The project involves construction of bulkhead wall in a highly seismic location in the United States of America. Several boring logs in the area of interest were assessed to develop an idealized cross section. Preliminary liquefaction analysis showed high soil liquefaction susceptibility. Thereafter, decisions were made on the need of ground improvement to limit the effect of soil liquefaction on the bulkhead wall. ASCE 61-14 requires numerical analysis to substantiate the design of bulkhead wall in liquefiable soils. In this article, bending moments and soil displacements are assessed for a single wall type.

2. Development of Input Time Series

Based on the deaggregation from the United States Geological Survey (USGS) Unified Hazard Tool, the probabilistic seismic hazard analysis (PSHA) is dominated by the a subduction interface seismic source, with magnitude of about nine point two (9.2). We selected records using the metadata obtained from the NGA-Sub Flatfile R211022, dated October 2021. Time series were developed for three design categories, i.e., Design Earthquake (DE), Contingency Level Event (CLE), and Operating Level Event (OLE).

3. Material Properties

To determine representative properties for all soil units (summarized in Tables 1 and 2), we used the SPT data from the relevant borings in the area of the interest. The SPT data was classified into corresponding soil units based on their location and depth. For each soil unit, we calculated the best estimate of $(N_1)_{60}$ values and shear wave velocity (V_s). We then assigned the effective friction angle

(f'), coefficient of lateral earth pressure (K_0) and Poisson's ratio (ν) for each soil units based on $(N_1)_{60}$. Best estimate for PM4SAND [1] properties is developed from empirical correlations.

Table 1. Best estimate of properties of soil units modeled as Mohr Coulomb.

	$(N_1)_{60}$	V_s (ft/s)	f' (°)	K_0	ν
Fill	54	545	41	0.35	0.26
Loose sand	11	355	34	0.44	0.30
Medium sand	23	725	37	0.40	0.28
Dense sand	46	805	41	0.35	0.26
Glacial	41	955	40	0.36	0.26
Bedrock		2,493		0.25	0.20

Table 2. Best estimate of PM4SAND material properties.

	Soil zone	RD	Go	h_{p0}
Loose sand	Unimproved	48%	405	0.05
Medium sand		70%	775	0.01
Loose sand (85% RD)	Improved	85%	835	0.05
Medium sand (85% RD)		85%	1,125	0.01

4. Model Geometry

To develop the geometry of the slope and soil stratigraphy (Figure 1), we used the data from eleven boring logs. The boring locations were superimposed on a satellite photo. One idealized subsurface cross section, A-A', was selected as the basis of our subsequent analyses in this article and is shown in Figure 1. We identified six major soil and rock units at the site, including (1) fill, (2) loose sand, (3) medium-dense sand, (4) dense sand, (5) glacial soils, and (6) bedrock for the idealized cross sections. The model contains predominantly quadrilateral elements approximately 3ft long. The bulkhead wall is 70 ft long which extends from el. 20 ft to el. -50 ft. The location between the wall and insitu material is filled with structured fill with properties same as fill.

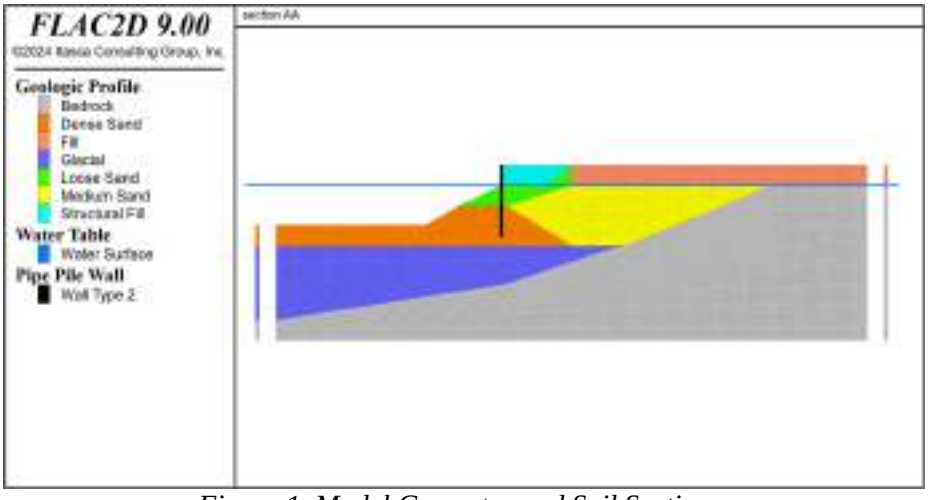

Figure 1. Model Geometry and Soil Sections.

5. Modeling Considerations

Using the computer program FLAC2D [2], we modeled a two-dimensional section shown on Figure 1. The analysis was performed for pipe-pile wall having an equivalent bending stiffness of 118*106 kips-in^2 per foot. A final relative density (RD) of 85% was modeled for the improved sandy layers

behind the wall (land side only) subjected to 3 ground motions of the Design Earthquake (DE) level. Input motions were applied as stress waves at the bottom of the model and the sides of the model had free-field elements. Liquifiable soils were modeled as PM4SAND material whose properties are shown in Table 2.

6. Results

Figure 2 presents the post-earthquake residual displacements for the input motion which resulted in the largest residual displacements. Figure 3 presents the envelope of the instantaneous bending moments with depth for the pipe wall and post-earthquake residual lateral displacement for the DE level motions.

From the examination of the results presented in Figure 3, we note that maximum instantaneous bending moment of about 940 kip-ft/ft. The maximum residual movement is about 7 feet, with a maximum differential between the top and the toe of the wall of about 5 feet.

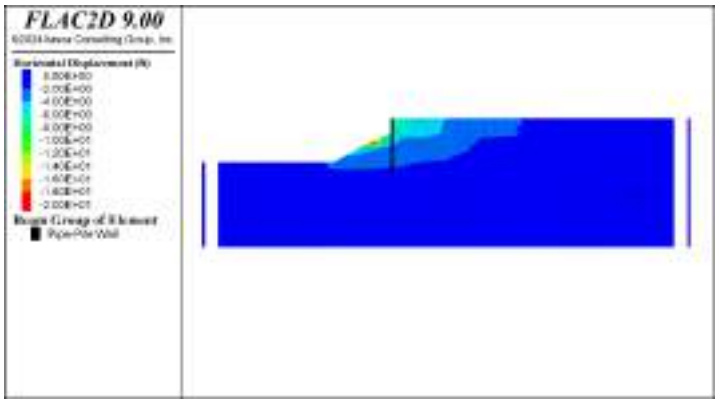

Figure 2. Post-earthquake soil residual displacement after being subjected to DE level earthquake.

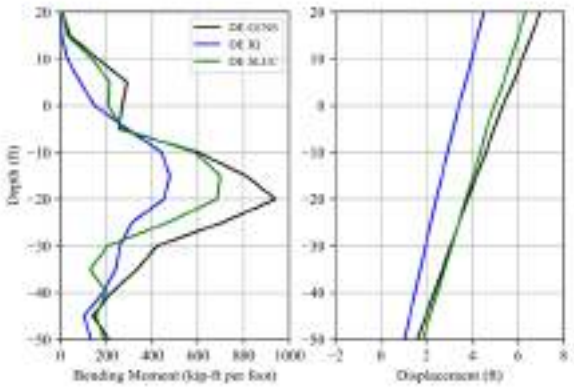

Figure 3. Envelope bending moment with depth for the pipe wall, and post-earthquake residual lateral displacement for the DE level earthquake.

7. References

[1] Boulanger, R. W., Ziotopoulou, K. (2022). PM4Sand (Version 3.2): A sand plasticity model for earthquake engineering applications, Report No. UCD/CGM-22/02, Department of Civil and Environmental Engineering, University of California, Davis, CA, March, 112 pp

[2] Itasca Consulting Group, Inc. (2024) FLAC3D — Fast Lagrangian Analysis of Continua in Two-Dimensions, Ver. 9.0. Minneapolis: Itasca

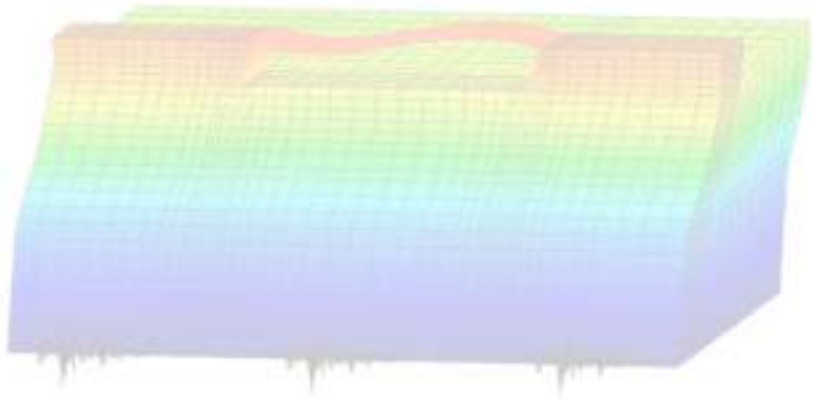

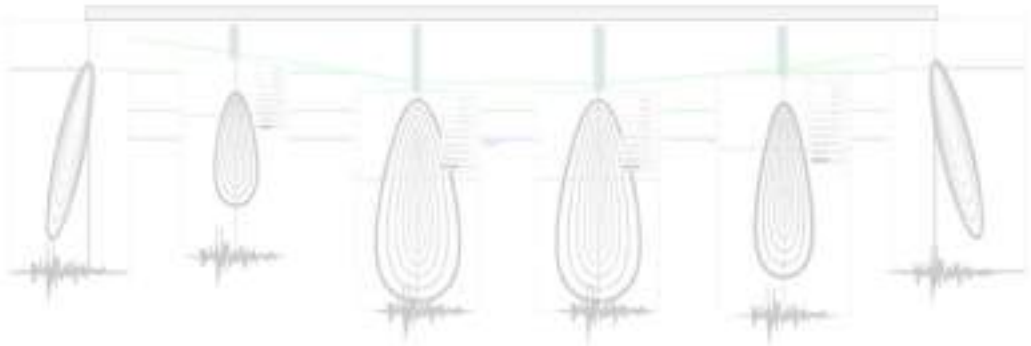

2. Artificial Intelligence-based approaches to dynamic soil-structure interaction

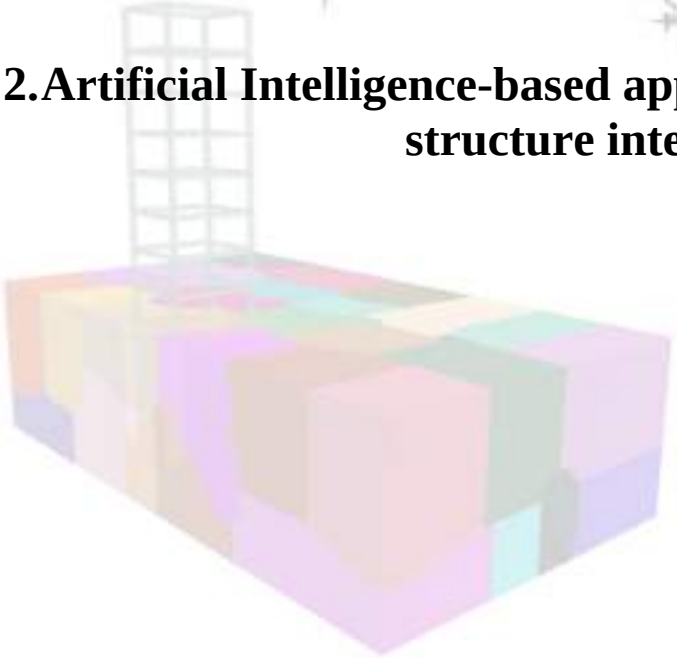

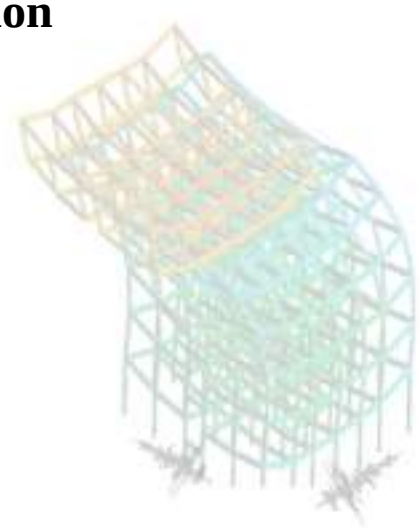

Region-Scale Seismic Simulations and Opportunities to Exploit their Output through Machine Learning Techniques

E. Taciroglu[1] and W. Zhang[2]
[1] University of California Los Angeles, Los Angeles, California, USA
[2] Texas Advanced Computing Center, Austin, Texas, USA

Abstract

Regional-scale earthquake simulations are becoming more readily available due, in part, to advances in computational capabilities and the availability of metadata to develop detailed input models, including regional geotechnical/geological data and civil engineering asset inventories. Massive data/metadata bracket both ends of these simulations as input and output, which bear inherent aleatory and epistemic uncertainties, requiring ensembles of analyses. However, each simulation typically has a very high cost and is unfeasible to execute (or re-execute) on-demand to explore the sample space through simple grid searches, even with access to the most advanced computing hardware. Machine learning techniques provide opportunities in multiple subdomains of these simulations, from devising large asset inventories to imputing missing metadata on the input side, from interpreting and rapidly classifying results on the output side to establishing models that link input to output to bypass the simulations altogether. This paper provides a brief overview of opportunities in this realm of research, attempting to delineate major avenues. The prior related studies discussed herein are only meant to illuminate the subject matter and are not meant as a comprehensive review.

1. Regional Earthquake Simulations: Rupture to Rafters

It is now well understood that region-scale assessments are needed in order to accurately quantify seismic resilience due to the inherently interconnected and distributed nature of the built environment [1, 2]. While there are numerous pathways to achieve this, there appears to be a consensus that is building around computational tools that enable so-called "rupture-to-rafters" type analyses, which encompass characterization of site-specific hazards [3], development and analysis of structure-specific models to determine asset and system fragilities [4], and examination of holistic loss and recovery simulations under ensembles of scenario events [5-8].

While the concept of "rupture-to-rafters" analyses was articulated more than a decade earlier [9], the development of requisite tools and databases took some time and have only recently become adequately mature and effective, at least for research purposes (see, for example,[10]). On the hazard characterization side, data-driven [11] and semi-analytical models [3] with ever-increasing complexity [12, 13] have dominated both research activities and engineering practice. Nevertheless, advances in computational capabilities continuously paved the way for fully physics-based simulation tools [14, 15]. The validity of such simulation codes as Hercules [16], SPEED [17], and SW4 [18] have been well examined, and their abilities have routinely increased in capturing regional seismic wave propagation at resolutions that will now impact earthquake engineering practice (e.g., > 10 Hz). Multiple efforts around the world have also aimed to make both the simulation codes and their output readily available in databases [19] and in formats adaptable as input to commercial or open-source codes for localized nonlinear analyses of soil-foundation-structure systems [20-22]. Not surprisingly, the regional scale analyses utilizing these tools are becoming more common and impactful [21, 23].

One of the aforementioned tools is by Taciroglu and co-workers [21]. It incorporates Hercules and various other tools for model inventory generation and localized soil-structure interaction analyses, such as the domain reduction method and perfectly matched layers [22]. Its workflow begins with the construction of ensemble fault-rupture scenarios and utilization of these in seismic wave propagation simulations, ending with structure-specific analyses (Figure 1). As stated above, all ingredients of such workflows are laden with data and metadata (whether physical input data extracted from field

surveys or computed/synthetic—albeit physics-based—output data from the simulations. The following section outlines a few opportunities to use these data to generate effective and accurate machine-learning models, which can enhance the utility and impact of regional simulations.

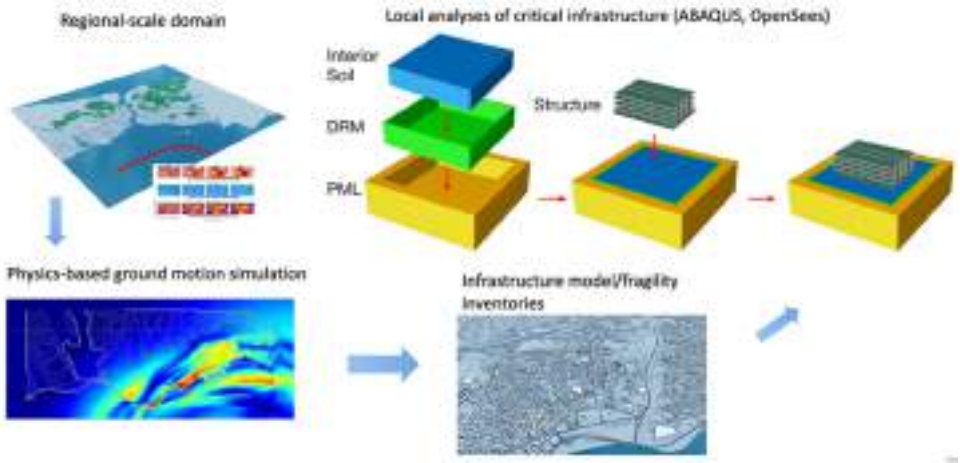

Figure 1. "Rupture-to-rafters" seismic assessment workflow by Taciroglu and co-workers [23, 24].

2. Machine Learning Applications to Regional Earthquake Simulations

The past decade brought extreme advances in Artificial Intelligence (AI) and Machine Learning algorithms. Coupled with commensurate progress in computing hardware (e.g., GPUs), applications have rapidly proliferated, including those in earthquake engineering [24], with a promise of more to come that will potentially dominate the research activities in this area. Omitting a detailed review for the sake of brevity, Table 1 outlines potential threads of research that can make use of regional simulation or help improve their effectiveness and accuracy.

Table 1. Potential ML/AI applications in regional seismic simulations.

Learning Class	Description	Common Algorithms	Potential Applications
Supervised	Train on labeled datasets to learn mapping from inputs to outputs, make predictions on new data.	Linear Regression, Random Forests, SVM, ANN	- Predict structural performance and damage - Improve eq. early warning
Unsupervised	Works with unlabeled data to find hidden patterns or groupings.	k-Means Clustering, PCA	- Anomaly detection (e.g., liquefaction)
Semi-Supervised	Use a small amount of labeled data combined with a large amount of unlabeled data to improve accuracy.	Self-training	- Develop model inventories through imputation - Improve model accuracy
Transfer	Applies knowledge from one domain to a related problem	Pre-trained NNs, Domain Adaptation	- Rapid damage classification
Ensemble	Combines multiple models to reduce variance.	Random Forests, Gradient Boosting, Bagging, Stacking	- Predict earthquake impacts
Physics-Informed	Integrates physical laws into learning, ensuring predictions adhere to known physics.	Physics-Informed NNs, Hybrid Models	- Modeling SSI - Simulating struct. response under seismic load

3. References

[1] Du, A., Wang, X., Xie, Y., Dong, Y. (2023). Regional seismic risk and resilience assessment: Methodological development, applicability, and future research needs – An earthquake engineering perspective, *Reliability Engineering & System Safety*, 233, 109104

[2] Davis, C., Johnson, L., Kiremidjian, A., Kwasinski, A., O'Rourke, T., Stanley, E., Yu, K., Zareian, F., Johnson, K., Hortacsu, A. (2024). Initial Framework to Design Lifeline Infrastructure for Post-Earthquake Functional Recovery Volume 1, *Special Publication*, NIST, Gaithersburg, MD

[3] Field, E. H., Jordan, T. H., Cornell, C. A. (2003). OpenSHA: A Developing Community-Modeling Environment for Seismic Hazard Analysis, *Seismological Research Letters*, 74(4), 406-419

[4] Wang, C.F., Law, K., McKenna, F., Yu, S., Taciroglu, E., Zsarnoczsay, A., Elhaddad, W., Cetiner, B. (2021). Machine Learning-based Regional Scale Intelligent Modeling of Building Information for Natural Hazard Risk Management, *Automation in Construction*, 122, 103474

[5] Koc, E., Cetiner, B., *et al*., (2020). CRAFT: Comprehensive Resilience Assessment Framework for Transportation Systems in Urban Areas, *Adv. Eng. Informatics*, 46, 101159

[6] Virtucio MB, Cetiner B, et al. (2023). A granular framework for modeling the capacity loss and recovery of regional transportation networks under seismic hazards: a case study on the Port of Los Angeles, *Int. J. Disaster Risk Reduction*, 100, 104164

[7] Hosseinpour, V., Saeidi, A., et al. (2021). Seismic loss estimation software: a comprehensive review of risk assessment steps, software development and limitations, *Engineering Structures*, 232

[8] Gidaris, I., et al. (2017). Multiple-hazard fragility and restoration models of highway bridges for regional risk and resilience assessment in the US: state-of-the-art review, *ASCE J Struct Eng*, 143(3)

[9] Swaminathan, K., Muto, M., et al. (2011). Rupture-to-Rafters Simulations: Unifying Science and Engineering for Earthquake Hazard Mitigation, *Computing in Science & Engineering*, 13(4), 28-43

[10] Deierlein, G. G., McKenna, F., et al. (2020). A Cloud-Enabled Application Framework for Simulating Regional-Scale Impacts of Natural Hazards on the Built Environment, *Frontiers in Built Env*., 6, 196

[11] Atkinson, G. M., Boore, D. M. (2006). Earthquake Ground-Motion Prediction Equations for Eastern North America, *Bulletin of the Seismological Society of America*, 96(6), 2181–2205

[12] Milner, K. R., Shaw, B. E., et al. (2021). Toward physics-based nonergodic PSHA: A prototype fully deterministic seismic hazard model for Southern California, *Bull. Seism. Soc. Am.*, 111(2), 898-915

[13] Lavrentiadis, G., Abrahamson, N. A., Nicolas, K. M. et al. (2023). Overview and introduction to development of non-ergodic earthquake ground-motion models, *Bull Earthquake Eng* **21**, 5121–5150

[14] Bao, H., Bielak, J., Ghattas, O., Kallivokas, L. F., O'Hallaron, D. R., Shewchuk, J. R., Xu, J. (1998). Large-scale simulation of elastic wave propagation in heterogeneous media on parallel computers, *Computer Methods in Applied Mechanics and Engineering*, 152(1–2), 85-102

[15] Petersson, N. A., Sjogreen, B. (2017). *SW4, version 2.0 [software], Computational Infrastructure of Geodynamics.* Switzerland: Zenodo, doi: 10.5281/zenodo.1045297

[16] Taborda, R., Bielak, J. (2013). Ground-Motion Simulation and Validation of the 2008 Chino Hills, California, Earthquake, *Bulletin of the Seismological Society of America*, 103(1), 131–156

[17] Mazzieri, I., Stupazzini, M., Guidotti, R., Smerzini, C. (2013). SPEED: SPectral Elements in Elastodynamics with Discontinuous Galerkin: a non-conforming approach for 3D multi-scale problems, *Int. J. Numer. Meth. Eng.*, 12: 991-1010

[18] Rodgers, A. J., et al., (2019). Broadband (0-5 Hz) Fully Deterministic 3D Ground-Motion Simulations of a Magnitude 7.0 Hayward Fault Earthquake: Comparison with Empirical Ground-Motion Models and 3D Path and Site Effects from Source Normalized Intensities, *Seismol. Res. Lett.*, 90:17

[19] Paolucci, R., Smerzini, C., Vanini, M. (2021). BB-SPEEDset: A validated dataset of broadband near-source earthquake ground motions from 3D physics-based numerical simulations, *Bulletin of the Seismological Society of America*, 111(5), 2527-2545

[20] McCallen, D., Petersson, N. A., Rodgers, A., Pitarka, A., et al. (2021a). EQSIM - A Computational Framework for Fault-to-Structure Earthquake Simulations on Exascale Computers Part I: Computational Models and Workflow, *Earthquake Spectra*, 37(2), 707-735

[21] Zhang, W., Restrepo, D., Crempien, J. G., Erkmen, B., Taborda, R., Kurtulus, A., and Taciroglu, E. (2021) A computational workflow for rupture-to-structural-response simulation and its application to Istanbul, *Earthquake Engineering and Structural Dynamics*, 50(1), 177-196

[22] Zhang, W., Esmaeilzadeh, W., Taciroglu, E. (2019). A verified ABAQUS toolbox for soil-structure interaction analysis, *Computers & Geotechnics*, 114, 103143

[23] Karimzadeh, S., Askan, A., Erberik, M.A., Yakut, A. (2018). Seismic damage assessment based on regional synthetic ground motion dataset: a case study for Erzincan, Turkey, *Nat. Haz.* 92, 1371–1397

[24] Xie, Y., Sichani, Y.E., Padgett, J. E., DesRoches, R. (2020). The promise of implementing machine learning in earthquake engineering: A state-of-the-art review, *Earthquake Spectra* 36 (4), 1769-180

Neural network-aided multi-directional Real-Time Hybrid Simulations of soil-structure systems: the case of a multi-story MRF-DBF frame

F. N. Malik[1], D. N. Gorini[2], J. Ricles[1], T. Marullo[1]
[1] Lehigh University, Bethlehem, Pennsylvania, United States
[2] University of Trento, Trento, Italy

Abstract

Real-Time Hybrid Simulation (RTHS) is a technique where the system is decomposed into analytical and experimental subdomains. These are kinematically linked, and the equations of motion are solved in real-time to obtain the response of the complete system. In this study, a Neural Network (NN) based macroelement is developed for introducing soil-foundation interaction into a nonlinear RTHS. The macroelement is shown to effectively capture the response of the soil-foundation domain when compared to full soil-foundation-superstructure numerical representations. The NN macroelement is 2400 times faster compared to a continuum numerical model of the soil domain, leading to a substantial extension of the RTHS framework for multi-directional assessments of soil-structure systems under complex loading.

1. Introduction

Nonlinear dynamic analysis is rapidly becoming the primary solution for assessing the performance of structural systems under natural and man-made hazards. However, this approach entails the use of a very refined numerical representation of the whole system, whose characterization can be compromised by the lack of detailed information or the presence of sub-components showing complex behavior. Real-Time Hybrid Simulation (RTHS) is a powerful technique overcoming these limitations, based on which the system is discretized into an analytical and an experimental subdomain. The latter is used to simulate physically critical system components which refined analytical models do not exist for. The remaining system is instead modelled numerically. Through the equations of motion, the subdomains are kinematically linked and synchronized in real-time.

In this view, the present study extends the RTHS approach to the simulation of soil-structure interaction in the time-domain dynamic analysis of structures. This is a critical task as, on the one hand, it is well known that soil-structure interaction can substantially alter the dynamic response of a structural system and, on the other hand, physical modeling of the soil-foundation system is mostly impractical. Furthermore, numerical modeling of the soil domain requires a non-trivial implementation, a broad characterization of the behavior at the meso-scale and is computationally expensive, making highly problematic the real time transmission of information between the numerical and physical subdomains. To address these issues, in the present study the nonlinear and frequency-dependent effects relating to soil-structure interaction are lumped into a macroelement, whose response is formulated using neural network (NN) models. The NN-based macroelement simulates the soil-foundation restoring forces at the interface with the superstructure at an extremely low computational effort, making RTHSs feasible.

2. The NN-based macroelement: development and validation

The approach delineated in Section 1 is applied to a three-story building equipped with a selected seismic hazard resistant system, composed of steel moment and damped braced resisting frames (named MRF and DBF, respectively) combined with nonlinear viscous dampers [1]. The respective 2D finite element model is shown in Figure 1. The prototype structure presents three stories above ground and a basement embedded into the soil for a depth of 2.8 m. Beams and columns of the MRF are modeled by means of explicit force-based fiber elements [2] exhibiting an elastic-plastic behavior with combined isotropic and kinematic hardening. In the DBF layout, the columns are modeled using explicit force-based fiber elements, whilst the beams and braces as elastic elements since they are

designed to remain elastic under dynamic loading. Geometric nonlinearities are accounted for by an appropriate geometric transformation considering P-Δ effects. Overall, the superstructure model had 289 degrees of freedom and 138 elements.

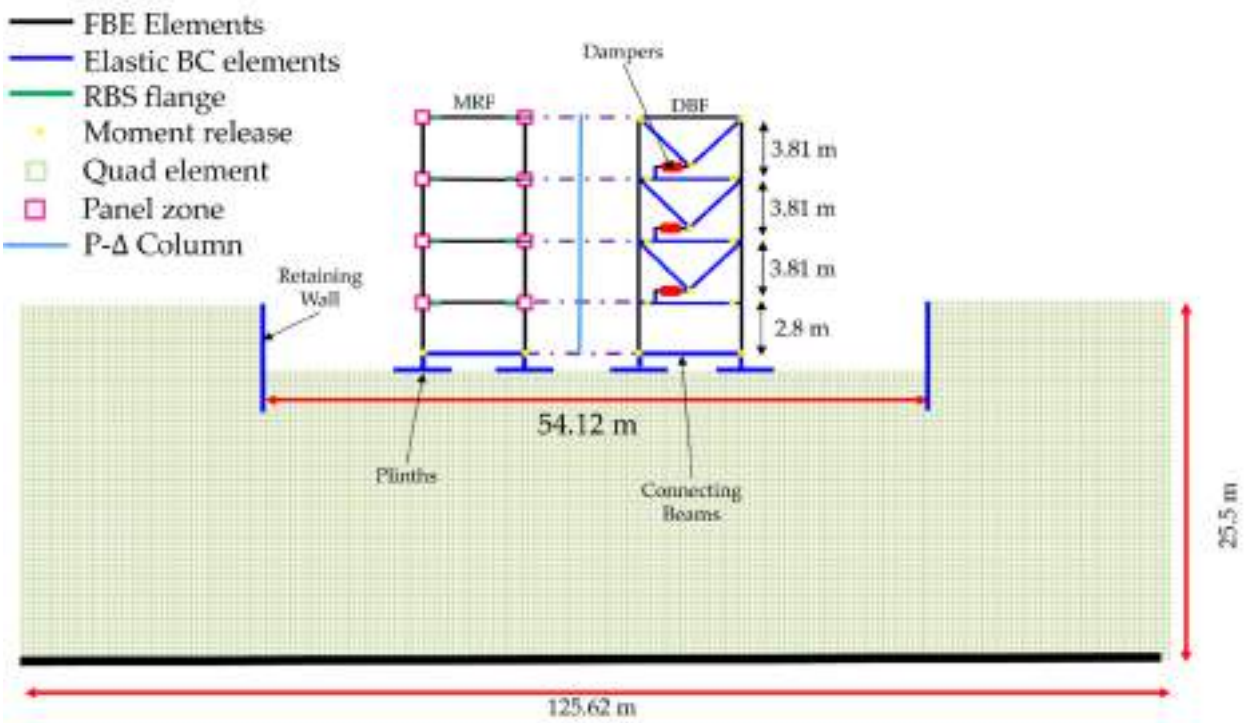

Figure 1. Finite element model of the three story MRF DBF frame and soil-foundation system.

The NN-based macroelement is trained in Python using the results of a coupled soil-foundation-superstructure (SFS) model for the considered layout in Fig. 1, implemented in OpenSees [3]. The soil domain is composed of 2429 four-node quadrilateral elements with a total of 4868 degrees of freedom, where the element behavior is described by a multi-surface plasticity constitutive law with kinematic hardening [4], known as PDMY. The latter is calibrated to reproduce the subsoil conditions of a well-documented sandy deposit in Italy [5]. The superstructure rests on shallow footings and the excavation produced for the installation of the basement is supported by retaining walls. The foundation structural members are modelled through elastic beam column elements. To train the NN-based macroelement, it is implemented into a 2D model of the sole superstructure layout created with the collaborative use of Simulink [6] and HyCoM-3D [7]. A total of 100 seismic records are selected from PEER NGA ground motion database [8] to train the NN model, where the selected ground motion records are representative of the seismic hazard on a stiff outcrop for the case at hand. Nonlinear dynamic time history analyses are carried out on the complete SFS model to compute: (i) the generalized restoring forces; and (ii) the corresponding displacements and rotations at the interface between the superstructure and the soil-foundation domain. These are quantities used to train the NN macroelement.

The NN-based macroelement consists of four Long Short-Term Memory (LSTM) layers followed by a dense fully connected layer. The input for the macroelement is represented by the ground acceleration at the base of the soil domain along with the displacements and velocities at the foundation-superstructure interface (a total of 13 inputs). Accordingly, the macroelement provides the 6 generalized forces exchanged with the superstructure. The Adam optimizer [9] is used during training to update the weights of the NN and mean square error of the loss function.

The effectiveness of the proposed model to reproduce the seismic performance of the considered structure is illustrated in Figure 2 in terms of the time histories of the horizontal (X) and vertical (Y)

roof displacements for a generic seismic scenario (not included among the ones used for training the NN model) scaled to MCE hazard level. The NN macroelement accurately reproduces the response predicted by the complete SFS model. The normalized root mean square error in the X and Y directions is 0.48% and 1.09%, respectively. It is also worth mentioning the extremely high computational efficiency of the proposed approach: the NN-based macroelement requires 0.5 seconds of CPU to perform the analysis compared to the 20 minutes associated with the 2D soil-foundation OpenSees model (that is, the proposed approach is 2400 times faster than the reference one).

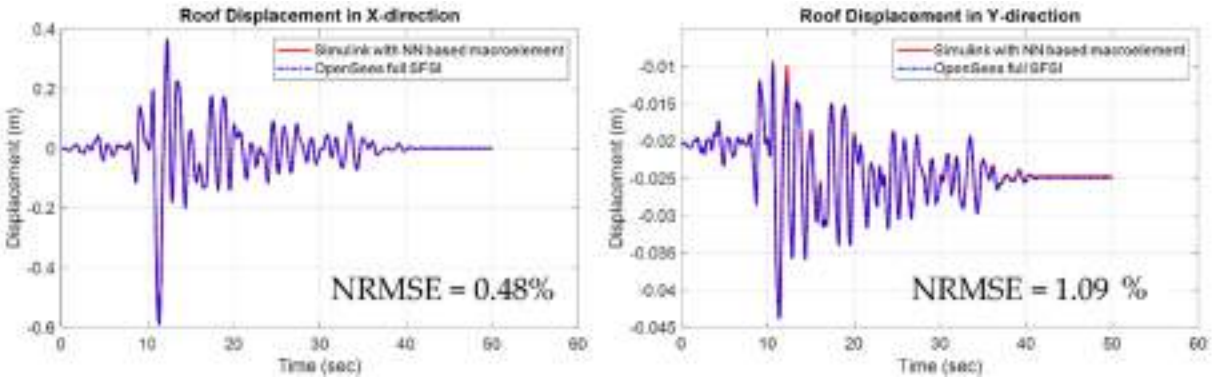

Figure 2. Comparison of OpenSees full SFSI model with the Simulink model of the structure and NN-based macroelement.

The proposed integration of the RTHS framework with artificial intelligence paves the way to new-generation approach for simulations, in which the development and real-time cyber-physical testing of novel hazard mitigation solutions for civil infrastructure can be used to assess the entire system accounting for soil-foundation-structure interaction effects.

3. References

[1] Dong, B., Sause, R., Ricles, J. (2016). Seismic Response and Performance of a Steel MRF Building with Nonlinear Viscous Dampers under DBE and MCE, *Journal of Structural Engineering*, 142(6), doi: https://doi.org/10.1061/(ASCE)ST.1943-541X.000148

[2] Kolay, C., Ricles, J. (2017). Force-Based Frame Element Implementation for Real-Time Hybrid Simulation Using Explicit Direct Integration Algorithms, *Journal of Structural Engineering*, 144(2) 4017191

[3] McKenna, F., Feneves, G., Scott, M. (2000). Open System for Earthquake Engineering Simulation, Berkeley: University of California, Berkeley

[4] Yang, Z., Elgamal, A., Parra, E. (2003). A computational model for liquefaction and associated shear deformation, *J. Geotech. Geoenviron. Engng.*, ASCE, 129(12), 1119–1127

[5] Gallese, D., Gorini, D.N., Callisto, L. (2024): Seismic design of integral abutment bridges using nonlinear static analysis of soil-structure numerical models, Geotechnique, doi: 10.1680/jgeot.22.00229MathWorks. (2022).

[6] MATLAB. Natick, Massachusetts: MathWorks. Retrieved from https://www.mathworks.com

[7] Ricles, J. M., Kolay, C., Marullo, T., Malik, F. N. (2024). HyCoM-3D: A Program for 3D Multi-Hazard Nonlinear Analysis and Real Time Hybrid Simulaiton of Civil Infrastructure Systems, Version 4.2.1, ATLSS Report No. 20-02 - Appended Feb 2024, ATLSS Engineering Research Center, Lehigh University, Bethlehem, PA

[8] Ancheta, T. D., Darragh, R., Stewart, J. P., Seyhan, E., Silva, W., Chiou, B., Wooddell, K., Graves, R., Kottke, A., Boore, D., Kishida, T., Donahue, J. (2014). NGA-West2 database, *Earthquake Spectra*, 30(3), 989-1005

[9] Kingma, D., Ba, J. (2014). Adam: A Method for Stochastic Optimization. *ArXiv*

Data-driven offshore monopile design and safety assessment

***B. Kato*[1]**
[1] *Shenzhen University, Shenzhen, China*

Abstract

Monopiles support 60% of existing offshore wind turbines (OWTs). However, their effective design remains expensive and challenging due to complex, nonlinear soil-structure interaction (SSI) under varying loads. Moreover, during their lifetime, OWTs will experience large storm surges that may negatively affect their structural safety. Current design codes do not provide sufficient guidance on tackling these problems. To address these issues, firstly, this study provides simple equations derived from numerical data, that estimate the change in the fundamental frequency of OWTs due to soil stiffness degradation, post-storm. Secondly, it presents an explainable AI, p**AI**le, using the long short-term memory model that can predict pile head displacements and rotations in response to cyclic environmental loads. This AI can also be used for rapid monopile size optimization and post-storm deformation assessment. 108 parametric finite element analyses were conducted, considering different pile diameters, lengths, soil strengths, and loading scenarios to build the data base for both aspects of this study. Shear stiffness degradation ratios were utilized to predict the change of natural frequency, given the mudline loads. Testing results showed that p**AI**le efficiently predicts pile head displacements and rotations (R^2=0.995), by reproducing non-linear SSI. Finally, feature importance analysis showed that it correctly understands which physical parameters govern pile head deformations.

1. Introduction

With climate change in mind, expanding energy generation via offshore wind turbine (OWT) farms along extensive coastlines becomes a viable solution to achieve carbon neutrality. Monopiles, supporting 60.2% of existing OWTs [1], are critical structures influencing the safety and energy efficiency of these dynamic systems. However, their effective design remains expensive and challenging. Moreover, accurate guidelines are lacking on how common storm surges may affect the natural frequency and performance of OWTs [2]. Current OWT monopile design challenges stem from complex nonlinear soil-structure interaction (SSI) under varying loads, often oversimplified in design codes, such as neglecting intermediate pile behaviour (not rigid or flexible), soil damping, inertia of soil, and pile gapping [3]. To address these issues, firstly, this study provides a simplified method to estimate the natural frequency change of OWTs post-storm, due to soil stiffness degradation. Secondly, it presents an AI model, p**AI**le, that predicts fully nonlinear pile head deformations in response to cyclic loads, and can also be used to rapidly size monopiles at the preliminary design stage, readily considering nonlinear SSI.

2. Methodology

To generate the data necessary for the above solutions, high-fidelity finite element (FE) models of monopile-supported OWTs in clay were built and validated against dynamic centrifuge tests conducted by Lai et al. [4]. Subsequently, a parametric analysis of 108 scenarios was conducted, considering different pile diameters, lengths, soil strengths, and loading scenarios. All permutations of the parameters listed in Table 1 were modelled in FE. OpenSees was selected as the FEM platform for high-fidelity modeling and STKO [5] for facilitating the use of the open-source software. A multi-axial cyclic bounding surface plasticity soil constitutive model [6] was adopted to capture the undrained cyclic behavior of clays, and a beam-solid contact element [7] based on the Mohr-Coulomb frictional model with tension cutoff to facilitate pile gapping and realistic soil-pile interaction. The utilized FE elements and environmental loading scenarios are depicted in Figure 1.

Table 1. The range of variables considered in FEM simulations.

Diameter:	4 m	5 m	6 m	7 m
Length:	26 m	30 m	40 m	
Clay soil parameters:	s_u = 40 kPa G_{max} = 14 MPa	s_u = 75 kPa G_{max} = 29 MPa	s_u = 120 kPa G_{max} = 46.5 MPa	
Load scenarios:	M_{max} = 141 MNm F_{max} = 2.9 MN	M_{max} = 267 MNm F_{max} = 4.3 MN	M_{max} = 360 MNm F_{max} = 5.3 MN	

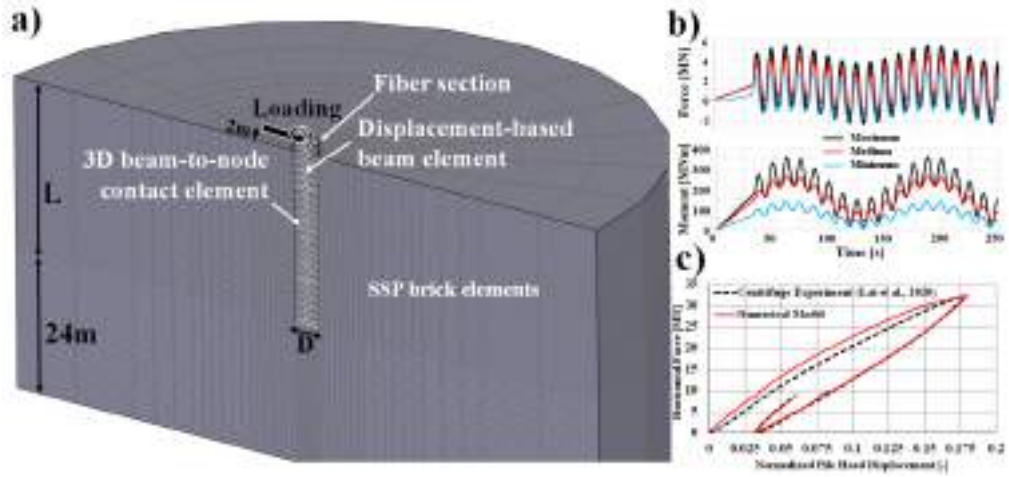

Figure 1. Dimensions and adopted elements of FEM models a). The three considered pile head loading time histories b). FEM model validation results c).

Table 2. Input and output variables of pAIle.

Input	*Output*
Horizontal force and moment time history (F, M) [N, Nm]	Pile head displacement time history (d) [m]
Pile diameter, length, bending stiffness (D, L, EI) [m, Pam^4]	
Undrained shear strength and shear modulus (s_u, G_{max}) [Pa]	Pile head rotation time history (θ) [rad]

During simulations, the shear stiffness degradation ratios (G/G_{max}) at 1D (pile diameter) depth were recorded and utilized for the estimation of post-storm OWT natural frequency changes. Secondly, pile head displacements and rotations were collected to train p**AI**le. The parameters that fully define the problem of OWT monopole design, and as such are used to train p**AI**le are listed in Table 2.

3. Results

For post-storm natural frequency change, G/G_{max} around the monopile can be estimated using a set of curves derived from the FE data, for given soil and pile parameters and according to maximal mudline forces that occur during a storm. These curves are published in Kato et al. [8]. Subsequently, a set of formulae were derived that correlate the natural frequency change of the whole OWT with estimated post-loading G/G_{max} values around the monopile. Following the data published in Kato et al. [8], separate formulas were identified for flexible (Eq. 1) and rigid (Eq. 2) piles. The coefficient of determination (R^2) is 0.97 for Eq. 1 and 0.9 for Eq. 2.

$$\mathbf{f_0^{post-storm} = f_0\left(1 - \left(19.45e^{-5(G/G_{max})}\right)/100\right)} \quad (1)$$

$$\mathbf{f_0^{post-storm} = f_0\left(1 - \left(0.67(G/G_{max})^{-1.18}\right)/100\right)} \quad (2)$$

where $f_0^{post\text{-}storm}$ is the post-storm natural frequency of the OWT, f_0 is its undamaged natural frequency, and G/G_{max} is the stiffness degradation value at 1D below the mudline. Such simple but reliable formulae can aid in the post-storm safety assessment of wind turbines at offshore farms.

p**AI**le is an explainable AI trained on high-fidelity FE data using the long short-term memory (LSTM) model and explained via a feature importance analysis. p**AI**le predicts pile head displacement and rotation histories of an arbitrarily sized monopile in clay, subjected to sinusoidal wind and wave loading. Testing results showed that p**AI**le accurately ($R^2 = 0.995$) predicts pile head deformations both at small strains and at post-failure flow state. It was able to reproduce nonlinear SSI phenomena, such as cyclic accumulation of plastic strains, plastic flow, and damping, as shown in Figure 2. Feature importance analysis showed that p**AI**le correctly understands which physical parameters govern pile head deformations. Finally, p**AI**le was wrapped into a Python loop to optimize monopole size by varying pile length, diameter, and flexural rigidity until the predicted deformations satisfy serviceability and ultimate limit criteria. The procedure takes 2 seconds and only requires readily available inputs: design wind and wave loads, and basic soil parameters.

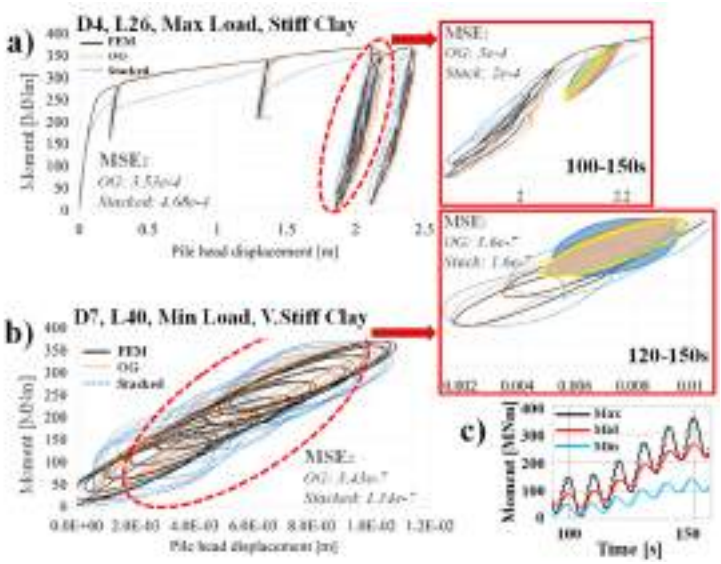

Figure 2. Pile head load-displacement predictions by pAIle against FEM results for a post-failure scenario a) and a pre-yield scenario b). The applied load corresponding to the highlighted (red) time intervals is shown in c). Prediction errors are quantified in terms of mean squared error (MSE).

4. References

[1] Musial, W., Spitsen, Sathish, S. (2023). Offshore Wind Market Report: 2023 Edition (No. NREL/TP-5000-87232), National Renewable Energy Laboratory (NREL), Golden, CO (United States)

[2] Abdullahi, A., Bhattacharya, S., Li, C., Xiao, Y., Wang, Y. (2022). Long term effect of operating loads on large monopile-supported offshore wind turbines in sand, *Ocean Eng.*, 245, 110404

[3] Abdullahi, A., Wang, Y., Bhattacharya, S. (2020). Comparative modal analysis of monopile and jacket supported offshore wind turbines including SSI, *Int. J. Struct. Stab. Dyn.*, 20(10), 2042016

[4] Lai, Y., Wang, L., Hong, Y., He, B. (2020). Centrifuge modeling of the cyclic lateral behavior of large-diameter monopiles in soft clay: Effects of episodic cycling and reconsolidation, *Ocean Eng.*, 111967.

[5] Petracca, M., Candeloro, F., & Camata, G. (2017). STKO user manual, ASDEA: Pescara, Italy

[6] Wang G. & Sitar N. (2006). Nonlinear Analysis of a Soil-Drilled Pier System under Static and Dynamic Axial Loading, PEER Report, 2006/06, University of California, Berkeley

[7] Arduino, P., Petek, K. A., & Helnwein, M. (2007). Three-Dimensional Beam-Solid Contact Element Formulation for Analysis of Pile Interaction. Mecánica Computacional, (33), 2909-2918

[8] Kato, B., Bhattacharya, S., Wang, Y. (2023). Evaluation of post-storm soil stiffness degradation effects on the performance of monopile-supported offshore wind turbines in clay, *Ocean Eng*, 114338

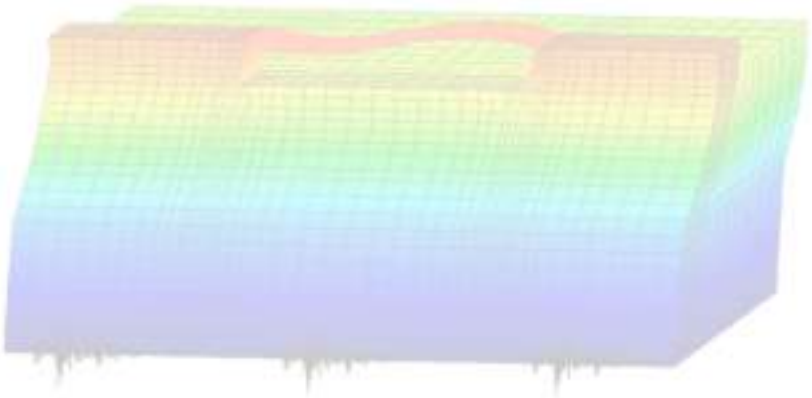

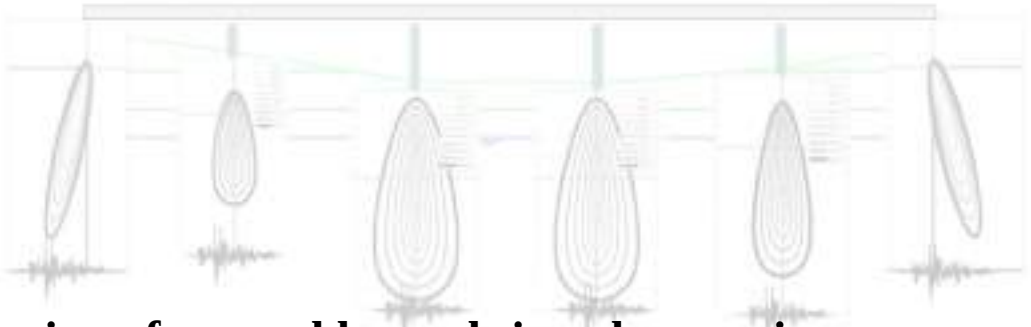

3.Mitigation of natural hazards in urban settings

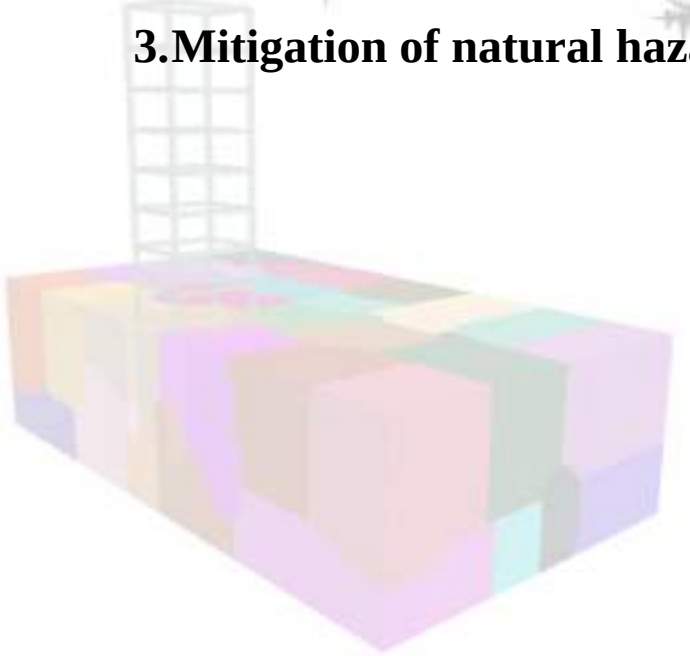

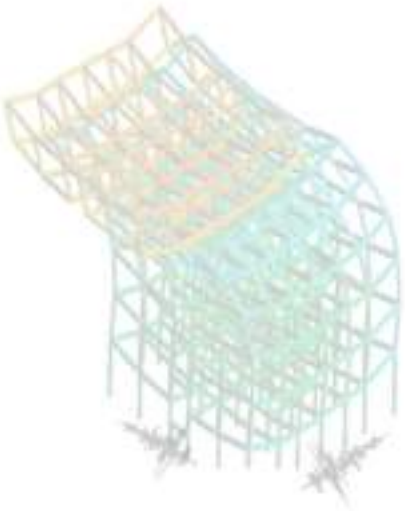

Mitigation of Seismic Liquefaction in Stratigraphically-Variable and Urban Sites

S. Dashti[1], C. Bessette[1] and Y.W. Hwang[2]
[1] University of Colorado Boulder, Boulder, CO, United States
[2] National Yang Ming Chiao Tung University, Hsinchu, Taiwan

Abstract

The existing engineering methodologies for liquefaction mitigation rely on free-field triggering in uniformly layered granular soil deposits. These methods routinely ignore cross-layer interactions in realistically stratified deposits, soil-structure interaction (SSI) on shallow foundations, or interactions between closely spaced structures in urban settings (structure-soil-structure interaction [SSSI]). In this presentation, through an experimental-numerical-statistical study, we show that these methods are unreliable, jeopardizing our ability to assess and mitigate liquefaction vulnerability. More than 4,000 fully-coupled, 3D, dynamic finite element analyses in OpenSees, validated with centrifuge experiments, show that combining ground reinforcement with drainage and densification improve foundation's settlement. These methods, however, may increase foundation's tilt potential, which must be evaluated on a case-by-case basis. The combined influence of seismic coupling and stratigraphic variability on mitigation efficacy is shown to be significant in terms of foundation tilt, spectral accelerations, and flexural drifts experienced within the superstructure of both mitigated and unmitigated neighbors. These effects are notable for spacing-to-foundation width-ratios (S/W) as large as 1.0, which are common in cities. Additional measures and technologies may be needed to reduce tilt to acceptable levels in closely-spaced cluster configurations and realistically stratified deposits, while simultaneously strengthening both the ground and structures at an area-level. Physics-informed machine learning is subsequently used to identify the key predictors and models for foundation's settlement ratio, which can guide the future design of mitigation near buildings.

1. Background and introduction

Recent case histories as well as experimental and numerical studies have demonstrated that methods for liquefaction triggering, consequence, and mitigation in the free-field do not apply to buildings on shallow foundations [1,2], because of differing seismic demands, deformations, and flow patterns. Much effort has been directed toward improving our understanding of soil-structure interaction (SSI) and structure-soil-structure interaction (SSSI) on uniformly layered deposits of liquefiable clean sand with or without mitigation [4-7]. Though insightful, saturated and susceptible granular deposits in the field often have non-uniform stratification and uncertain layer continuity, including low-permeability silt or clay interlayers [8]. Previous studies have revealed that liquefaction-induced lateral spreading can manifest even in slopes with inclinations as gentle as 0.3-1°, resulting in substantial displacements of up to 2 m and posing risks to critical infrastructure and lifelines (O'Rourke and Lane 1989). Similar displacements may result from non-uniform or sloped stratigraphies. Additionally, the severity of liquefaction manifestation can be strongly influenced, if not controlled, by interactions among soil layers in interbedded deposits, as demonstrated during the 2010-2011 earthquake sequence in Christchurch, New Zealand [9]. Nevertheless, these system-level effects are poorly understood and are not included in existing triggering and settlement procedures, particularly near structures. Hence, they are also not included in designing mitigation strategies. The next generation of liquefaction procedures need to account for complexities associated with SSI, SSSI, and stratigraphic variability.

2. Fully coupled 3D dynamic finite element simulations

Three-dimensional (3D), fully-coupled, effective stress, nonlinear finite element (FE) simulations were performed within the object-oriented, parallel computation platform OpenSEES [11] on the Alpine supercomputer at CU. These simulations were first validated with a series of centrifuge

experiments and then expanded with additional input parameters. To model the nonlinear response of the granular soil layers, we used the pressure-dependent, multi-yield surface, version 2, soil constitutive model (PDMY02) implemented in OpenSEES [3]. A small-strain Rayleigh damping value of 3% at frequencies corresponding to the soil column's first and third initial modes was used in addition to the model's hysteresis damping, following a similar methodology adopted in [7].

Following calibration and validation, a comprehensive numerical parametric study followed in 3D (a sample of which is shown in Fig. 1 schematically). Soil stratigraphy, interlayering, and mitigation properties (with dense granular columns) were varied in these simulations to evaluate their effects on the performance of isolated and adjacent, similar and dissimilar structures and identify the key predictors of performance. The parameter space was determined using Quasi-Monte Carlo sampling, leading to more than 4,000 total simulations.

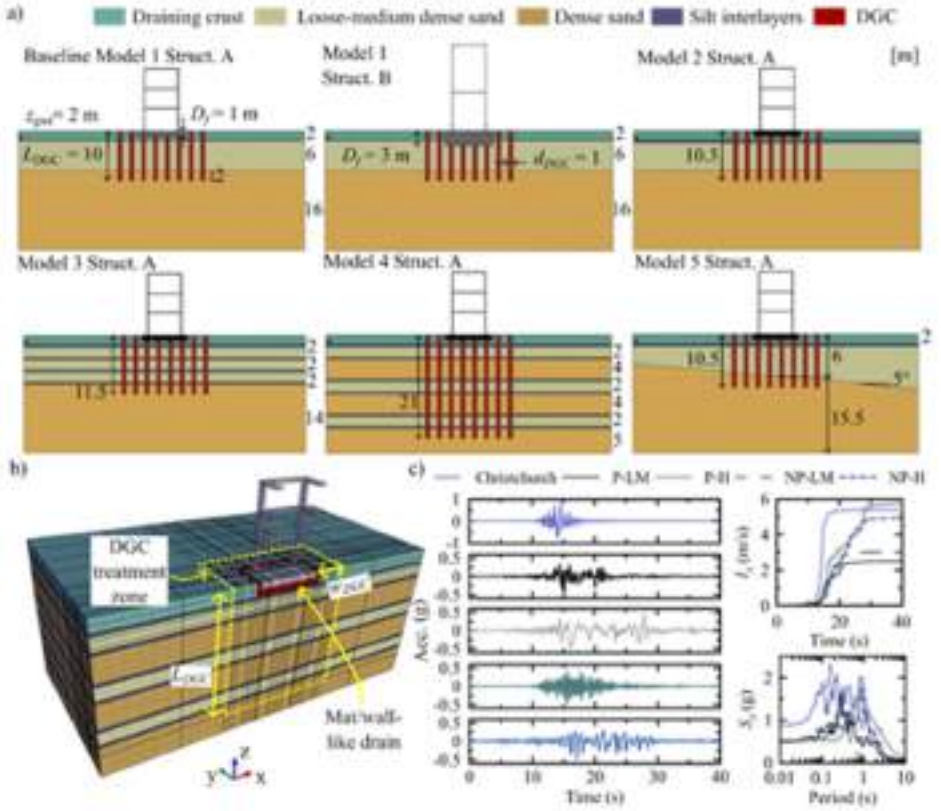

Figure 1. Schematic view of a subset of numerical model configurations in the parametric study.

3. Effects of interlayering and SSSI on foundation performance and mitigation effectiveness

Fig. 2 describes the trends from a small subset of 3D simulations on the effectiveness of various DGC mechanisms for isolated structures. We compare the EDP_{DGC}/EDP_{NM} predictions from five of the soil models (Fig. 1) for two structures and z_{gwt} = 2 m, along with their absolute values (NM or DGC), to evaluate the effect of stratigraphic variability on DGC performance. The results highlight the effectiveness of draining DGCs (k_r = 100) in reducing δ compared to NM. The simulations also indicate that interlayering in the deposit can notably amplify the negative influence of SSSI and seismic coupling on foundation tilt. The key predictors of δ_{NM} for an isolated structure are identified as CAV of the outcropping rock as well as the thickness of the loosest sand layer and thickness to depth ratio of silt and clay interlayers. The key predictors of δ_{DGC}/δ_{NM} are identified as foundation width, thickness, relative density, and depth to critical layers within the foundation's influence zone. Two machine-learning methods (i.e., the random forest and lasso with classical regression) are used to develop predictive models of foundation performance and optimize model uncertainty.

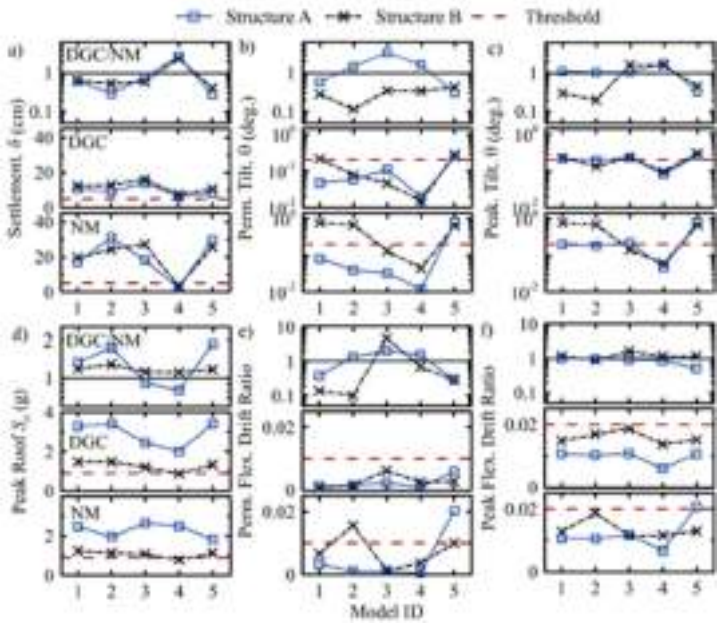

Figure 2. Median normalized (ratio of mitigated to unmitigated) response, mitigated response (with DGCs), and response with no mitigation (NM) for different models for a subset of numerical simulations.

4. References

[1] Dashti, S., Bray, J., Pestana, J., Riemer, M., Wilson, D. (2010a). Mechanisms of seismically induced settlement of buildings with shallow foundations on liquefiable soil, *J. Geotech. Geoenviron. Eng.*, 136(1), 151-164

[2] Dashti, S., Bray, J., Pestana, J., Riemer, M., and Wilson, D. (2010b). Centrifuge testing to evaluate and mitigate liquefaction-induced building settlement mechanisms, *J. Geotech. Geoenviron. Eng*., 136 (7), 918-929

[3] Elgamal, A., Yang, Z., Parra, E. (2002). Computational modeling of cyclic mobility and post liquefaction site response, *Soil Dyn. Earthquake Eng*., 22 (4): 259–271, doi: https://doi.org/10.1016/S0267-7261(02)00022-2

[4] Karimi, Z., Dashti, S., Bullock, Z., Porter, K., Liel, A. (2018). Key Predictors of Structure Settlement on Liquefiable Ground: A Numerical Parametric Study, *Soil Dynamics and Earthquake Engineering*, 113, 286-308, doi: https://doi.org/10.1016/j.soildyn.2018.03.001

[5] Bullock, Z., Karimi, S., Dashti, S., Porter, K., Liel, A., Franke, K. (2019a). A Physics-Informed Semi-Empirical Probabilistic Model for the Settlement of Shallow-Founded Structures on Liquefiable Ground, Géotechnique, doi: https://doi.org/10.1680/jgeot.17.P.174

[6] Bullock, Z., Dashti, S., Karimi, Z., Liel, A., Porter, K., Franke, K. (2019b). Probabilistic Models for the Residual and Peak Transient Tilt of Mat-Founded Structures on Liquefiable Soils, *ASCE Journal of Geotechnical and GeoEnvironmental Engineering*, 145(2)

[7] Hwang, Y.W., Dashti, S., Kirkwood, P. (2022). Impact of Ground Densification on the Response of Urban Liquefiable Sites and Structures, *ASCE Journal of Geotechnical and GeoEnvironmental Engineering*, doi: 10.1061/(ASCE)GT.1943-5606.0002710

[8] Kokusho, T., Fujita, K. (2001). Water films involved in post-liquefaction flow failure in Niigata City during the 1964 Niigata earthquake, Proc., Fourth Int. Conf. on Recent Advances in Geotechnical Earthquake Engineering and Soil Dynamics, Univ. of Missouri-Rolla, Rolla, Mo

[9] Cubrinovski, M., Rhodes, A., Ntritsos, N. (2017). System response of liquefiable deposits, 3rd Int. Conf. on Performance-based Design in Earthquake Geotechnical Engineering, Vancouver, Canada

[10] O'Rourke, T.D. and Lane, P.A. (1989). Liquefaction Hazards and Their Effects on Buried Pipelines, National Center for Earthquake Engineering Research, Technical Report NCEER-89-0007

[11] Mazzoni, S., McKenna, F., Scott, M. H., Fenves, G. L. (2006). Open System for Earthquake Engineering Simulation (OpenSees) Command Language Manual, Berkeley, CA: Network for Earthquake Engineering Simulations

Assessment of the attenuation of 3D basin ground motions by a Rigid Inclusion System

F. Lopez-Caballero[1] and V. Soto-Moncada[1]
[1] Université Paris-Saclay, CentraleSupélec, ENS Paris-Saclay, CNRS, LMPS - Laboratoire de Mécanique Paris-Saclay, 91190, Gif-sur-Yvette, France

Abstract

Surface waves might cause significant building damage at large distances from an earthquake epicenter, particularly when they are amplified by sedimentary layers in basins. The rotational components of these ground motions, often neglected in traditional assessments, can further exacerbate seismic damage. Therefore, accounting for three-dimensional ground motions, including rotational effects, in seismic risk management could be important. To reduce structural vulnerability, one approach is to prevent earthquake motion from reaching the structure's foundation. A practical solution involves using vertical rigid materials, or rigid inclusions (RIs), in the soil, which serve as wave barriers to attenuate seismic waves through frequency bandgaps. RIs can be installed beneath the foundation or around it as a barrier, especially in cases dealing with existing structures. This study examines a soil-structure interaction (SSI) model under 3D seismic loading, focusing on a structure with a foundation reinforced by RIs, situated over a sedimentary basin. The research assesses the seismic response and damage potential using a three-dimensional wave propagation model that incorporates local geology using a Performance Based approach. The findings evaluate the effectiveness of RIs in mitigating seismic damage through parametric dynamic analyses, exploring both the beneficial and detrimental effects of this mitigation strategy.

1. Introduction

Seismic surface waves, particularly those affecting structures located above sedimentary basins, can significantly amplify and extend the duration of seismic events. This phenomenon has been well-documented in previous studies [1, 2], indicating that the unique geological features of basins can exacerbate seismic amplification in both intensity and duration. Moreover, the geological features in sedimentary basins impose in the full seismic wavefield a complex three-dimensional (3D) aspect, characterized by ground motions including both horizontal and rotational components. While rotational components of ground motions are often overlooked in traditional earthquake engineering assessments, these can be especially induced by surface waves (Love and Rayleigh) in basins, substantially increasing the destructive potential of moderate earthquakes in such areas and, therefore, pose significant challenges in seismic risk management.

In response to these challenges, treating the subsoil to modify its mechanical characteristics has emerged as a potential mitigation strategy, as it can reduce the amplitude of seismic waves reaching structures [3, 4]. This can be achieved by either increasing the inertia of the foundation with respect to the soil, or by creating a dynamic altering system in the soil. Among the various techniques available, one solution is the use of vertical rigid materials in the soil. These materials act as wave barriers, mitigating seismic waves and surface waves by exhibiting bandgaps at different frequencies that result in seismic wave attenuation [5]. In this topic, a Rigid Inclusion System (RI) is a soil improvement technique commonly employed to increase the soil-bearing capacity and limit the settlement of the superstructure, making them a viable option for creating such an altering system. In situations where existing structures are concerned, upgrading the structure is not always feasible or cost-effective, thus, an alternative solution is the retreat of the foundation. In this case, the same vertical rigid materials are inserted into the soil around the foundation and serve as a periodic wave barrier by restraining the wave's arrival at the foundation.

This study builds on this foundation by exploring the use of RIs as a method for altering soil

characteristics to protect infrastructure in earthquake-prone urban areas. The study uses a Performance Based approach [6] to compare both the demand and the capacity of the infrastructure and therefore have a comprehensive assessment of the effectiveness of the RIs in mitigating the structural damage from 3D basin-induced ground motions.

2. Modelling approach for the quantification of structural response due to regional 3D ground motions

The numerical study presented here represents a realistic soil-structure interaction (SSI) model under seismic loading, focusing on a reinforced concrete bridge pylon in soil reinforced by RIs over a sedimentary basin. The time-domain nonlinear response-history analyses (NRHAs) are performed with a three-dimensional wave propagation from the earthquake source to the structure, including local geology (i.e., the basin), using the coupled method based on the Domain Reduction Method (DRM) based on the work of [7]. The study utilized the spectral element code SEM3D [8] for large-scale wavefield generation, considering the earthquake source, regional geological features and local soil layers. The regional model is coupled with the finite element method (FEM) software CodeAster [9], which models local interactions involving the surficial soil layers, the infrastructure, and the RIs. The transition of wavefields from the 3D regional scale to a reduced, more focused domain is facilitated by paraxial boundaries, ensuring an accurate representation of local effects on structures. Regional wave propagation simulations and subsequent localized analyses are conducted in order to capture the distinct characteristics of surface waves impacting the barrier-soil-structure system. A schematical representation of the main features of the 3D numerical model, as well as the size of both regional and local domains, is illustrated in Figure 1.

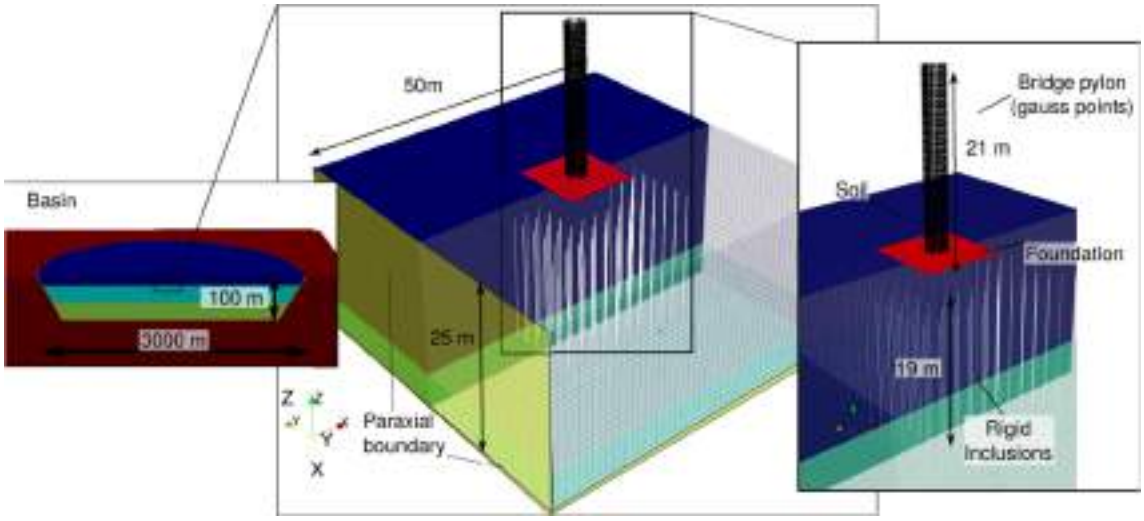

Figure 1. Schematic representation of the regional and reduced domains, including RI foundation and infrastructure.

Parametric dynamic analyses are carried out by considering either the rigid inclusions beneath the foundation or on the outside, working as a barrier. Each pile is implemented with beam elements, and their mechanical properties are carefully selected to match typical reinforced concrete, ensuring realistic simulation conditions. A comparative analysis is designed where three models are developed: two incorporating the RIs (beneath or as a barrier) and another without them.

3. Main outcomes of the study and perspectives

The study pretends to achieve a deeper understanding of the relationship between the characteristics of RIs and the attenuation of seismic waves in the frequency domain, particularly those with rotational components such as Love and Rayleigh waves. It also aims to clarify the extent to which RIs can

mitigate seismic-induced structural damage by using a Performance Based approach. By comparing the performance of structures with and without RIs, the research will provide valuable insights into the potential benefits of this retrofitting method.

Initial findings showed similar results from the two RI configurations tested in this study in terms of attenuation bands, indicating the feasibility of retrofitting existing structures. While initial findings suggest that the implementation of RIs can significantly reduce several Intensity Measures (IMs) as indicators of the seismic response at the ground level, the introduction of RIs also altered the mechanical characteristics of SSI, leading to complex structural responses under 3D ground motions. These findings highlight the need for further research to fully understand the implications of using RIs in seismic risk mitigation. Future work should focus on refining the understanding of these complex interactions and exploring additional configurations and materials for optimizing the performance of RIs in different seismic scenarios.

4. References

[1] Miura, H., Midorikawa, S. (2001). Effects of 3-D Deep Underground Structure on Characteristics of Rather Long-Period Ground Motion, *Zisin (Journal of the Seismological Society of Japan 2nd ser)*, 54, 381–395, doi: https://doi.org/10.4294/zisin1948.54.3_381

[2] Cruz-Atienza, V.M., Tago, J., Sanabria-Gómez, J.D., et al (2016). Long Duration of Ground Motion in the Paradigmatic Valley of Mexico, Sci Rep, 6:38807, doi: https://doi.org/10.1038/srep38807

[3] Achaoui, Y., Antonakakis, T., Brûlé, S., et al. (2017). Clamped seismic metamaterials: Ultra-low frequency stop bands, New J Phys, 19, doi: https://doi.org/10.1088/1367-2630/aa6e21

[4] Wang, H.F., Zhang, R.L. (2021). Dynamic structure-soil-structure interaction of piled high-rise buildings under earthquake excitations I: Influence on dynamic response, *Latin American Journal of Solids and Structures*, 18, 1–23, doi: https://doi.org/10.1590/1679-7825622

[5] Mandal, P., Somala, S.N. (2020). Periodic pile-soil system as a barrier for seismic surface waves, SN Appl Sci, 2, 1–8, doi: https://doi.org/10.1007/s42452-020-2969-8

[6] Porter, K.A. (2003). An Overview of PEER's Performance-Based Earthquake Engineering Methodology, In: Ninth International Conference on Applications of Statistics and Probability in Civil Engineering (ICASP9), San Francisco. pp 1–8

[7] Korres, M., Lopez-Caballero, F., Alves Fernandes, V., et al (2023). Enhanced Seismic Response Prediction of Critical Structures via 3D Regional Scale Physics-Based Earthquake Simulation, *Journal of Earthquake Engineering*, 27, 546–574, doi: https://doi.org/10.1080/13632469.2021.2009061

[8] CEA and CentraleSupélec and IPGP and CNRS (2017). SEM3D Ver 2017.04 Registered at French Agency for Protection of Programs (Dépôt APP)

[9] CodeAster (2017). General public licensed structural mechanics finite element software, included in the Salomé-Meca simulation platform. Website http://www.code-aster.org

Numerical analyses for the assessment of the isolation effects by a gravel-rubber mixture layer at the base of a building

G. Abate[1], A. Fiamingo[1] and M.R. Massimino[1]
[1] University of Catania, Catania, Italy

Abstract

Seismic hazard is recognized as one of the main causes of structures and infrastructure failure worldwide. Geotechnical Seismic Isolation (GSI) systems have emerged as a mitigation technique that enhances soil behavior through natural or modified geomaterials. Soil-rubber mixtures (SoRMs) are recognized as an effective eco-sustainable solution for protecting structures in earthquake-prone regions [2]. The main idea is to improve the soil immediately underneath the foundations using SoRMs so that seismic energy will be partially dissipated within SoRMs before being transmitted to the structures. SoRMs are generally obtained by mixing sand or gravel and granulated tyre rubber. Rubber grains for the mixtures are manufactured from End-Of-Life Tyres (ELTs), the disposal of which has become a severe environmental problem worldwide. Recent laboratory tests on gravel-rubber mixtures (GRMs) have highlighted their good static and dynamic properties [3-4]. Comprehensive investigations, including numerical analyses and small-scale experiments, evaluated the effectiveness of GRMs as GSI systems [5]. Only one full-scale test was recently performed on the EuroProteas prototype structure located in the Euroseistest site (Greece), after replacing the foundation soil with GRMs characterized by different rubber contents [2]. These tests demonstrated that a GRM characterized by a rubber content per weight equal to 30% (GRM 70/30) can effectively dissipate the seismic energy within it before being transmitted to the structure. Following these promising outcomes, the dynamic interaction between GRMs and buildings was further investigated numerically, focusing on the effects of the GRM 70/30 layer beneath the shallow foundations of a real structure.

1. The FEM models

Parametric analyses were performed varying the seismic motions and the GRM layer thickness.

The analyses were performed developing three different FEM models (Figure 1): i) without the GRM layer as a benchmark model (Model 1); ii) with a 0.80 m GRM layer (Model 2); iii) with a 1.50 m GRM layer (Model 3). The main dimensions of the FEM models are reported in Figure 1. The hypothesized GRM, as previously introduced, was the same mixture adopted for the large tests carried out in Greece [2], (GRM 70/30). The chosen structure was a typical reinforced-concrete Italian building, damaged by the 2018 Catania earthquake. It was modelled by 2-node Hermitian beam elements, considering different moment-curvature curves to consider nonlinear behavior [6]. Both the soil-structure system without the GRM and with the GRM were modelled, using plane-strain 4-node 2D-solid elements and adopting an equivalent visco-elastic constitutive model for the soil and the GRM. The main properties of the structure, soil deposit and GRM layer are reported in [6]. The element size was 1/6 ÷ 1/8 of the ratio between shear waves velocity in the GRMs layer and the maximum significant frequency of the dynamic input. In addition, a finer discretization near the structure was considered to consider the areas with high stress concentrations. As regards the boundary conditions, the horizontal displacements of the structure beams in the y-direction were linked by "constraint equations" to simulate an axial rigid diaphragm. The nodes at the soil's lateral boundaries were connected by "constraint equations" that ensured the same y- and z-translations at the same depth. Nodes at the model's base were constrained only in the vertical direction and, to simulate the bedrock, dashpots were applied at the base of the model, following Lysmer and Kuhlemeyer [7] formulation. Contact surfaces were appropriately defined between the foundation and the soil for Model 1, and between the foundation and the GRM layer for Models 2 and 3, to simulate interaction phenomena such as uplifting and/or sliding, assuming a friction angle of $\delta = 2\phi/3$. The material viscosity was modelled according to the Rayleigh damping. The loading conditions

applied to each model included: the weight of the entire model, distributed loads on the beams (evaluated in the seismic design combination), and vertical forces on the columns. Nine accelerograms were applied to the dashpots as input motions: two recorded and seven spectrum-compatible according to [8]. For more details see [6].

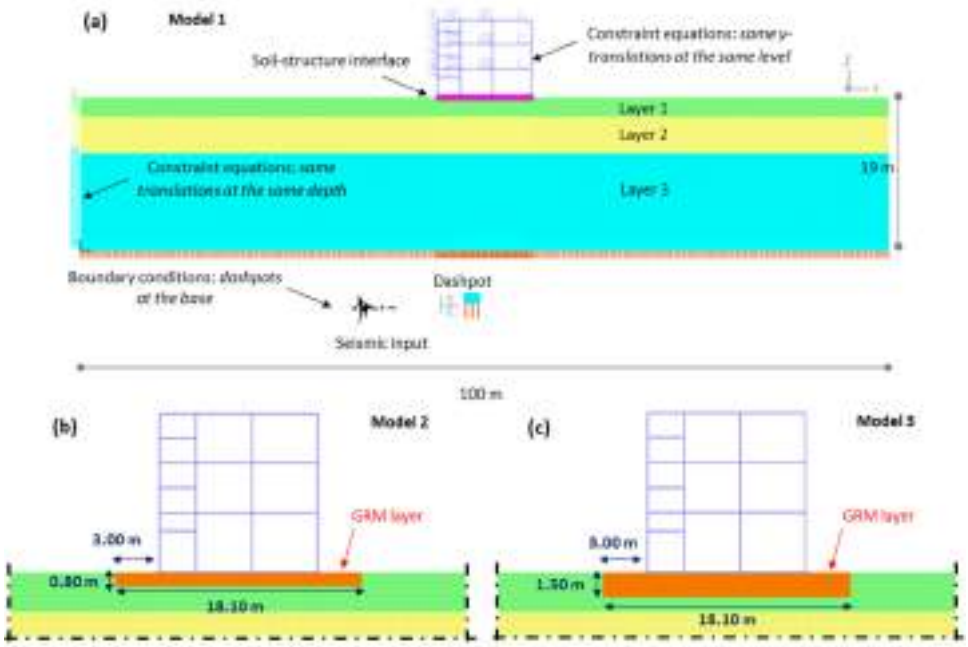

Figure 1. FEM models: (a) Model 1: soil-structure system, without the GRM layer; Models 2 and 3: a zoomed view (near the building) of the two FEM models including the GRM layer underneath the structure of 0.80 and 1.50 m, respectively, modified by [8].

2. Results and conclusions

The performance of the GRM 70/30 layer as a GSI system was assessed by examining the seismic responses of Models 1, 2 and 3, considering the nine accelerograms. Among the results evaluated, by way of example, the envelope of the elastic response spectra in acceleration for the configuration without the GRM layer (Model 1) and with the GRM layer of 0.80 m and 1.50 m (Models 2 and 3, respectively) for the foundation and the roof motion, assuming a damping ratio equal to 5% are shown (see Figure 2).

In general, the GRM layer leads to a general decrease in spectral acceleration and a translation of the spectral acceleration peaks toward higher periods. This result is typical of all those systems where valuable DSSI phenomena occur. The spectral accelerations decrease as the GRM layer thickness increases. This effect is due to the different strain level activated by the GRM layer: the strain level induced by the GRM layer with a thickness of 1.50 m is more significant that that with a thickness of 0.80 m, leading to a more pronounced decrease in shear modulus and an increase in the damping ratio. More specifically, at the roof level, the GRM determines an excellent reduction (average value = 40%) in spectral accelerations for the period range 0–0.8 s and 0–0.9 s, by using the 0.80 m and the 1.50 m GRM layer, respectively. At the foundation level, a significant reduction of the spectral accelerations is obtained for periods lower than 0.2 s and 0.3 s, as well as for periods in the range 0.4–0.9 s and 0.5–0.9 s, by using the 0.80 m (average value = 15%) and the 1.50 m GRM layer (average value = 25%), respectively. But the effects of soil-GRM-structure interaction could not always be beneficial: for period ranges equal to 0.2–0.4 s and 0.9–2 s by using the 0.80 m GRM layer, as well as for period ranges equal to 0.3–0.5 s and 0.9–2.0 s by using the 1.50 m GRM layer, there is an increase (up to 20%) in the spectral accelerations at the foundation, the more significant, the higher the GRM layer thickness. So, GRM layers underneath foundations appear to be a valuable GSI solution even with reduced thicknesses. Nevertheless, careful attention should be devoted to the

period ranges inside which GRM have irrefutable positive effects. Further Authors' studies will be aimed at parametric analyses involving different site seismicity, soil types and structures, as well as analyses concerning the static behaviour of GRM-structure systems, also considering the durability of the overall performance over time.

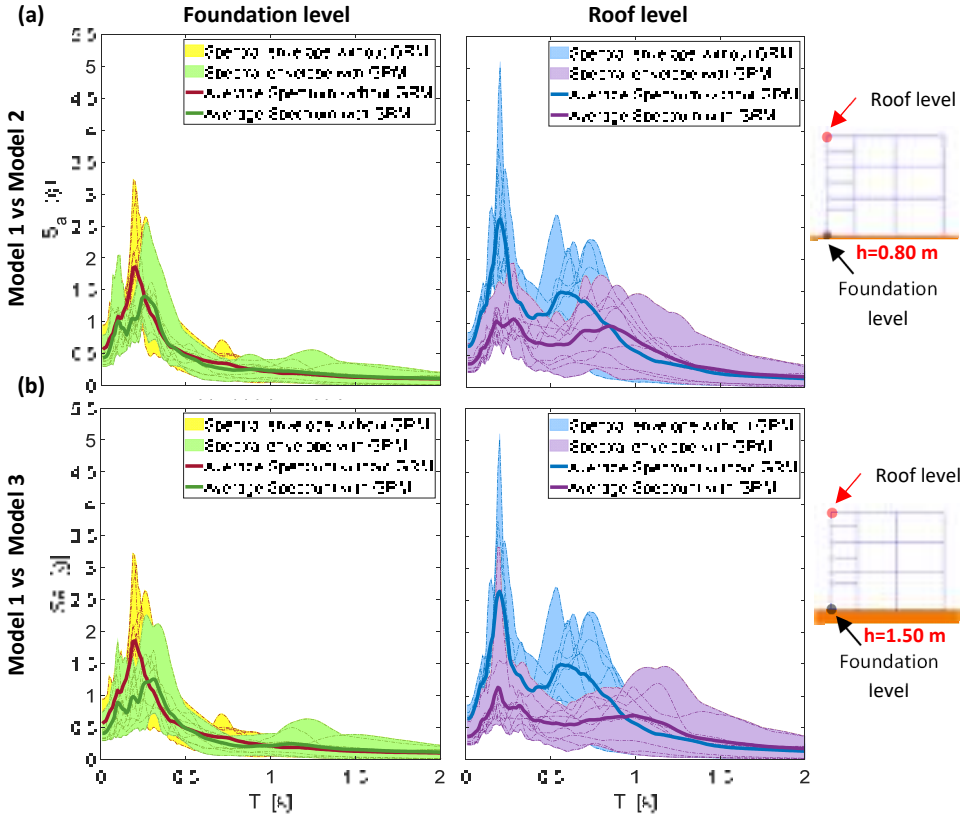

Figure 2. Comparison between the envelopes of the elastic response spectra in acceleration at the foundation and the roof: (a-b) without and with GRM layer having a thickness h = 0.80 and 1.50 m.

3. References

[1] Tsang, H. (2009). Geotechnical seismic isolation, in Takumi Miura and Yuuki Ikeda (Eds.), Earthquake Engineering: New Research, Nova Science Publishers Inc., New York, 55-87

[2] Pitilakis, D., Anastasiadis, A., Vratsikidis, A., Kapouniaris, A., Massimino, M.R., Abate, G., Corsico, S. (2021). Large-scale field testing of geotechnical seismic isolation of structures using gravel-rubber mixtures, *Earthq. Eng. Struct. Dyn.*, 50: 1-20, doi:10.1002/eqe.3468

[3] Senetakis, K., Anastasiadis, A., Pitilakis, K. (2012). Dynamic properties of dry sand/rubber (GRM) and gravel/rubber (GRM) mixtures in a wide range of shearing strain amplitudes, *Soil Dyn. Earthq. Eng.*, 33: 38-53, doi: 10.1016/j.soildyn.2011.10.003

[4] Pasha, S.M.K., Hazarika, H., Yoshimoto, N. (2019). Physical and mechanical properties of gravel-tire chips mixture (GTCM), *Geosynth. Int.*, 26(1), 92-110, doi: 10.1680/jgein.18.00041

[5] Abate, G., Fiamingo, A., Massimino, M. R., Pitilakis, D. (2023). FEM investigation of full-scale tests on DSSI, including gravel-rubber mixtures as geotechnical seismic isolation, *Soil Dyn. Earthq. Eng.*, 172, 108033, doi: 10.1016/j.soildyn.2023.108033

[6] Abate, G., Fiamingo, A., Massimino, M. R. (2023). An eco-sustainable innovative geotechnical technology for the structures seismic isolation, investigated by FEM parametric analyses, *Bull. of Earthq. Eng.*, 21(10), 4851-4875, doi:10.1007/s10518-023-01719-6

[7] Lysmer, J., Kuhlemeyer, R. L. (1969). Finite dynamic model for infinite media, *J. Eng. Mech.*, 95:859-877, doi:10.1061/JMCEA3.0001144

[8] NTC 2018, D.M. 17/01/18 - Updating of technical standards for buildings, Official Journal of the Italian Republic, 17th January 2018 (In Italian)

Soil-structure interaction as a means for optimising hazard resistant solutions: the case of Tuned Mass Dampers

D. N. Gorini[1], P. R. Marrazzo[2], E. Nastri[2], R. Montuori[2]
[1] University of Trento, Trento, Italy
[2] University of Salerno, Fisciano, Italy

Abstract

The dynamic behavior of foundation soils can compromise the performance of Tuned Mass Dampers (TMDs) aimed at mitigating earthquake- and wind-induced vibration in structures. Therefore, the present study illustrates a multi-scale analysis of dynamic soil-structure-TMD interaction, as a framework to design TMDs accounting for the soil compliance. In a first stage, advanced numerical simulations on a coupled soil-building model were carried out to grasp soil-structure interaction effects controlling the seismic performance of TMDs. This led to the development of an up-scaling process, setting up a simplified, interpretative model reproducing cardinal features of soil-structure-TMD interaction. Its extensive use pointed out critical soil-structure layouts in which TMDs can partly or fully loose their effectiveness. Therefore, optimised correlations between the TMD parameters and the ones featuring the soil-structure system were devised, exploiting the dynamic coupling of the whole system. The effectiveness of the optimised design was finally validated against the results of time-domain dynamic analyses.

1. Understanding: advanced numerical modelling

The frequency-dependent and nonlinear interactions between soil, structure and classically designed TMDs (i.e., nelecting soil-structure interaction) was investigated through nonlinear dynamic analyses on a comprehensive numerical model of a 3D soil-building system [1] developed in OpenSees [2], shown in Fig. 1. The model simulates a case study situated in the earthquake-prone Pantano region (Messina Strait, Italy), whose subosil is composed of a coarse-grained deposit (Cat. C in European standards, EN 206-1) with friction angle of 38° [3,4]. The subosil is discretised by brick elements exhibiting a highly nonlinear, hardening behaviour [5]. The building is a RC existing strcuture designed in accordance with an outdated Italian code [6]. Its members are modelled as elastic-plastic fiber section elements. The TMD is integrated into the system as masses placed at the top of the building and connected to the latter by means of rheological devices. Because the TMD effectiveness is sensitive to the mass ratio MR=m_{TMD}/m_{st} between the TMD mass and the one of the building, a large variability of MR was explored.

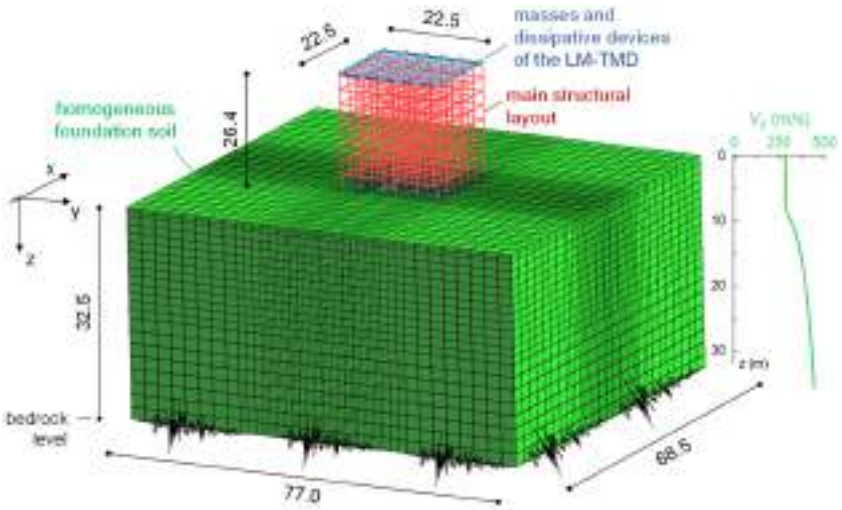

Figure 1. Mesh of the 3D soil-building-TMD model.

Figure 2 plots the effectivness η of the TMD, taken as the reduction of the maximum interstorey drift of the building compared to the case with no TMD, as a function of MR and for different intensities of a spectrum-compatible seismic record (IM=0.5, 0.75, 1.0, 1.25 for the Full Operational, Damage Control, Life Safety and Near Collapse Limit State, respectively). The TMD effectiveness appears very sensitive to the intensity of the seismic input, due to the the detrimental effect induced by the nonlinear soil response. This unfavourable effect dominates the one produced by the nonlinear structural response as the alteration of η produced by IM is much more limited when soil-structure interaction is neglected (Fig. 2a vs 2b). Nonethless, large MRs can lead to a positive TMD effectiveness even under strong ground motion.

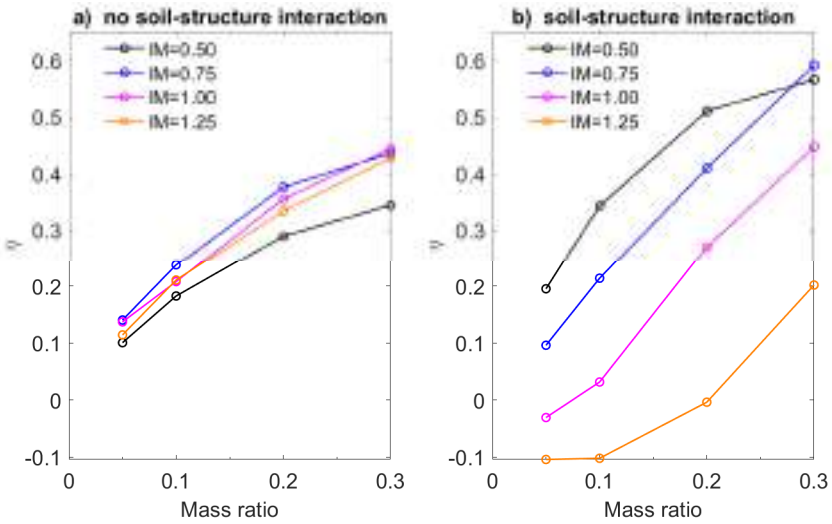

Figure 2. TMD effectiveness in the a) fixed-base model and b) soil-building model.

2. Interpretative model

On the basis of the understanding gained by advanced modelling, an interpretative model, named SimilSDOF, was developed as a manageable tool for extensive assessments [7]. This model extends the two-masses system (m_{st} + m_{TMD}) used in standard design to soil-structure interaction. The SimilSDOF was initially used in a global sensitivity analysis to point out the non-dimensional parameters controlling the TMD performance [7], which, in addition to the ones used in conventional design, were found to be the structure-to-soil relative stiffness, the structural slenderness, the foundation aspect ratio and the radius of gyration of the structure. This paved the way for an optimised design criterion for TMDs.

3. Optimised design criterion for TMDs

The SimilSDOF was therefore used to carry out a parametric analysis varying the dominant parameters, with the aim of identifying optimal configurations of the TMD minimising seismic-induced structural deformations. As a result, optimum analytical expressions were devised for the TMD fundamental frequency and damping ratio, with the aid of multi-objective, multi-dimensional best-fitting methodologies. These parameters were correlated to MR and the ones dominanting soil-structure interaction effects (see Section 2). The soil-driven optimised criterion is expressed in a rigorous non-dimensional form and can be directly used for design purposes, enhancing structural performance by a convenient tuning of the device to the soil-structure system.

4. Standard practice vs soil-driven optimised design

A comparative assessment was performed between the proposed soil-driven TMD design (OPT) and the largely diffused Den Hartog (DH) criterion [8] neglecting the soil compliance. A variety of soil-

structure layouts equipped with a TMD were investigated by means of time-domain dynamic analyses using the SimilSDOF, considering MR=5-30 % and multiple ground motions.

Preliminary results of the parametric study are consicely depicted in Figure 3, as the ratio η_{OPT}/η_{DH} plotted as a function of the TMD effectiveness obtained with the conventional design, η_{DH}. Three regions can be identified, corresponding to negligible soil-structure interaction (DH is still the optimum), significant coupling between the dynamic response of the structure and the soil (DH loses partly its effectiveness) and response dominated by the soil (η_{DH} reduces to a minimum).

In a minor percentage of cases, the soil-driven design worsens slightly the performance provided by DH. Conversely, in most of the cases, the optimised design improves evidently the performance, with maximum values of η_{OPT}/η_{DH} attained when soil-structure interaction impacts significantly structural performance.

The discussion above is a preliminary demonstration of the capability of the soil-driven design to tune conveniently the characteristics of TMDs to the overall dynamic response for enhancing structural safety and usability. By virtue of these promising results, the proposed methodology is currently being extended to a broader class of hazard protection devices.

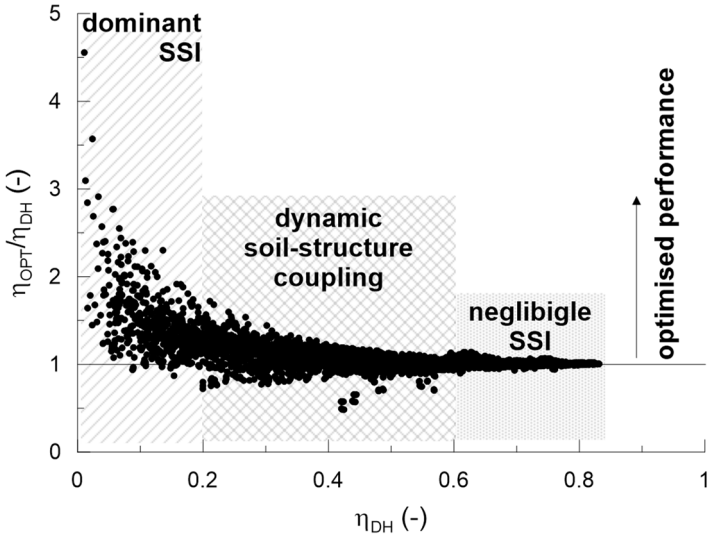

Figure 3. Comparison of the effectiveness in an optimized and a classic procedure for TMDs.

5. References

[1] Gorini, D.N., Marrazzo, P.R., Nastri, E., Montuori, R. (2024). Effectiveness of an innovative seismic resilient superelevation in an archetype, existing soil-structure system. Accepted for publication on *Bull. Earthq. Eng*

[2] McKenna, F., Scott, M.H., Fenves, G.L. (2010). OpenSees. Nonlinear Finite-Element Analysis Software Architecture Using Object Composition, *J. Comput. Eng*., 24, 95-107

[3] Gorini, D.N. (2019). Soil-structure interaction for bridge abutments: two complementary macro-elements. *PhD thesis*, Sapienza University of Rome. https://iris.uniroma1.it/handle/11573/1260972

[4] Gorini, D.N., Callisto, L. (2019). A coupled study of soil-abutment-superstructure interaction, IN: *Springer Lecture Notes in Civil Engineering*. "Geotechnical Research for Land Protection and Development" (CNRIG2019)., 565-574, doi https://doi.org/10.1007/978-3-030-21359-6_60

[5] Yang, Z., Elgamal, A., Parra, E. (2003). Computational Model for Cyclic Mobility and Associated Shear Deformation, *J. Geotech. Geoenv. Eng*., 129, 1119-1127, doi: https://doi.org/10.1061/(asce)1090-0241(2003)129:12(1119)

[6] Decreto Ministeriale 16 giugno 1976 (1976). Norme tecniche per la esecuzione delle opere in cemento armato normale e precompresso e per le strutture metalliche

[7] Gorini, D.N., Chisari, C. (2022). Impact of soil-structure interaction on the effectiveness of Tuned Mass Dampers, Earthq. *Eng. Struct. Dyn*., 51, 1501-1521

[8] Den Hartog, J.P. (1956). Mechanical vibrations. McGraw Hill, New York

Modelling Liquefaction Effects – From Lateral Spreading to Soil-Structure Interaction

Pedro Arduino[1] and Alborz Ghofrani[2]
[1] University of Washington, Seattle, WA, United States
[2] Google Corporation, San Francisco, CA, United States

Abstract

Soil liquefaction induced by earthquakes can cause significant damage to adjacent structures and lead to considerable economic loss. The mechanism and effects of soil liquefaction have been studied extensively throughout the years. With the development of computational tools and advanced constitutive models which can capture complex soil behavior under various loading and drainage conditions, numerical modeling has become popular for predicting liquefaction-induced ground failure, deformations, and effects induced by this phenomenon. This is particularly true for Soil Structure Interaction (SSI) problems where the interaction between the liquefied soil and pile foundations is highly nonlinear and inherently complex in nature. In this paper, we examine important considerations that must be taken into account when numerically evaluating soil structure interaction effects due to liquefaction effects including the capabilities of the constitutive model, boundary conditions, solution strategies, and soil-pile interface representation.

1. Problem Statement

In this presentation, we focus on addressing the significant risks posed by soil liquefaction, a phenomenon triggered by seismic events that compromises the integrity of structures built on loose, saturated soils. Liquefaction causes soils to lose their strength and stiffness, transforming into a fluid-like state, which can result in severe structural damage. One of the most critical consequences of this process is lateral spreading, where large horizontal displacements of soil occur, particularly in sloped areas or near riverbanks. These displacements exert substantial forces on structures such as bridge foundations, increasing design demands and potentially leading to failures. The complex and nonlinear interaction between liquefied soil and structural foundations, known as Soil-Structure Interaction (SSI), presents a challenging problem that requires advanced computational techniques and robust constitutive models to model accurately.

2. Scope of Work

In this study, we explore and evaluate various methods for the numerical modeling of liquefaction effects, with a particular emphasis on lateral spreading and SSI. The study [3] covers several key areas:

a. **Finite Element Formulations:** We examine finite element (FE) methods, including the widely used u-p and u-p-U formulations based on Biot's theory of poroelasticity [3]. These formulations are crucial for modeling the coupled behavior of the soil skeleton and pore fluid during seismic events, providing the necessary framework for understanding the dynamic response of soils.

b. **Constitutive Models:** We include a critical analysis of constitutive models, particularly those designed to simulate cyclic loading in soils. The focus is on the Manzari-Dafalias model, a sophisticated plasticity model capable of capturing both dilatant and contractive behaviors of sands under seismic loading conditions [Fig-1a][1][2]. This model's ability to represent the critical state conditions and cyclic response of soils is discussed in detail, highlighting its relevance for accurate seismic soil modeling.

c. **Boundary Conditions:** We emphasize the importance of implementing appropriate boundary conditions in FE models to achieve accurate simulations. Various strategies, including transmitting boundaries and the Domain Reduction Method (DRM), are reviewed to simulate seismic wave propagation and its effects on local soil-structure systems, ensuring that boundary effects do not distort the simulation outcomes [3].

d. **Soil-Structure Interaction (SSI):** We explore the interaction between structural elements (e.g., piles) and liquefied soil, with a focus on advanced modeling techniques like the embedded element approach [Fig-1b][4]. We discuss the challenges of simulating SSI, including the need for accurate representation of the soil-pile interface and the complexities introduced by large deformations and soil-structure contact mechanics.

e. **Validation and Case Study:** We highlight validation efforts using experimental data from the LEAP (Liquefaction Experiments and Analysis Projects) initiative. A case study involving the lateral spreading of a soil-pile system is presented to illustrate the practical application of the discussed modeling techniques and to demonstrate the effectiveness of the proposed methods in real-world scenarios [3].

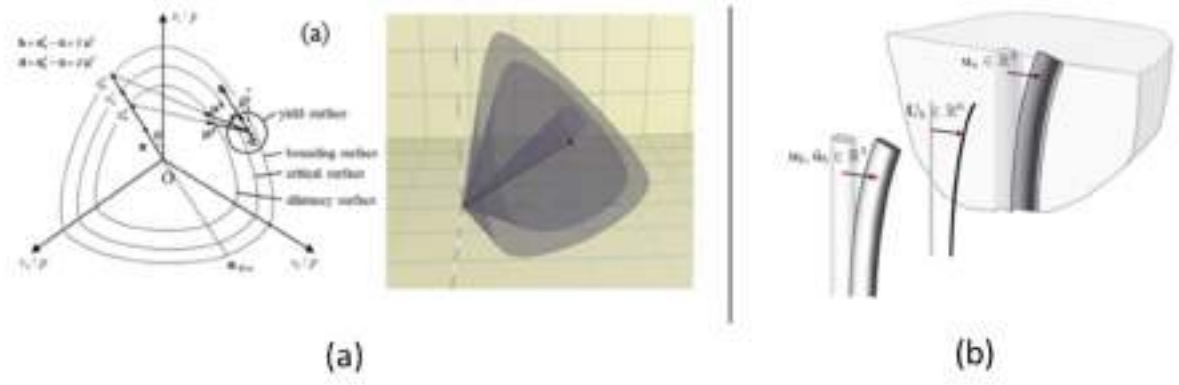

Figure 1. a) Manzari Dafalias yield surfaces and mapping method, b) Embedded beam-solid element for SSI

3. Findings

The findings of this study indicate that advanced constitutive models, like the Manzari-Dafalias model, when coupled with robust FE formulations, are critical for accurately predicting the effects of soil liquefaction and lateral spreading on structures. Validation efforts using LEAP data demonstrate that while current models can reasonably simulate seismic soil behavior, challenges remain, particularly in capturing large deformations and the transition from solid to fluid-like behavior in soils. The embedded element approach for SSI modeling is highlighted as an effective method for simulating the complex interactions between piles and surrounding soil, though further refinement is needed to improve the accuracy of large-scale simulations.

In this study, the case study demonstrates that the orientation of seismic motion relative to the slope direction [Fig-2a] significantly influences the structural demands on piles [Fig-2b]. Simulations indicate greater displacements and higher structural demands when the seismic motion is applied parallel to the slope, underscoring the importance of considering directionality in seismic design.

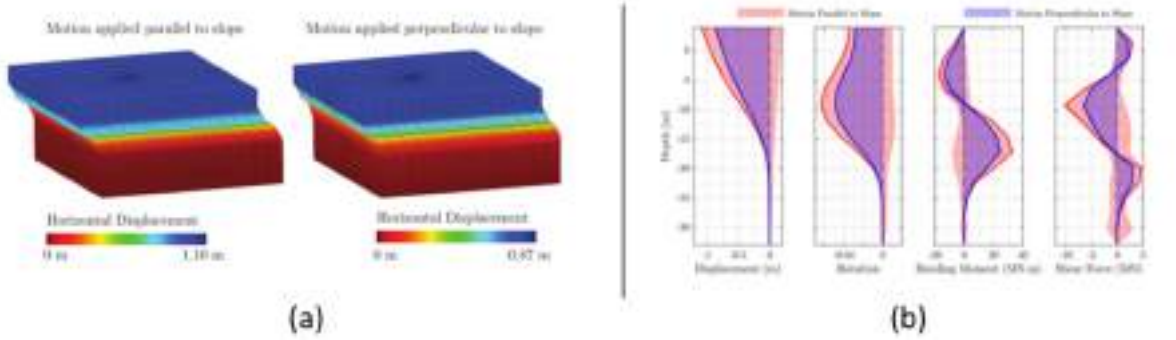

Figure 2. (a) Liquefied soil response to loading in different directions, b) Pile structural response

4. Conclusion

In this work, we provide a comprehensive overview of the numerical modeling approaches required to simulate the complex phenomena associated with soil liquefaction and SSI during seismic events. The study integrates advanced constitutive models with effective FE formulations and boundary conditions, enhancing the predictive capabilities of simulations. The results suggest that continued research and development are necessary to address the limitations of current models, particularly in dealing with large deformations and nonlinear SSI effects, ultimately contributing to safer and more resilient structural designs in liquefaction-prone areas.

5. References

[1] Dafalias, Y.F., Manzari, M. T. (2004). Simple plasticity sand model accounting for fabric change effects, *J Eng Mech*, 130(6):622–34

[2] Ghofrani, A., Arduino, P. (2016). Prediction of LEAP Centrifuge Test Results Using a Pressure-Dependent Bounding Surface Constitutive Model, *Soil Dynamics and Earthquake Engineering*, doi: http://dx.doi.org/10.1016/j.soildyn.2016.12.001

[3] Ghofrani, A. (2018). Development of numerical tools for the evaluation of pile response to laterally spreading soil, PhD Dissertation, University of Washington, Seattle, WA

[4] Turello, D. F., Pinto, F., Sánchez, P. J. (2016). Embedded beam element with interaction surface for lateral loading of piles, *International Journal for Numerical and Analytical Methods in Geomechanics*, 40(4), 568-582

The role of site effects on the seismic response of an existing r.c. bridge

A. Ambrosino[1] and S. Sica[1]
[1] University of Sannio, Benevento, Italy

Abstract

To accurately evaluate the seismic response of bridges, it is often necessary to develop complex numerical models that include a significant portion of the soil deposit, especially when the bridge is not directly founded on rock. The subsoil model should be as precise as possible to capture the main stratigraphic and topographic irregularities of the bridge valley, along with key aspects of soil behavior under seismic loading conditions. In this study, both 1D and 2D site response analyses were conducted to calculate the seismic input at the base of a reinforced concrete bridge that was extensively studied from both structural and geotechnical perspectives. Soil nonlinearity was considered in two ways: a simplified approach using the equivalent linear procedure and a more advanced approach utilizing a refined constitutive model of the soil. The results of these analyses revealed significant differences in the ground response at the pier locations depending on the assumptions made (1D vs. 2D geometry and equivalent linear vs. nonlinear soil behavior). The resulting acceleration response spectra were then compared to the design response spectra prescribed by the Italian technical code for the same soil category as the bridge piers. The primary focus of the study is on site response at the bridge piers. The outcomes of these analyses serve as inputs for the assessment of the structural safety of the bridge.

1. Introduction

Soil-Structure Interaction (SSI) may play a significant role in the seismic response of bridges that are not founded on rock. To determine whether SSI is beneficial or detrimental to the bridge response and its structural components [1], coupled approaches are generally considered the most effective solution. As highlighted in the literature, local site features such as ridges, slopes, and canyons can strongly influence the seismic wave propagation within a given soil deposit, thereby affecting the seismic response of bridges located on such sites.

The objective of this study is to assess the influence of site effects on the seismic response of a pre-stressed concrete bridge built in Italy in the 1950s. A highly accurate numerical model of the superstructure was developed and validated in a previous study [4]. Modal analysis was performed to validate this model, and the results were compared with the experimental findings by De Angelis et al [5]. To quantify the modifications in seismic motion at the base of the bridge piers due to valley and stratigraphy effects, both 2D equivalent linear and true nonlinear analyses were conducted. In the latter case, soil behavior was modeled using the Hardening Soil with Small Strain Stiffness constitutive model [6]. The results indicate a significant amplification of seismic motion at the base of the bridge piers due to site effects, which has important implications on the response of the superstructure.

2. Case study

The San Nicola Bridge is located in the city of Benevento (Italy). The structure was designed in between 1952 and 1955 by the engineer Riccardo Morandi. A detailed analysis of the San Nicola Bridge can be found in previous papers by the authors [4-5, 7], while the most important data are recalled hereinafter. The bridge deck is made of pre-stressed concrete, cast in situ, while the piers and foundations are made of reinforced concrete. For the geotechnical characterization of the site, three boreholes with SPT were carried out together with laboratory tests (oedometer test and triaxial tests) on the fine-grained materials of the soil deposit. In correspondence of the right pier of the bridge, the shear wave velocity Vs was measured through a Down Hole test while the fundamental frequencies of the subsoil was identified through an HVSR analysis. The performed investigations lead to the 2D

geotechnical model shown in Figure 1. The following soil layers have been identified: an artificial fill (AF), alluvial deposits consisting of sand and gravel (YS), fluvial colluvial deposits (FC), alluvial deposits consisting of sandy silt to clayey places (LS), and blue-grey clayey silt (BGC). The rigid bedrock formation, represented by the bottom blue-grey clay layer, was detected at a depth of 65 m from the ground level in correspondence of the east pier (borehole S1-2020).

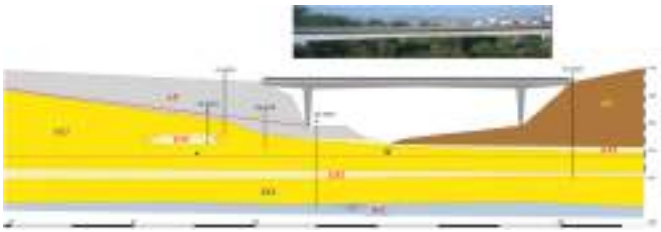

Figure 1. Longitudinal section of the valley with a superimposed picture of the bridge.

3. Numerical model and results

To assess the seismic response of the bridge by accounting for site effects and the likely spatial variability of seismic motion at the two bridge piers, the finite-element software MIDAS FEA NX was adopted. The structure was modelled trough three-dimensional (solid) finite elements. A linear-elastic constitutive model was attributed to the bridge material, with the mechanical properties identified as described in [5].

Regarding the soil model, both 1D, 2D and 3D models were extensively validated in a previous study [7]. To evaluate the topographic and stratigraphic effects on ground motion at the bridge piers, 2D sections were identified along the longitudinal axis of the bridge and transversely at the locations of the two piers. Beyond the geometric considerations, the results of site response analysis (SRA) are significantly influenced by the nonlinear behavior of the various soil layers that make up the deposit. In this phase of the study, soil nonlinearity was modeled using both a simplified equivalent linear procedure and a more advanced soil model [6].

To perform a time-history seismic analysis of the bridge, seven groups of spectrum-compatible acceleration signals were selected for the horizontal (x and y) and vertical (z) components. These signals were selected with reference to a peak acceleration on rock a_g = 0.349g, use class IV and topographic category T2 (SLV limit state). For brevity, the discussion will focus on the motion computed at the base of the two bridge piers, specifically addressing the y-component and the longitudinal section B-B as shown in Figure 2.

The predictions obtained from 1D site response analyses solved with the STRATA software were compared with those provided by the 2D equivalent linear or nonlinear analyses through MIDAS. The response spectra of the acceleration signals provided by the 1D and 2D analyses at the bridge bases (Figures 2a) were compared to the design spectrum prescribed by the Italian technical code (NTC2018). In particular, the design spectrum at the pier site was computed for a soil category B. Even taking into account soil nonlinearity, the 2D models provide for a higher amplification than the 1D analyses. In addition, the spectral accelerations obtained through the 2D site response analyses are higher than those corresponding to the requirements of the Italian technical regulation. This difference could be attributed to both stratigraphic and geometric features of the valley. The impact of these results on the bridge response is illustrated in Figure 2b, which shows the profiles of peak accelerations along the bridge piers. It is clear that a response-spectrum analysis, traditionally used in structural engineering, is insufficient for capturing the actual response of the piers. Although soil nonlinearity improves the pier response compared to linear approaches, it is evident that incorporating 2D effects is essential for accurately assessing the pier response.

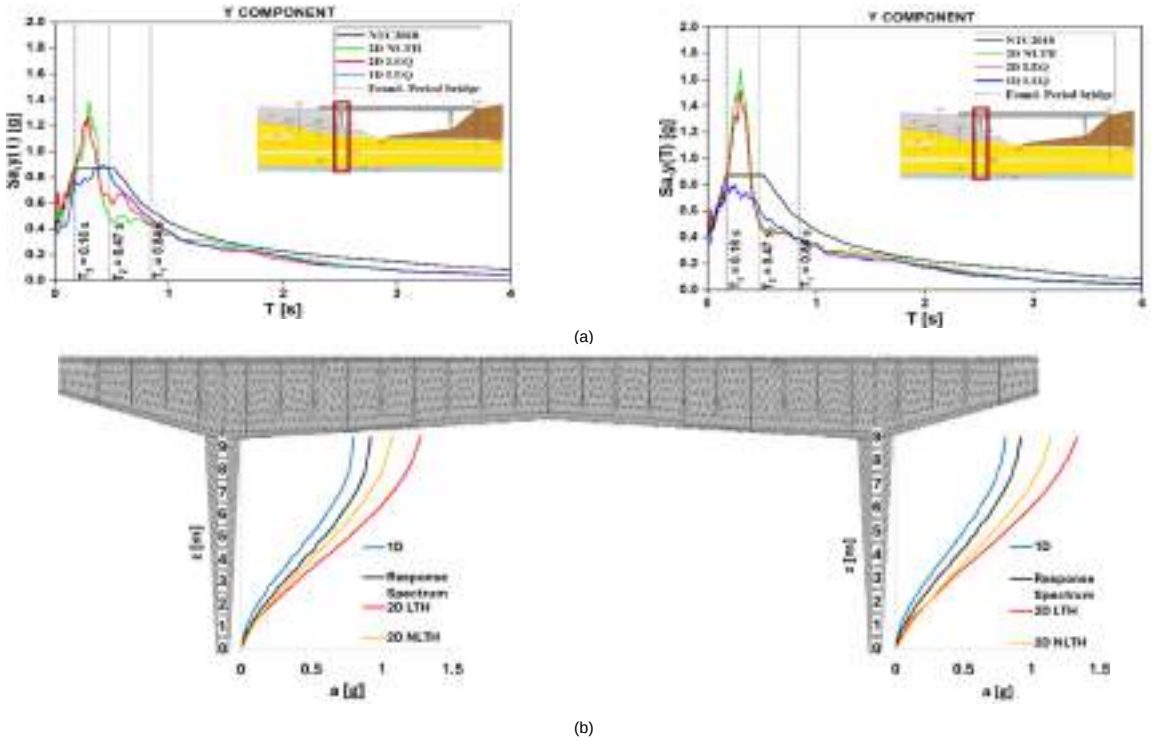

Figure 2. Results of 1D and 2D site response analyses in y direction.

4. Conclusions

The paper examined the influence of site effects on the ground motion computed at the two piers of a reinforced concrete bridge in Italy. Both 1D and 2D soil models were developed, with the 2D models encompassing the entire alluvial valley of the bridge. The study findings indicated that the 2D models predicted higher peak ground accelerations (PGAs) compared to the 1D models. For periods close to the bridge fundamental frequencies, the acceleration response spectra obtained from both the 1D and 2D analyses exceeded the design spectrum specified by the seismic code for the soil classification at the piers. Finally, the study highlighted the effects of ground response analysis on the acceleration profile along the pier height.

5. References

[1] Mylonakis, G., Gazetas, G. (2000). Seismic soil-structure interaction: beneficial or detrimental, *J Earthq Eng*, 4:277–301

[2] Luo, Y., Fan, X., Huang, R., Wang, Y., Yunus, A. P., & Havenith, H. B. (2020). Topographic and near-surface stratigraphic amplification of the seismic response of a mountain slope revealed by field monitoring and numerical simulations, *Engineering Geology*, 271, 105607

[3] Paolucci, R. (2002). Amplification of earthquake ground motion by steep topographic irregularities, *Earthquake engineering & structural dynamics*, 31(10), 1831-1853

[4] Ambrosino, A., De Angelis, A., Pecce M.R. & Sica, S. (2023). Effect of soil-structure interaction on the dynamic identification of a prestressed concrete bridge, In 9th ECCOMAS Thematic Conference on Computational Methods in Structural Dynamics and Earthquake Engineering, M. Papadrakakis, M. Fragiadakis

[5] De Angelis, A., Pecce, M. R. (2023). Model assessment of a bridge by load and dynamic tests, *Engineering Structures*, 275, 115282

[6] Schanz, T., Vermeer, P. A., Bonnier, P. G. (2019). The hardening soil model: Formulation and verification, In Beyond 2000 in computational geotechnics (pp. 281-296), Routledge

[7] Ambrosino, A., Sica, S. (2023). Calibration of a 3D numerical model to perform modal analysis of coupled systems of soil and structure, Proceedings 10th European Conference on Numerical Methods in Geotechnical Engineering, Zdravković L, Konte S, Taborda DMG, Tsiampousi A (eds), NUMGE 2023

Assessing and Increasing Resilience of Soil-Structure Systems for Seismic Loads

Boris Jeremić[1]
[1] *University of California, Davis, CA, USA*

Earthquake mechanical waves carry seismic energy and excite soil-structure systems (buildings, bridges, tunnels, dams, power plants...). The Earthquake-Soil-Structure-Interaction (ESSI), the propagation of seismic energy in time and space, through nonlinear soil-structure system, determines the extent of damage, possible collapse and casualties. Controlling, directing propagation of seismic energy through the soil-structure system can be used to improve safety and economy of infrastructure, built environment. If seismic energy can be deflected from and/or dissipated outside of structure or dissipated within structures using designated dissipation devices and SSI system components, earthquake damage can be reduced and even completely alleviated.

Briefly presented are methods, modeling and simulation tools, that can be used to better understand seismic energy propagation and practical design recommendations to control and direct propagation of seismic energy within soil-structure systems. Analysis methodology, including modeling and simulation tools are based on recent work [1; 2; 3; 4] that is implemented and available in a public domain program Real-ESSI Simulator [5]. Proposed methodology to control and direct propagation of seismic energy encompasses:

1. Soil, hard and/or soft, adjacent to and beneath the structure, and the soil-foundationinterface zone [6; 7],
2. Energy dissipators, energy sinks, within structure, for example buckling restrained braces (BRBs), frictional pendulum, lead core elastomers, etc. [8; 9; 7],
3. Viscous dampers and viscous coupling between fluid and structure [10; 8; 11],
4. External trenches surrounding the structure [12; 13],
5. Meta-materials, meta-devices, for example resonant unit cells, negative stiffness metamaterials, etc., adjacent to or within the structure [14; 15].

Of particular interest is investigation of relative contribution of each of the above noted measures for seismic energy dissipation, seismic energy deflection and seismic energy conversion. Presented will be details about and design guidance for relative efficiency of seismic protection approaches. In addition, presented will be analysis methods, simulation tools and models that are available in public domain and that are used by the engineering community for design, assessment and upgrades of soil-structure systems.

High fidelity models of soil-structure building systems, ASCE-7-21 standard buildings [7; 16] will be used to illustrate and asses seismic energy control approaches, as noted above. Presented analysis methodology and tools are used to improve safety and economy in designing new objects, as well as improving safety and economy of existing objects through upgrades.

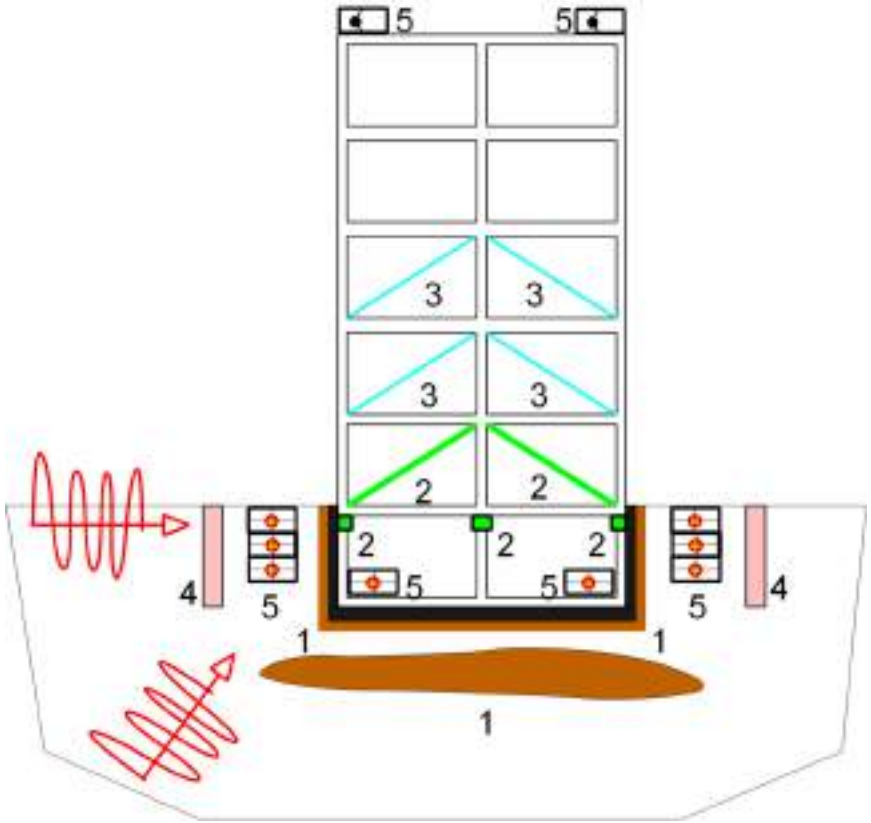

Figure 1. Seismic energy management, control methods and devices for a typical soil-structure system.

1. References

[1] Yang, H., Sinha, S. K., Feng, Y., McCallen, D. B., Jeremić B. (2018). Energy dissipation analysis of elastic-plastic materials, *Computer Methods in Applied Mechanics and Engineering*, 331:309– 326

[2] Yang, H., Feng, Y., Wang, H., Jeremić, B. (2019). Energy dissipation analysis for inelastic reinforced concrete and steel beam-columns, *Engineering Structures*, 197:109431, ISSN 0141-0296, doi: https://doi.org/10.1016/j.engstruct.2019.109431.
URL http://www.sciencedirect.com/science/ article/pii/S0141029618323459

[3] Yang, H., Wang, H., Feng, Y., Wang, F., Jeremić B. (2019). Energy dissipation in solids due to material inelasticity, viscous coupling, and algorithmic damping, *ASCE Journal of Engineering Mechanics*, 145(9)

[4] Yang, H., Wang, H., Jeremić B. (2024). Energy balance for earthquake soil structure interaction systems, analysis of input and dissipated energy. *Engineering Structures*, In Print.

[5] Jeremić B., Jie, G., Cheng, Z., Tafazzoli, N., Tasiopoulou, P., Pisanò, F., Abell, J. A., Watanabe, K., Feng, Y., Feng, Y., Behbehani, F., Yang, H., Wang, H., Staszewska, K. D. *The Real-ESSI Simulator System*. University of California, Davis, 1988-2024, http://real-essi.us/

[6] Jeremić B. (2010). High fidelity modeling and simulation of sfs interaction: energy dissipation by design, In Rolando P. Orense, Nawawi Chouw, and Michael Pender, editors, *Soil-Foundation-Structure Interaction*, pages 125–132, CRC Press, Taylor & Francis Group, ISBN 978-0-415-60040-8 (Hbk); 978-0-20383820-4 (eBook)

[7] Jeremić B., Yang, H., Wang, H., Lizundia, B. (2020). Direct analysis of soil structure interaction case studies for ATC-144 project, Technical Report UCD-CompMech-Sep2020, UCDavis and Rutherford+Chekene

[8] Symans, M. D., Charney, F. A., Whittaker, A. S., Constantinou, M. C., Kircher, C. A., Johnson, M. W., McNamara, R. J. (2008). Energy dissipation systems for seismic applications: current practice and recent developments, *Journal of structural engineering*, 134(1):3–21

[9] Nucera, F., Vakakis, A. F., McFarland, D. M., Bergman, L. A., Kerschen, G. (2007). Targeted energy transfers in vibro-impact oscillators for seismic mitigation. *Nonlinear Dynamics*, 50:651–677, doi: https://doi.org/10.1007/s11071-006-9189-7

[10] Symans, M. D., Constantinou, M. C. (1998). Passive fluid viscous damping systems for seismic energy dissipation, *ISET Journal of Earthquake Technology*, 35(4):185–206

[11] Roh, H., Reinhorn, A. M. (2010). Modeling and seismic response of structures with concrete rocking columns and viscous dampers, *Engineering Structures*, 32(8):2096–2107

[12] Woods, R. D. (1968). Screening of surface waves in soils, ASCE *Journal of the Soil Mechanic and Foundations Division*, 94(4):951–979

[13] Bolt, B. A., Morrison, H. F. (1981). Modification by trench barriers of the seismic input to nuclear power plants, Technical Report NUREG/CR-1777, UCB-ENG-4723, Department of Engineering Geosciences, UC Berkeley

[14] Kanellopoulos, C., Jeremić, B., Anastasopoulos, I., Stojadinović, B. (2020). Use of the domain reduction method to simulate the seismic response of an existing structure protected by resonating unit cell metamaterials, In M. Papadrakakis, M. Fragiadakis, and C. Papadimitriou, editors, *Proceedings of the EURODYN 2020, XI International Conference on Structural Dynamics*, pages 2926–2938, Athens, Greece, EASD Procedia

[15] Chondrogiannis, K. A., Dertimanis, V., Jeremić, B., Chatzi, E. (2021). On the vibration attenuation properties of metamaterial design using negative stiffness elements. In Walter Lacarbonara, Balakumar Balachandran, Michael J. Leamy, Jun Ma, J.A. Tenreiro Machado, and Gabor Stepan, editors, *Advances in Nonlinear Dynamics - Proceedings of the Second International Nonlinear Dynamics Conference (NODYCON 2021)*, volume 3, Sapienza, Università di Roma, Springer Nature

[16] Lizundia, B., Crouse, C.B., Harris, S., Jeremić, B., Stewart, J. P., Valley, M. (2020). A practical guide to soil-structure interaction, FEMA P-2091, Technical Report FEMA P-2091, Applied Technology Council, Redwood City, CA, USA

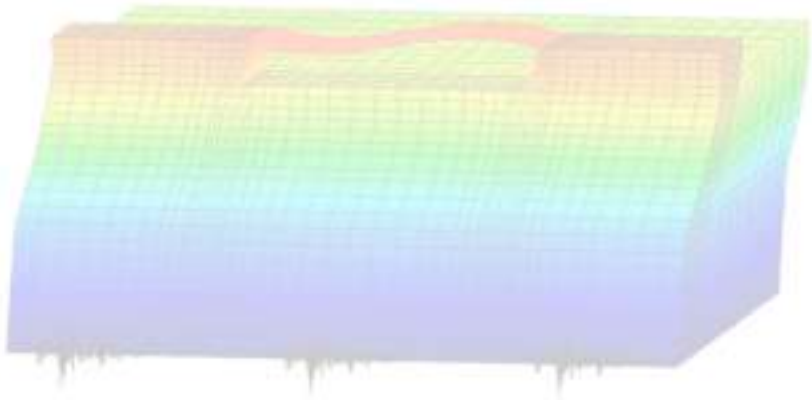

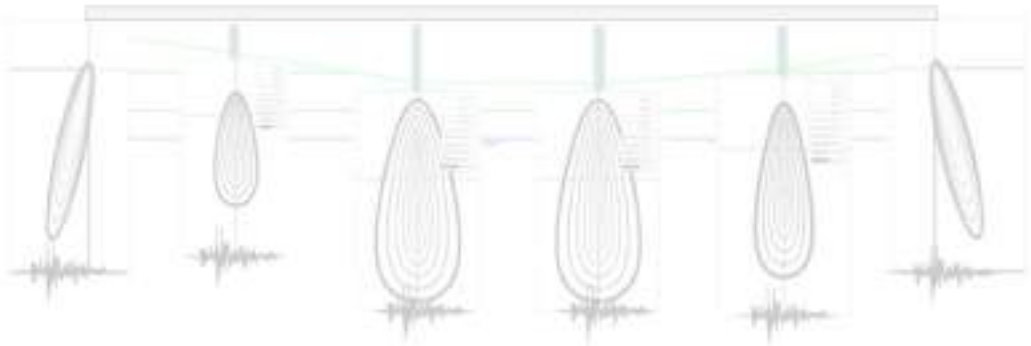

4.Underground structures

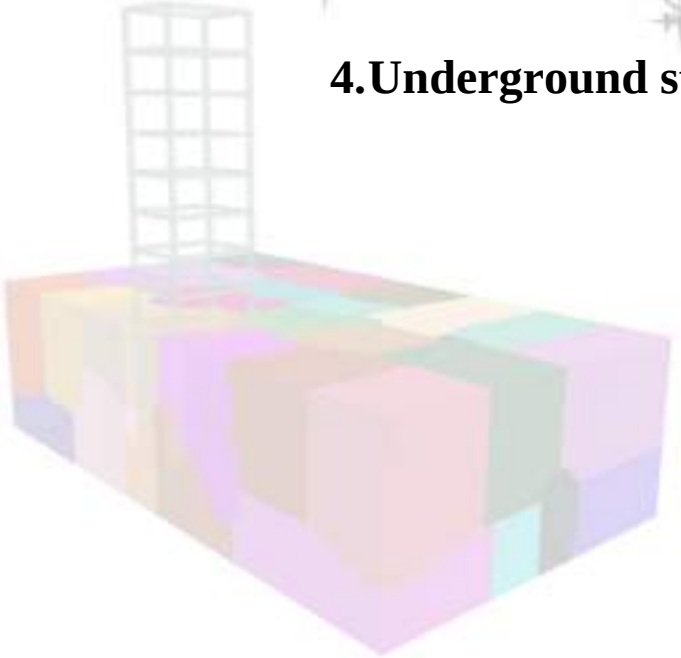

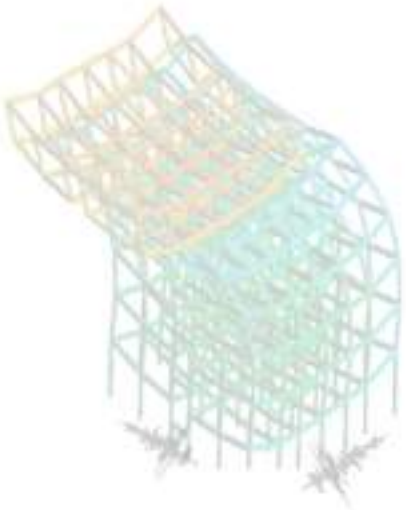

The role of constitutive and numerical modelling in seismic design and retrofitting of tunnels

D. Boldini[1], G. Caldarini[1] and L. Vignali[2]
[1] Sapienza University of Rome, Rome, Italy
[2] University of Bologna, Bologna, Italy

Abstract

The contribution examines the seismic behaviour of tunnels and proposes strategies for designing new structures and evaluating existing ones. During the design stage, accurately estimating the inertial response of the surrounding soil is crucial, which necessitates the selection of an appropriate constitutive model. In certain scenarios, conducting fully-coupled dynamic analyses becomes essential to capture significant soil-structure interaction effects. These analyses are also particularly valuable for assessing the seismic performance of existing structures, especially when dealing with damaged or inadequately thick linings, or flexible linings at the invert arch, as discussed with reference to the case-history of the TT10 tunnel at CERN.

1. Introduction

Tunnels have traditionally been regarded as inherently resistant to seismic events. However, recent evidence suggests that, during significant earthquakes, tunnels can suffer damage, collapse, and become the weak link in an infrastructural network, thereby reducing its resilience [1].

In the state-of-the-practice, the seismic design of tunnels typically follows a decoupled approach where: 1) the inertial response of the soil to seismic actions is assessed through a free-field seismic site response analysis assuming a visco-elastic model for the soil, and 2) the evaluation of the force increments in the lining is performed by modelling the tunnel as an elastic beam resting on an elastic soil [2]. This approach may be appropriate or even overly conservative for low to medium earthquake intensities in terms of soil response, as soil plasticity tends to reduce the seismic forces induced in the lining [3, 4]. However, during intense earthquakes, soil behaviour can include stiffness degradation, volumetric-deviatoric coupling, and potential soil liquefaction in shallow saturated sands, which are typically associated with more severe conditions than those predicted by the simplified decoupled approach. These distinctive features can be effectively simulated using state-of-the-art numerical simulations employing advanced soil constitutive formulations [5]. Results also demonstrate that fully-coupled analyses are sometimes necessary to accurately capture dynamic soil-structure interaction effects that cannot be adequately predicted using a decoupled approach alone [5, 6].

Fully-coupled analyses are also a fundamental tool for the analysis and retrofitting design of existing tunnels. Many of these tunnels were often constructed without consideration of seismic actions. Additionally, particularly in developed countries, numerous structures over 50 years old may have been damaged due to construction inadequacies (such as the absence of waterproofing membranes, or very flexible invert arches). Numerical simulations can accurately consider the unique geometry and initial conditions of the tunnel lining, helping to identify the most suitable solutions for enhancing seismic performance.

This contribution aims to analyse the transversal response of tunnels during seismic events. Initially, the response of a circular shallow tunnel excavated in a saturated sand deposit is investigated using different constitutive models, properly calibrated to account for the initial stiffness profile with depth and stiffness decay with increasing strain levels. Then, from a design perspective, the required constitutive elements for various seismic intensity scenarios are highlighted, and cases requiring fully-coupled analyses are identified. Finally, the role of these types of analyses is discussed with reference to existing tunnels. In particular, a vulnerable section of the TT10 tunnel, part of the underground CERN infrastructure, is evaluated [7, 8].

2. The role of constitutive and numerical modelling in the seismic design of tunnels

Different constitutive formulations were adopted to reproduce the seismic response of the saturated sand deposit in which the tunnel is excavated. Specifically, the simplest visco-elastic (VE) formulation, with stiffness and Rayleigh damping parameters properly calibrated against an equivalent-linear visco-elastic analysis (VE-LE) [4, 9], are investigated together with the HSsmall [10] and SANISAND [11] models.

The input signal, recorded during the 1999 Turkey earthquake, was scaled down to different values of *PGA*, from 0.05 g to 0.25 g. It is characterised by a predominant frequency of 1.284 Hz, similar to the natural frequency of the deposit at small strain, equal to 1.134 Hz. Figure 1a,b shows that the shear stress-strain response calculated at the depth of 6.5 m by the different constitutive models is comparable up to an input *PGA* of 0.05 g. However, marked differences are observable for the largest *PGA* of 0.25 g due to plastic strain accumulation, volumetric-deviatoric coupling (Fig. 1c), and overall stiffness decay. The SANISAND model is associated with the higher forces in the lining.

The soil around the tunnel displays liquefaction during the seismic event and the tunnel lining is pushed towards the ground surface, which suffers a centimetric heave (Fig. 2c). This behaviour is significantly different from that recorded by the VE (Fig. 2a) and HSsmall (Fig. 2b) analyses. This indicates that, at least for the investigated problem, the simple VE approach could be acceptable for simulating the inertial soil response up to shear strain levels on the order of 0.1-0.2%, as already pointed out in [3]. However, more advanced constitutive laws are needed at higher shear strain levels. Additionally, especially when liquefaction phenomena occur, using a fully-coupled approach becomes essential to correctly capture the seismic soil and tunnel responses.

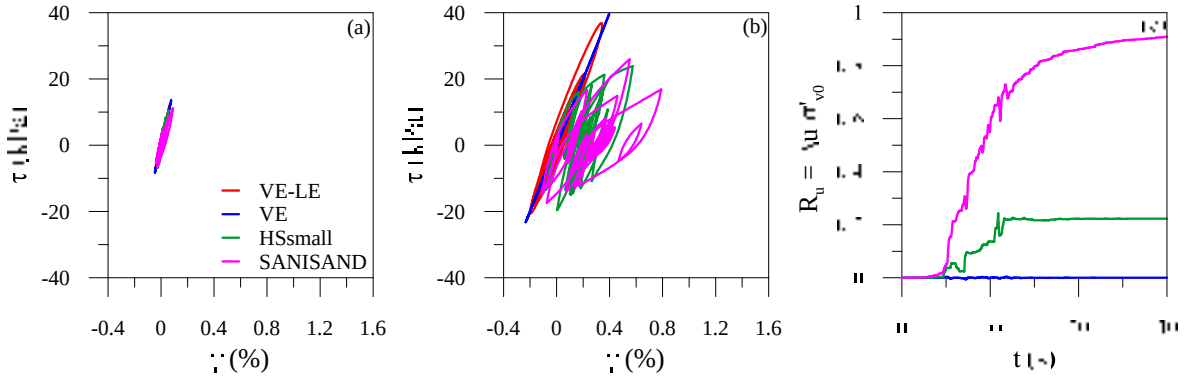

Figure 1. Shear stress-strain curves in the case of PGA equal to 0.05 g (a) and 0.25 g (b) and excess pore water pressure ratio for PGA = 0.25 g (c) for a point at the depth of 6.5 m [5].

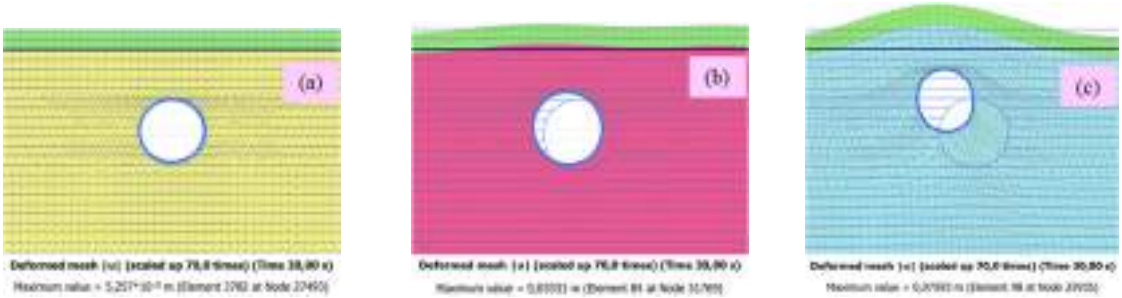

Figure 2. Deformed configuration at the end of the earthquake (30 s) in the case of VE (a), HSsmall(b) and SANISAND models for the soil.

3. The role of numerical modelling in the seismic retrofitting of tunnels

Fully-coupled numerical analyses are essential for assessing the seismic performance of existing tunnels and designing appropriate retrofitting measures. Figure 3 refers to a cross-section of the TT10

tunnel at the CERN underground laboratories, located between the moraine and molasse regions, showing cracks along the concrete lining [7]. Simulations were conducted to investigate the potential impact of damage on the lining's response to the 1995 Port Island earthquake record, scaled to a *PGA* of 0.15 g. The force distribution, in terms of the minimum and maximum values of the increment in hoop force and bending moment on the tunnel lining during the seismic event, is plotted in the figure as a function of the angle θ for five different scenarios of lining deterioration. Results reveal that, from a structural point of view, the most severe scenarios are those involving an asymmetric reduction in the stiffness or thickness of the lining (i.e., scenarios 3 and 5).

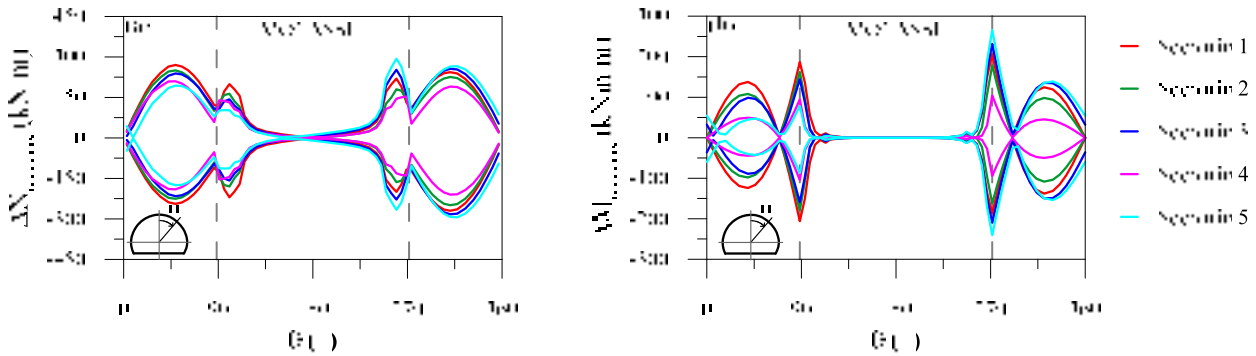

Figure 3. Maximum and minimum envelopes of hoop force (a) and bending moment (b) during the seismic event on the tunnel lining for the 5 following scenarios: 1) E_{lin} = 20 GPa for 0° ≤ θ ≤ 360°; 2) E_{lin} = 10 GPa for 0° ≤ θ ≤ 360°; 3) E_{lin} = 10 GPa for 0° ≤ θ ≤ 113°; 4) t_{lin} = 0.15 m for 0° ≤ θ ≤ 113°, 247° ≤ θ ≤ 360°, t_{lin} = 0.185 m for 113° ≤ θ ≤ 247°; 5) t_{lin} = 0.15 m for 0° ≤ θ ≤ 113°.

4. References

[1] Callisto, L., Ricci, C. (2019). Interpretation and back-analysis of the damage observed in a deep tunnel after the 2016 Norcia earthquake in Italy, *Tunn. Undergr. Space Technol.*, 89, 238–248, doi: 10.1016/j.tust.2019.04.012

[2] Wang, J.N. (1993). Seismic design of tunnels: a state-of-the-art approach, Monograph 7, Parsons

[3] Régnier, J. et al. (2016). International benchmark on numerical simulations for 1D, nonlinear site response (PRENOLIN): verification phase based on canonical cases, *Bull. Seismol. Soc. Am.*, 106(5), 2112-2135, doi: 10.1785/0120150284

[4] Amorosi, A., Boldini, D. (2009). Numerical modelling of the transverse dynamic behaviour of circular tunnels in clayey soils, *Soil Dyn. Earthq. Eng.*, 29, 1059–1072, doi: 10.1016/j.soildyn.2008.12.004

[5] Caldarini, G., Rollo, F., Amorosi, A., Boldini, D. (2024). Il ruolo del legame costitutivo nella modellazione di una galleria soggetta a sisma, IARG 2024, Gaeta, 6 pages

[6] Shen, Y., El Naggar, M.H., Zhang, D., Li, L., Du, X. (2024). Seismic response characteristics of shield tunnel structures in liquefiable soils, *Soil Dyn. Earthq. Eng.*, 182, 108701, doi: 10.1016/j.soildyn.2024.108701

[7] Di Murro, V. (2019). Long-term performance of a concrete-lined tunnel at CERN, PhD thesis, University of Cambridge

[8] Vignali, L. (2023). Analisi del comportamento sismico di gallerie: il caso della galleria TT10 del CERN, Master thesis in Ingegneria Civile, University of Bologna.

[9] Amorosi, A., Boldini, D., Elia, G. (2010). Parametric study on seismic ground response by finite element modelling, *Comput. Geotech.*, 37(4), 515-528, doi: 10.1016/j.compgeo.2010.02.005

[10] Benz, T., Vermeer, P.A., Schwab, R. (2009). A small overlay model, *Int. J. Numer. Anal. Methods*, 33(1), 25-44, doi: 10.1002/nag.701

[11] Dafalias, Y., Manzari, A. (2004). Simple plasticity sand model accounting for fabric change effects, *J. Eng. Mech.*, 130(6), 622-634, doi: /10.1061/(ASCE)0733-9399(2004)130:6(622)

State of Practice for Seismic Structure-Soil-Structure Interaction Analysis in California

K. Ellison[1], B. Shao[2] and M. Tatarsky[3]
[1] Arup, Portland, Oregon, United States
[2] Arup, San Francisco, California, United States
[3] Arup, New York City, New York, United States

Abstract

Over the past decade, seismic structure-soil-structure interaction (SSSI) analysis has evolved from being state of the art to common practice in the US State of California. Agencies such as BART, LA Metro, San Francisco Public Utilities Commission, Caltrans, and the Transbay Joint Powers Authority now routinely rely on SSSI analyses from their consultants to design underground structures or assess the potential impact of new construction on the performance of their nearby existing assets during a seismic event.
This presentation will focus on 4 short case studies (2 rail projects and 2 water projects) to highlight how model sophistication, agency requirements, and client expectations have evolved over the past 12 years. Each case study involves 3D nonlinear, fully coupled analysis with bedrock propagating ground motion time histories with the software LS-DYNA.

1. Rail Case Studies

SSSI analyses for the Salesforce Transit Center and adjacent high rises (circa 2013) in San Francisco (see Figure 1a) were novel at the time and effective at demonstrating the potential impact of new high-rise construction on the seismic performance of the Salesforce Transit Center being constructed simultaneously. Based on these analyses, minor modifications to the transit center were incorporated such as locally increased concrete strength in the ground level diaphragm and locally increased rebar density in the trainbox wall. Comparison of the Salesforce Transit Center case study with more recent analyses for the UCLA Metro Station and adjacent Wilshire-Gayley High Rise in Los Angeles (see Figure 1b) highlights several modeling advances and changes to the state of practice such as:

- more knowledgeable clients and reviewers
- tri-directional shaking (rather than uni- or bi-directional)
- non-Masing damping in the constitutive model
- automated stratigraphy-generation and soil model validation using conventional SRA software (i.e. DEEPSOIL)
- automated post-processing of large numbers of simulations via cloud computing.

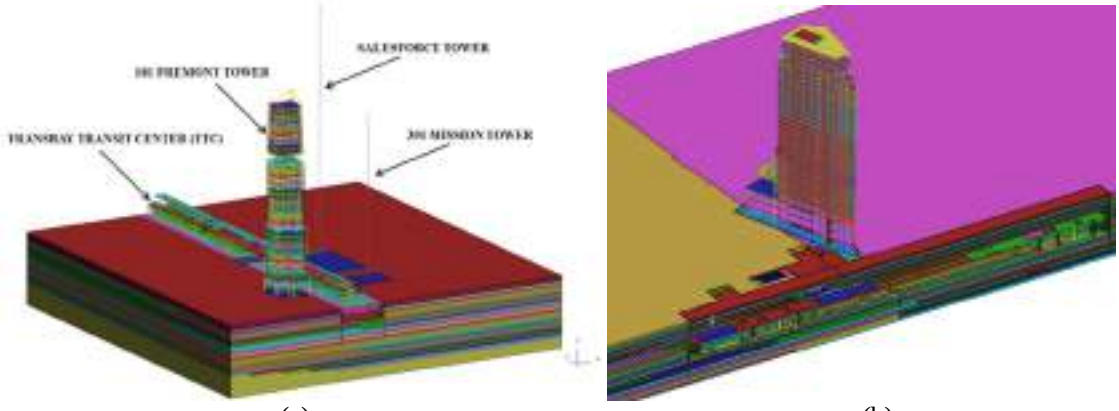

(a) (b)

Figure 1. SSSI Models of (a) Salesforce Transit Center and (b) UCLA Station.

Results from the UCLA Station analyses are currently being used to assess whether mitigative measures incorporated into the station design, such as CLSM placement between the Wilshire-Gayley tower and UCLA Station, are sufficient to mitigate the SSSI impacts.

2. Water Case Studies

Analyses for the Mariposa Pump Station and adjacent sewer box (see Figure 2a) in San Francisco performed circa 2017 borrowed the same techniques used for the Salesforce Transit Center project. Similar to the rail examples, this project consisted of a new structure (a pump station) being constructed adjacent to critical below-grade linear infrastructure (a transport/storage sewer box). Unlike the rail examples, the pump station did not impart significant inertial loading from its above-grade superstructure. Nevertheless, kinematic effects from introducing a stiff embedded structure had significant SSSI implications on the seismic performance of the sewer box. The analysis was ultimately useful to specify a suitable strength and stiffness of CLSM to be placed in a small gap between the two structures.

A unique finding from the Mariposa Pump Station case study was that averaging effects that tended to reduce spectral accelerations for the stiff transport/storage (T/S Box) in the longitudinal direction had the effect of shedding this effect to the adjacent pump station. This phenomenon is shown in Figure 3 whereby the inclusion of the T/S box reduced shear demands in the pump station in the X direction but had relatively little effect on the maximum shear demands in the Y direction.

Comparison of the Mariposa Pump Station analyses with more recent analyses for the Lower Alemany Stormwater Tunnel and adjacent highway ramps (circa 2023) reinforces all the modeling advances listed above for the rail case studies. In addition, the Lower Alemany Stormwater Tunnel provides a useful case study to demonstrate an automated workflow combining soil columns from DEEPSOIL with soil stratigraphy from LEAPFROG to produce a large soil domain with complex topography and stratigraphy discussed in the next section.

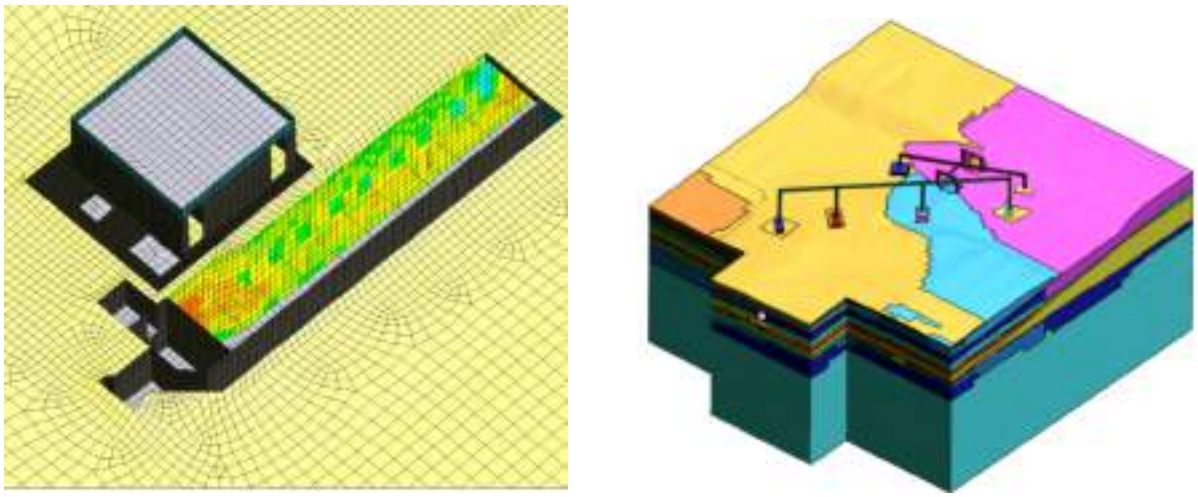

(a) (b)

Figure 2. SSSI Models of (a) Mariposa Pump Station and (b) Lower Alemany Stormwater Tunnel.

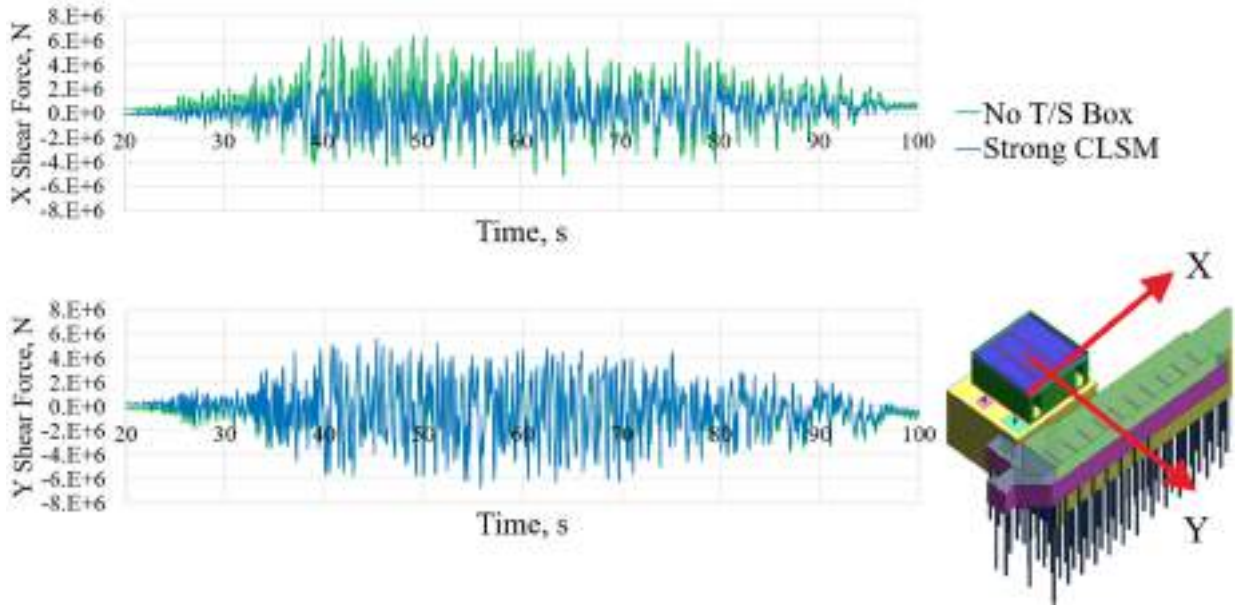

Figure 3. Shear forces in the pump station superstructure with/without the adjacent sewer box.

3. Advances on digital workflow

The SSSI model creation process for simulations in LS-DYNA has been streamlined to the point where it is now economically feasible for relatively small projects. An example SSSI workflow for the Lower Alemany Stormwater Tunnel project is shown in Figure 4. Parameter generation for a single soil column can be directly exported from the nonlinear SRA software DEEPSOIL. Python scripts have been developed to automatically create and run equivalent SRA models in LS-DYNA with uni-directional shaking (for verification of equivalence with DEEPSOIL) and multi-directional shaking. One or more of the LS-DYNA SRA models can then be combined with surfaces from the geologic modeling software LEAPFROG to automatically develop a 3D SRA model. 3D SRA models are useful to provide a continuous assessment of the seismic hazard throughout a project area and to evaluate the impact of 3D stratigraphy on the site response. Finally, all or a portion of the soil domain from the 3D SRA can be recycled to perform SSI or SSSI models.

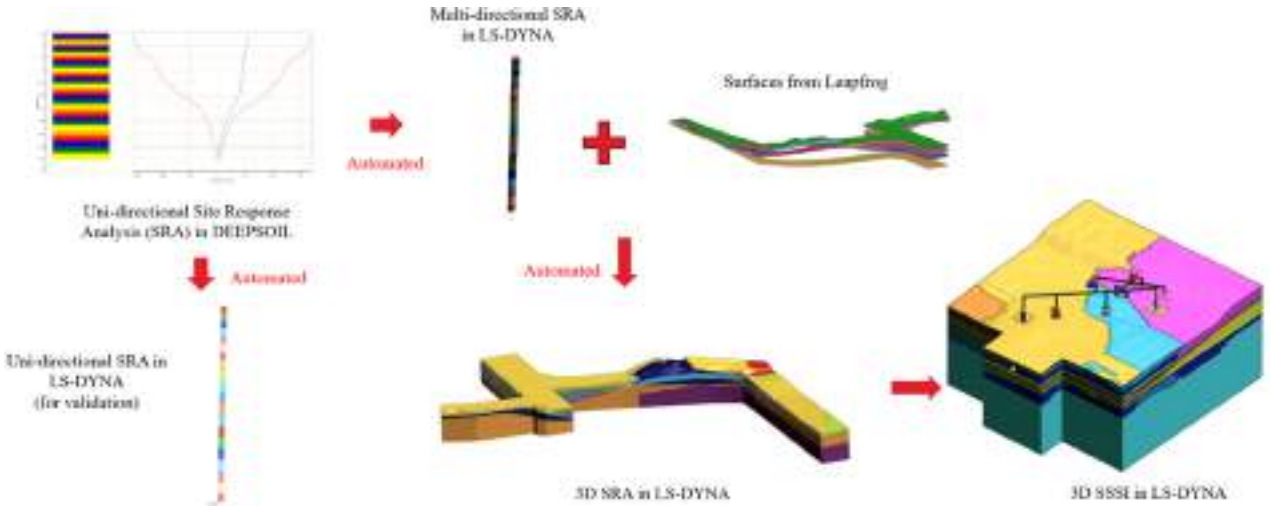

Figure 4. General workflow for developing 3D SRA and SSSI models.

In addition, the workflow leverages cloud computing resources to fully utilize the parallel processing capabilities of LS-DYNA where sophisticated models can be run on many multi-core machines simultaneously, which significantly reduces the run time needed for analysis iteration.

Evaluation of the seismic behaviour of the underground facilities hosting CMS experiment at the Large Hadron Collider at CERN using Real – ESSI Simulator

U. Carmando[1], A. Mubarak[2], A. Bilotta[1], E. Bilotta[1], J. Knappett[2], S. La Mendola[3], M. Gastal[3], P. Mattelaer[3], D. Merlini[4], M. Falanesca[4], G. Bella[4], F. Gianelli[4], B. Jeremic[5] and M. Andreini[3]

[1] University of Napoli Federico II, Italy

[2] University of Dundee, United Kingdom

[3] CERN - European Organization for Nuclear Research, Geneva, Switzerland

[4] Pini Group SA, Switzerland

[5] University of California, Davis, US

Abstract

Understanding the seismic behaviour of underground structures is essential to assess the response of critical equipment for scientific experiments, such as those housed in the cutting–edge infrastructure of CERN. The latter is one of the world's largest research centres located at the border between France and Switzerland and consists of linear and circular accelerators of nuclear particles. In the field of seismic geotechnical engineering, the code Real–ESSI (Realistic modelling and simulation of Earthquakes, Soils, Structures and their Interaction) permits simulating the behaviour of underground infrastructure when subjected to seismic waves, integrating advanced finite element modelling techniques with high-performance computing capabilities. Real–ESSI was used for assessing the seismic performance of the underground caverns hosting the Compact Muon Solenoid experiment, as part of the Large Hadron Collider complex at CERN. According to the applicable French regulations in the matter of seismic safety, the site in which the CMS experiment is located is classified as a zone with moderate seismicity level. By considering three different seismic input motions applied at the model base, dynamic Finite Elements Analyses (FEA) have been carried out to benchmark results using Real–ESSI against analyses using the PLAXIS FEA software, as well as to investigate the effects of such input motions on the CMS infrastructures. This preliminary research provides a baseline for further investigations to be conducted into how the seismic motions vary through site layers and can affect the sensitive installations located inside the CMS cavities.

1. Introduction

This paper focuses on the modelling and simulating the behaviour of two deep caverns of the LHC Point 5 (CERN) hosting the Compact Muon Solenoid (CMS). Stratigraphic and lithological profiles have been simplified on the basis of previous studies [1]. This study aims to compare Real – ESSI Simulator [2] with FE software PLAXIS 2D v.20 [3] by applying to the base of the model Ricker Wavelet as imposed motion in order to assess the amplification of the ground shaking through the layers up to ground level, as well as to identify the effect of seismic excitations on the cavern's boundaries under plane-strain conditions.

2. Verification phase: free – field conditions and LHC point 5

The model consists of three major layers, starting from the top: i) a Moraine deposits layer extending from ground level to 50 m depth; ii) an underlying Molasse rock layer, extending to 100 m depth, divided into sublayers by different stiffness degree; iii) a medium – stiff Molasse rock layer extending a further 70 m to the base of the model. A first verification phase in free – field conditions, i.e. without the CMS cavern, was initially carried out. As done in PLAXIS 2D [4] the vertical boundaries of the model were set at five times the caverns' depth to minimize the effect of boundary wave reflection in the area of interest.

A 1-km-length model has been created in Real – ESSI, by defining a regular mesh size of 8-node-brick elements, a linear visco – elastic behaviour and the same materials for soil layers, the same boundaries conditions, i.e. a full fixity at the base of geometry was generated, whereas roller supports to the vertical boundaries were assigned, as well as the same damping ratios equal to approximately 5% for all soil layers

via Rayleigh approach with double frequency control. For further comparison, a third software capable to compute a linear-elastic one-dimensional wave propagation through a layered medium, namely Strata, has been employed [5]. By applying a Ricker Wavelet as input motion at the base of the model, results observed in terms of acceleration time histories show good compatibility level between the two FE analyses in the time domain, and the corresponding solution in the frequency domain (Figure 1).

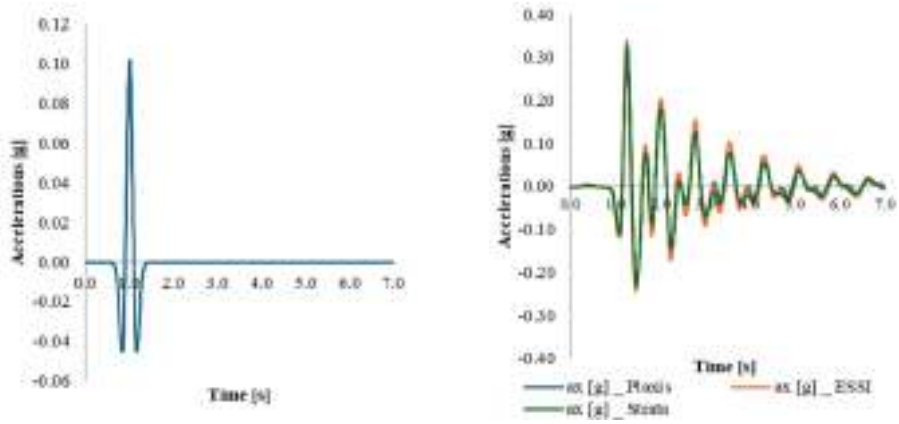

Figure 1. Input ricker wavelet (on the left) and acceleration time history computed at the ground level in free – field conditions (on the right).

Figures 2 and 3 show a further comparison between PLAXIS 2D and Real – ESSI with the presence of the LHC cavities, with the same ground conditions and having the same input motion as above. Damping ratios equal to 5% have been assumed for the concrete linings of caverns and pillar. Several points of the model have been compared in both models (Figure 3).

To better understand if the model can determine structural response of caverns when subjected to a seismic input motion, instead of the Ricker wavelet input, the recorded time history of acceleration during Friuli earthquake (1976) and a low intensity event recorded at CERN on November 1st, 2022, were employed and applied to the base of the model. The last event has a PGA value equal to 0.0002 g.

The amplification functions calculated in free-field conditions (Figure 4a) are almost overlapped, consistently with the linear elastic framework. Difference in the peak amplitude is due to possible diversities in the damping ratio among codes. Considering the presence of caverns (Figure 4b), the low intensity CERN signal produces very large amplifications, possibly due to numerical issues that need further investigation.

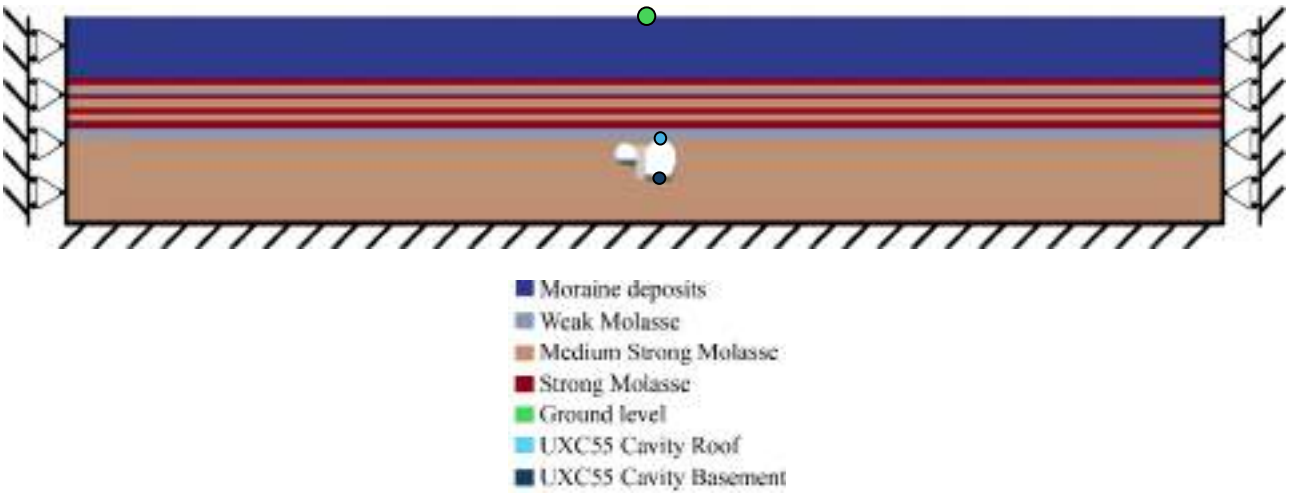

Figure 2. LHC Point 5.

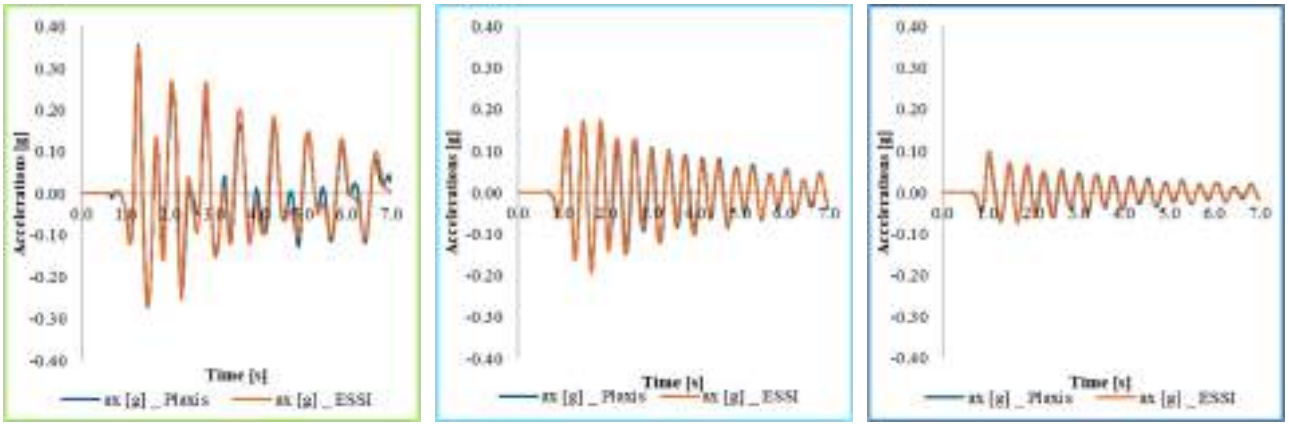

Figure 3. LHC Point 5: results in terms of acceleration time histories on ground level (on the left), UXC55 cavity roof (on the center) and UXC55 cavity basement (on the right).

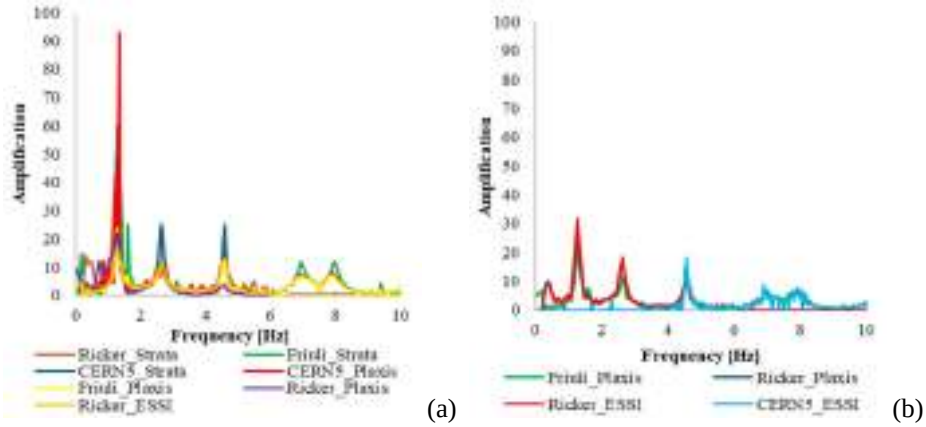

(a) (b)

Figure 4. Amplification functions observed for free – field conditions (a) and with the presence of LHC cavities (b).

3. Concluding remarks

These numerical simulations have shown the potential of Real-ESSI Simulator in the problem at hand. However, further analyses are currently being carried out to address the numerical issues of dynamic response of the lined caverns undergoing very low intensity shaking. This preliminary activity will permit to deeply investigate how the seismic motions can affect the sensitive installations located inside the CMS caverns.

4. References

[1] Mubarak, A. (2022). Numerical simulation of large tunnel systems under seismic loading conditions: CERN infrastructure as a case study, Doctoral dissertation, University of Dundee (UoD), UK

[2] Jeremic et al. (2024). Real – ESSI Simulator Lecture Notes, UCD California, Davis

[3] Plaxis. Bentley (2022). Material Models Manual and Reference Manual - Plaxis CONNECT Edition

[4] Carmando, U., Mubarak, A., Bilotta, A., Bilotta, E., Knappett, J., La Mendola, S., Gastal, M., Mattelaer, P., Sironi, L., Merlini, D., Falanesca, M., Bella, G., Gianelli, F., Andreini, M. (2023). Preliminary study for seismic assessment of the underground facilities at point 5 of the Large Hadron Collider (LHC) at CERN, COMPDYN 2023 9th ECCOMAS Thematic Conference on Computational Methods in Structural Dynamics and Earthquake Engineering M. Papadrakakis, M. Fragiadakis (eds.) Athens, Greece, 12-14

[5] Kottke, A. R., Wang, X., Rathje, E. M. (2013). Technical Manual for Strata, Department of Civil, Architectural, and Environmental Engineering, University of Texas

Simplified approach for assessing the risk of buried pipelines threatened by displacements induced by groundwater fluctuations

A. Tawalo[1,2], G. Urciuoli[2], G. Tsinidis[3]
[1] SSM - Scuola Superiore Meridionale, Naples, Italy
[2] DICEA - Dipartimento di Ingegneria Civile, Edile e Ambientale, Università degli Studi di Napoli Federico II, Naples, Italy
[3] Department of Civil Engineering, University of Thessaly, Volos, Greece

Abstract

Pipeline systems constitute an indispensable type of infrastructure due to their vital function in transporting essential resources, including gas, water, and data. Given their widespread nature, pipeline systems may cross unstable slopes, thereby exposing them to potential deformations triggered by slope movements which can reach critical levels, ultimately leading to pipeline failures. Enhancing the resilience of these systems against slope displacements requires proper assessment of the displacements magnitude, as well as of the vulnerability of the pipelines affected. This paper presents a simplified framework to assess the risk for buried pipelines exposed to slope displacements induced by groundwater fluctuations. The approach for assessing landslide displacements builds upon an existing analytical model that predicts slope displacements and velocities by solving the momentum equation with an added viscous term. The proposed framework expands this model into a probabilistic approach, accounting for spatial and temporal variability. Spatial uncertainty primary stems from variations in soil properties, sliding surface depth, and pore pressure in space. Meanwhile, temporal uncertainty is mainly attributed to fluctuations in groundwater level over time. Semi-variogram tool is used to model the spatial variability, while the temporal variability is modelled by using the annual rate of exceedance. The approach is illustrated using a case study (Miscano slope) in southern Italy. Fragility functions derived from existing literature data are utilized to assess the vulnerability of buried pipelines. Integrating the simplified approach for assessing groundwater-induced landslide displacements with the developed fragility functions for buried pipelines enables a comprehensive first-level risk assessment.

1. Assessment of PGD (Peak Ground Displacements)

The proposed framework for assessing the PGD takes advantage of the analytical model of Corominas et al. [1], Figure a, in which they could describe the slope movement by solving the momentum equation after adding the viscosity term:

$$\gamma l \sin\alpha \cos\alpha - [c' + (\gamma l cos^2\alpha - p_w)\tan\varphi'] - \tau \left(\frac{v}{A}\right)^{\frac{1}{X}} = ma \quad (1)$$

Where A and X are the viscosity parameters of the sliding surface which should be calibrated by back analysis of the measured displacments. c' and φ' are the cohesion and the effective friction angle, respectivily, and they refer to the sliding surface. p_w is pore pressure near the sliding surface. γ is the unite weight of the soil. l is the depth of the sliding surface.α is the slope angle. v is the velocity.

This analytical model was extended to a probabilistic approach by introducing the spatial variability in soil properties and the temporal variability in pore water pressure:

$$D = \lambda_{(D_w > d_w)} * \overline{D} + \varepsilon_{p\%} \quad (2)$$

D is a vector with d dimension, where d is the number of the examined sites along the slope, and represents the computed PGD with a specific probability of exceedance $p_{\%}$.

$\lambda_{(\boldsymbol{D_w} > d_w)}$ is the annual rate of exceedance, i.e. the number of the days in a reference period during which the groundwater table level (D_w) exceeds a specific value (d_w). It represents the temporal variability in pore pressure. Typically, a one-year period is selected as the reference period for the regular groundwater regime.

$\overline{D}$ is a vector, with d dimension. For each site along the slope the analytical model is calibrated using the measured displacements. For each site, the calibrated model is used to calculate the PGD for a specific groundwater table level (d_w) and time period equal to one day.

$\varepsilon_{p_{\%}}$ is a vector of residual values sampled from the probability distribution of the random function ε corresponding to a probability of exceedance of $p_{\%}$. It represents the spatial variability in soil properties. ε is a vector of spatially distributed residuals $\varepsilon = \{\varepsilon_1, \varepsilon_2, \dots, \varepsilon_d\}$, where ε_1 is the difference between the measured and predicted PGD at site 1, ε_2 represents the difference at site 2, and so on. This spatilly distributed residuals ε follows a multivariate normal distribution with zero vector and covariance matrix calculated using semi-variogram tool.

2. Assessment of the vulnerability of buried pipelines

Empirical data available from American Lifelines Alliance appendices (ALA-part 2) [2] are employed in the proposed framework, to develop the fragility functions of buried pipelines subjected to permanent ground deformations. This selection is based on the main assumption that permanent ground deformations that may cause potential damage on the examined pipeline constitute the main "loading" condition of the pipeline, regardless of the hazard causing these deformations. The limit state is defined as the state of the examined pipeline failure (having at least one repair for 100 m of pipeline length). In a first approximation, all data was selected to develop the fragility function used in the proposed framework through fitting them using lognormal probability distribution. Additional analysis was conducted to develop a fragility function to be used in the herein framework, by employing only the data referring to natural gas, NG, pipelines, Figure b.

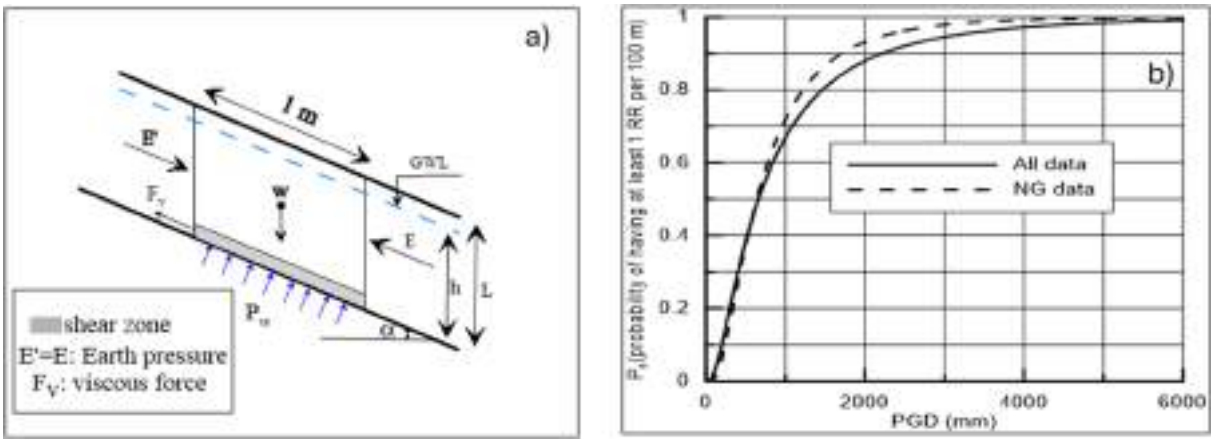

Figure 1. Geometry and variables used in the analytical model (modified from Corominas et al.[1])(a), fragility functions based on the available data from ALA [2] (b).

3. Assessment of the associated risk

The resulting risk is quantified solely on the basis of a number of required repairs in a reference period, without considering the severity of damage on the examined pipelines. To address this limitation and enhance the reliability of the assessed risk, it is recommended to follow the guidance of HAZUS [3]. According to HAZUS, for damage of buried pipelines associated with permanent ground deformations, approximately 80% of reported damage case should be considered as breaks , whereas the other 20% should be treated are leaks. Figure a illustrates the flowchart of the proposed framework.

4. Application of the proposed framework in a case study

Data available from Miscano landslide, located in southern Italy, was used to illustrate the application of the simplified framework proposed herein [4]. The landslide body consists of highly fissured sheared clay shales of high plasticity with isolated blocks or fragments of limestone. Field

investigations and measurements showed that three main zones can be distinguished, i.e., a sliding body consisting of remolded soil, a sliding surface and the intact soil, Figure b.

5. Results

Applying the previously summarized framework on a supposed natural gas pipeline embedded in the Miscano landslide, the probability of having at least one break per 100m length of the pipe for different locations along the slope (I4, I5, I6 and I7, see Figure b) and for time interval of 10 years:

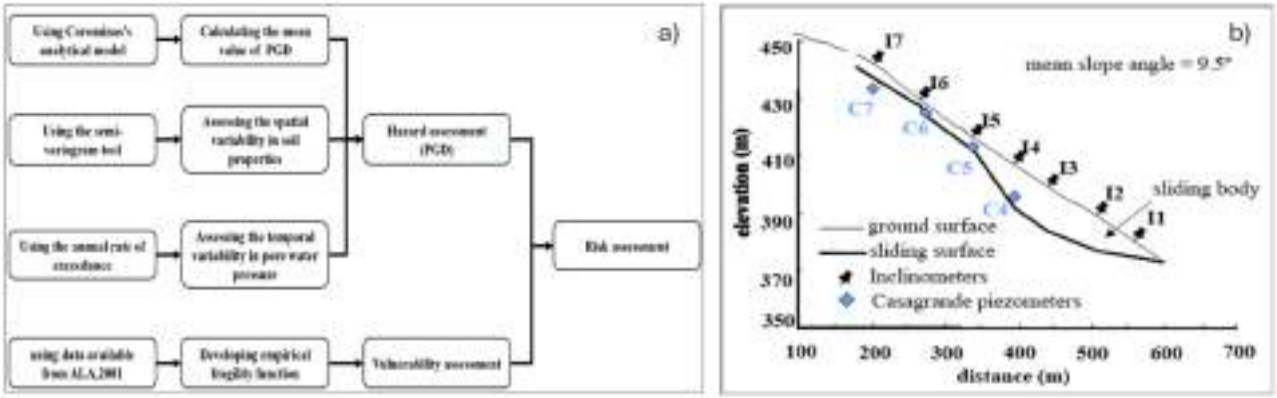

Figure 2. Flowchart illustrates the proposed framework (a), longitudinal section of Miscano slope (modified from Picarelli et al. [4])(b).

$$P_{break}(\%) = \begin{bmatrix} 0 \\ 37.6 \\ 0 \\ 76.8 \end{bmatrix} \tag{3}$$

And the probability of having at least one leak per 100m length of the pipe for different locations along the slope:

$$P_{leak}(\%) = \begin{bmatrix} 0 \\ 9.4 \\ 0 \\ 19.2 \end{bmatrix} \tag{4}$$

6. References

[1] Corominas, J., Moya, J.; Ledesma, A., Lloret, A., Gili, J. A. (2005). Prediction of Ground Displacements and Velocities from Groundwater Level Changes at the Vallcebre Landslide (Eastern Pyrenees, Spain), *Landslides*, 2 (2), 83–96, doi: https://doi.org/10.1007/s10346-005-0049-1

[2] ASCE-FEMA. (2001). Seismic Fragility Formulations for Water Systems, Part 2- Appendices

[3] National Institute of Building Sciences (NIBS) (2004). Earthquake Loss Estimation Methodology. HAZUS Technical Manual, Federal Emergency Management Agency (FEMA)

[4] Picarelli, L., Russo, C., Mandolini, A. (1999). Long-Term Movements of an Earthflow in Tectonized Clay Shales. In Slope Stability Engineering: Geotechnical and Geoenvironmental Aspects: Proceedings of the International Symposium (IS-Shikoku'99), Yagi, N., Yamagami, T., Jiang, J.-C. A. A., Eds., Matsuyama, Shikoku, Japan; Rotterdam, The Netherlands, Vol. 2, pp 1151–1158

Nonlinear static analyses for the seismic design of shallow tunnels

G. Lombardi[1], A. Manelli[1], D. N. Gorini[2], L. Callisto[1]
[1] Sapienza University of Rome, Rome, Italy
[2] University of Trento, Trento, Italy

Abstract

This paper introduces and validates a novel method for evaluating seismic-induced internal forces in the lining of a shallow circular tunnel. The method employs a static nonlinear analysis, typically used for structural systems, applied specifically to tunnels. In this decoupled approach seismic demand is represented by an elastic response spectrum, while seismic capacity is determined by applying horizontal static forces to the same numerical plane strain model used for the static design. The study outlines the key steps of the method and its effectiveness by comparing the results with time-domain dynamic analyses of the soil-tunnel model.

1. Introduction

In recent years there has been a growing awareness of the importance of seismic actions on tunnels, stimulated in part by damage to several underground structures during moderate to high intensity earthquakes. In current practice the seismic forces acting on the tunnel lining are assessed using rather simplistic methods that model the soil-lining interaction by linear springs connecting the lining to the free-field soil motion. More accurate methods would require time-domain dynamic analysis using full numerical models, but the relative complexity and cost are often impractical for standard projects. Therefore, this paper describes a decoupled design approach developed by the authors, as an intermediate complexity method exploiting the common static analysis performed to reproduce the construction sequence of the tunnel. In the method the seismic capacity of the system is represented by its capacity curve, derived from nonlinear pushover analysis of the soil-tunnel model. Then, the seismic demand is described by the elastic response spectrum of the considered action, modified to account for the tunnel's depth. The system performance is ultimately evaluated by comparing the demand and capacity on the acceleration-displacement (AD) response spectrum.

2. Case study

An idealized case, depicted in Figure 1, was developed to validate the method, described through a plane strain finite element model within the open-source analysis framework OpenSees [1]. The system's geometry consists of an 80×60 m soil domain, with a tunnel situated at a depth of 30 m. The tunnel has a diameter of 7 m, and its reinforced concrete lining is 0.5 m thick. This replicates a typical TBM-excavated urban tunnel.

The finite element grid was generated using a parametric mesh creator developed within the MATLAB framework. The soil domain was modeled using 4-noded stabilized single-point integration elements (SSPquad), and the soil mechanical behavior was simulated using an elastic-plastic constitutive model with kinematic hardening, known as PDMY [2]. The tunnel lining was discretised by two-noded elements characterized by linear elastic behavior (ElasticBeamColumn).

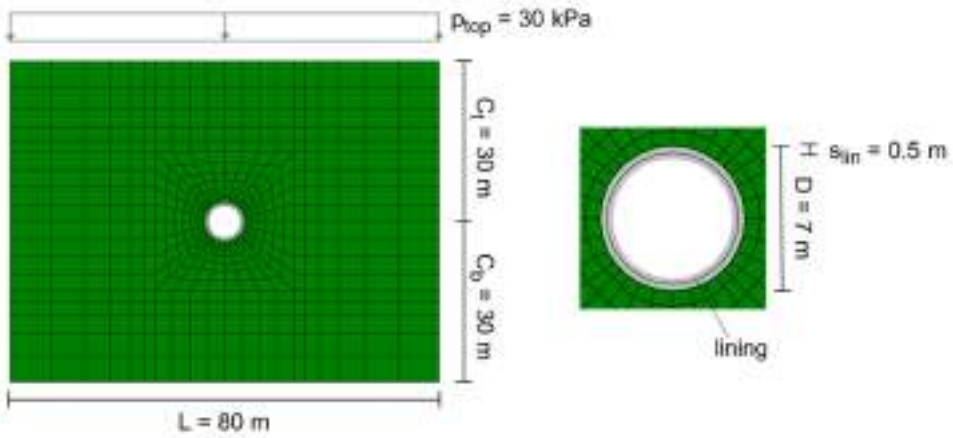

Figure 1. Finite element discretization of the reference model.

3. Capacity curve and seismic demand

In alignment with the Capacity Spectrum Method [3] for nonlinear static analysis of structural systems, this method derives independently the seismic capacity and demand, subsequently comparing these components on the AD plane. The capacity curve of the soil-tunnel system is derived by applying horizontal inertial forces incrementally to the numerical model, whose initial condition corresponds to the end of construction of the tunnel lining. The force distribution is assumed to be proportional to a uniformly distributed acceleration of amplitude $k_H \cdot g$ (g being the acceleration of gravity), that was see to reproduce with sufficient accuracy the deformation pattern associated with the first vibration mode of the system. In the pushover analysis the seismic coefficient k_H is gradually increased until a global plastic mechanism is activated. The capacity curve for the system at hand is shown in Figure 2a, where k_H is plotted as a function of the horizontal displacement d computed at the tunnel crown. Additionally, for each k_H, the pushover analysis provides the distribution of seismic-induced increments in internal forces across all lining sections. Figure 2a shows such increments in bending moment, normal force, and shear force in three lining sections of interest.

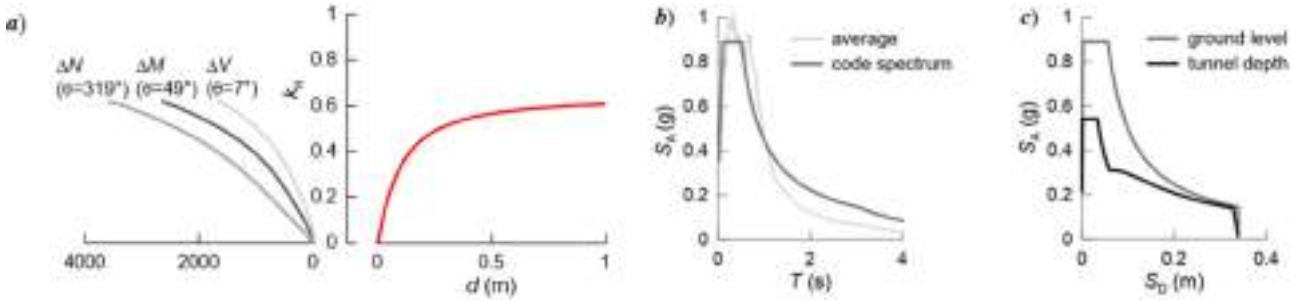

Figure 2. a) pushover curves in terms of displacement and seismic-induced increase of internal forces in the sections of interest; b) 5%-damped average elastic response spectrum at the ground level and interpolation with the Eurocode 8 shape; c) comparison between the AD spectrum considering or not the effect of the reduction factor β_D (tunnel depth and ground level, respectively).

In the validation of the proposed method, the seismic demand is represented by the average response spectrum at the ground surface. The latter was obtained by propagating eight selected accelerograms through a one-dimensional soil column that replicates the stratigraphic profile of the investigated deposit. This average spectrum, illustrated in Figure 2b, is interpolated using the spectral shape provided by Eurocode 8. Considering that the analysis focuses on the internal forces within the tunnel lining, it is essential to obtain the seismic demand at the tunnel depth. Figure 2c shows this adjustment, achieved by multiplying each point of the AD spectrum by the corresponding value of the reduction

factor β_D, which accounts for the effect of the tunnel depth. The reduction factor was obtained in analogy with the provisions of Eurocode 8 for retaining structures.

4. Implementation and validation

In the proposed method, the system performance is identified by the intersection of the seismic capacity and demand in the AD plane (performance point). In doing so it is necessary to adjust the elastic response spectrum to consider a damping ratio representative of the level of mobilised strength in the soil for the considered seismic scenario. This process begins with plotting the response spectrum for an initial damping ratio (e.g., ξ = 5%). The latter is then evaluated assuming a Masing-type uloading-reloading rule and the resonse spectrum is iteratively modified until convenrgence on the damping ratio is achieved. The acceleration at the performance point is subsequently used in the nonlinear static analysis to determine the internal forces in the lining sections. The design procedure was validated by comparing the force increments obtained in the lining sections of interest with those derived from nonlinear time-domain analyses of the soil-tunnel model applying to the base the same accelerograms used to derive the average response spectrum. As shown in Figure 3b, the simplified approach slightly overestimates the bending moment; on the other hand, shear and normal forces are somewhat underestimated. Despite these discrepancies, the agreement between the two methods is considered satisfactory, given the simplicity of the proposed design approach.

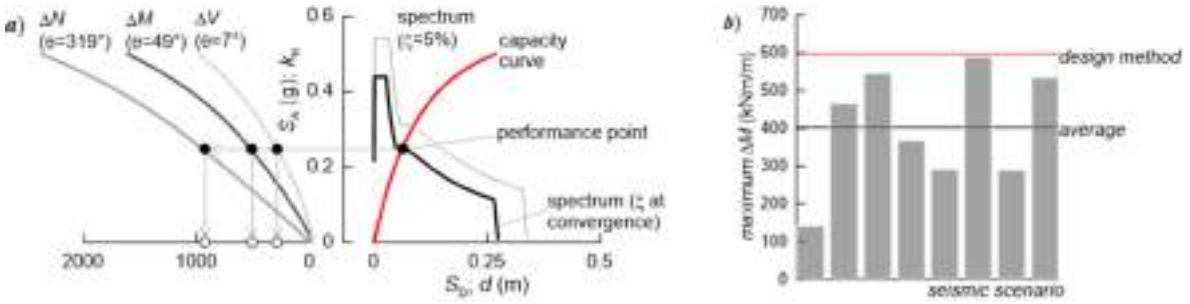

Figure 3. a) layout of the method implementation and b) reperentation of the maximum seismic bending moments in the lining obtained with time-domain dynamic analyses (gray bars), their average (black line) and using the proposed method (red line).

5. Conclusions

The proposed method regards seismic action as an equivalent static action, extending traditional design analyses related to construction phases. This approach allows for the design of the system without the need of time-domain dynamic analyses, whereas still accounting for the nonlinear behavior of the soil-tunnel system. The present study demonstrates that the method predicts earthquake-induced lining forces quite satisfactorily, specifically for the case of a shallow circular tunnel.

As a future development, the method will be utilized in a parametric study to enhance its general applicability and to facilitate the creation of design charts.

6. References

[1] McKenna, F. T. (1997). Object-oriented finite element programming: frameworks for analysis, algorithms and parallel computing, University of California, Berkeley

[2] Yang, Z., Elgamal, A., Parra, E. (2003). Computational model for cyclic mobility and associated shear deformation, *Journal of Geotechnical and Geoenvironmental Engineering*, 129(12), 1119-1127

[3] Freeman, S. A. (2004). Review of the development of the capacity spectrum method, *ISET Journal of Earthquake Technology*, 41(1), 1-13

List of Authors

(emails of the corresponding authors only)

Akan O.D. - University School for Advanced Studies IUSS Pavia, Italy, *onur.akan@iusspavia.it*
Abate G. - University of Catania, Italy, *glenda.abate@unict.it*
Abu-Kassab Q. - Lehigh University, United States
AlKhatib K. - Mott MacDonald, Cleveland, United States
Al-Subaihawi S. - Lehigh University, United States
Alver O. - Delft University of Technology, The Netherlands
Alves Fernandes V. - Electricité de France, France
Ambrosino A. - University of Sannio, Italy, *anambrosino@unisannio.it*
Andreini M. - CERN, European Organization for Nuclear Research, Switzerland
Arduino P. - University of Washington, United States, *parduino@uw.edu*
Batuhan Kocak M. - Istanbul Technical University, Turkey
Bella G. - Pini Group SA, Switzerland
Bilotta A. - University of Napoli Federico II, Italy
Bilotta E. - University of Napoli Federico II, Italy
Boldini D. - Sapienza University of Rome, Italy, *daniela.boldini@uniroma1.it*
Brito L. - University of Colorado Boulder, United States
Brunetti A. - Università Politecnica delle Marche, Italy
Callisto L. - Sapienza University of Rome, Italy
Camata G. - ASDEA Software Technology, Italy; University G. D'Annunzio of Chieti-Pescara, Italy
Carbonari S. - Università Politecnica delle Marche, Italy
Carmando U. - University of Napoli Federico II, Italy, *ugo.carmando@unina.it*
Dashti S. - University of Colorado Boulder, United States, *shideh.dashti@colorado.edu*
Dezi F. - Università di Camerino, Italy
Dizman Y. - Istanbul Technical University, Turkey
Ellison K. - ARUP, Portland, United States, *kirk.ellison@arup.com*
Eseller Bayat E.E. - Istanbul Technical University, Turkey
Falanesca M. - Pini Group SA, Switzerland
Fiamingo A. - University of Catania, Italy
Gallese D. - ARUP, London, UK, *domenicogallese@arup.com*
Gara F. - Università Politecnica delle Marche, Italy
Gastal M. – CERN, European Organization for Nuclear Research, Switzerland
Gatti F. - Université Paris-Saclay, France
Ghofrani A. - Google, USA, *alborzgh.uw@gmail.com*
Gianelli F. - Pini Group SA, Switzerland
Go J. - ARUP, London, UK
Gorini D.N. - Sapienza University of Rome, Italy, *davideno.gorini@uniroma1.it*
Goswami N. - Langan Engineering and Environmental Services, Unites States, *gopu16101989@gmail.com*
Hashash Y.M.A. - University of Illinois Urbana-Champaign, United States, *hashash@illinois.edu*
Jeremic B. - University of California, Davis, United States, *jeremic@ucdavis.edu*
Kanellopoulos C. - ETH Zurich, Zurich, Switzerland, *kkanello@ethz.ch*
Kato B. - Shenzhen University, China, *bkato@szu.edu.cn*
Knappett J. - University of Dundee, United Kingdom
Korres M. - Electricité de France, France, *michail.korres@edf.fr*

La Mendola S. - CERN, European Organization for Nuclear Research, Switzerland
Lai C.G. - University of Pavia, Italy; EUCENTRE, Italy
Liel A.B. - University of Colorado Boulder, United States
Lombardi G. - Sapienza University of Rome, Italy, *giuseppe.lombardi@uniroma1.it*
Lopez-Caballero F. - Université Paris-Saclay, France, *fernando.lopez-caballero@centralesupelec.fr*
Malik F.N. - Lehigh University, United States, *mamc22@lehigh.edu*
Manelli A. - Sapienza University of Rome, Italy
Marrazzo P.R. - University of Salerno, Italy
Martini R. - Università Politecnica delle Marche, Italy, *r.martini@pm.univpm.it*
Marullo T. - Lehigh University, United States
Massimino M.R. - University of Catania, Italy
Mattelaer P. - CERN, European Organization for Nuclear Research, Switzerland
McCallen D. - Lawrence Berkeley National Laboratory, United States, *dbmcallen@lbl.gov*
Merlini D. - Pini Group SA, Switzerland
Montuori R. - University of Salerno, Italy
Mubarak A. - University of Napoli Federico II, Italy
Nastri E. - University of Salerno, Italy
Pakzad A. - University of Washington, United States, *amnp95@uw.edu*
Petracca M. - ASDEA Software Technology, Italy
Pisanò F. - Norwegian Geotechnical Institute, United States, *federico.pisano@ngi.no*
Ricles J. - Lehigh University, United States, *jmr5@lehigh.edu*
Sasaki J. - ARUP, Tokyo, Japan
Sause R. - Lehigh University, United States
Shao B. - ARUP, San Francisco, United States
Sica S. - University of Sannio, Italy
Soto Moncada V. - Université Paris-Saclay, France
Spacone E. - University G. D'Annunzio of Chieti-Pescara, Italy
Stojadinovic B. - ETH Zurich, Switzerland
Suleiman M. - Lehigh University, United States
Syngros K. - Langan Engineering and Environmental Services, United States
Taciroglu E. - University of California Los Angeles, United States, *etacir@ucla.edu*
Tamagnini C. - University of Perugia, Italy
Tatarsky M. - ARUP, New York City, United States
Tawalo A. - SSM - Scuola Superiore Meridionale, Italy; University of Naples Federico II, Italy, *ali.tawalo-ssm@unina.it*
Tsinidis G. - University of Thessaly, Greece
Urciuoli G. - University of Naples Federico II, Italy
Varandas Ferreira J.N., Universidade NOVA de Lisboa, *jnsf@fct.unl.pt*
Voldoire F. - Electricité de France, France
Xing G. - Langan Engineering and Environmental Services, United States
Zentner I. - Electricité de France, France
Zeolla E. - University of Sannio, Italy, *ezeolla@unisannio.it*
Ziotopoulou K. - University of California, Davis, United States